MINIATURIZATION OF A SCREENING METHOD TO FIND NOVEL INHIBITORS OF *E. COLI* EFFLUX PUMPS

Sampo Kurvonen
Helsingin yliopisto
Farmasian tiedekunta
Farmaseuttisten biotieteiden osasto

Toukokuu 2019

HELSINGIN YLIOPISTO
HELSINGFORS UNIVERSITET
UNIVERSITY OF HELSINKI

Tiedekunta/Osasto Fakultet/Sektion – Faculty Farmasian tiedekunta	Osasto/Sektion– Department Farmaseuttisten biotieteiden osasto	
Tekijä/Författare – Author Sampo Kurvonen		
Työn nimi / Arbetets titel – Title Miniaturization of a screening method to find novel inhibitors of *E. coli* efflux pumps		
Oppiaine /Läroämne – Subject Biofarmasia		
Työn laji/Arbetets art – Level Pro gradu -tutkielma	Aika/Datum – Month and year Toukokuu 2019	Sivumäärä/ Sidoantal – Number of pages 77

Tiivistelmä/Referat – Abstract

Tausta: Antibiootit ovat olleet tärkeä tekijä bakteeriperäisten infektiotautien kuolleisuuden romahduksessa 1900-luvulla. Bakteerit ovat kuitenkin erittäin tehokkaita mukautumaan ympäristönsä muutoksiin lyhyen elinkaarensa vuoksi. Näin ollen bakteerien antibioottiresistenssin kehitys on luonnollisesti seurannut valtavaa maailmanlaajuista antibioottien käyttöä. Nykyinen tilanne on, että bakteerien antibioottiresistenssi kehittyy nopeammin kuin uusia antibiootteja löydetään ja kehitetään. Gram-negatiivisten bakteerien kolme pääasiallista resistenssistrategiaa ovat: antibiootin kohderakenteen muokkaus, antibiootin entsymaattinen inaktivaatio ja solun sisäisen antibioottikonsentraation laskeminen ulkokalvon toimintaa muokkaamalla. Bakteerit laskevat solun sisäistä antibioottikonsentraatiota muun muassa efluksipumpuilla, joista merkittävimpiä antibioottiresistenssin kannalta ovat RND-perheen effluksipumput. RND-efluksipumput toimivat tyypillisesti osana kolmiosaista rakennetta, joka mahdollistaa antibioottien pumppaamisen solun ulkoiseen tilaan. RND-pumppuja vastaan on kehitetty useita inhibiittoreita, mutta yksikään ei ole saavuttanut lääkekehityksen kliinistä vaihetta.

Tavoitteet: 384-kuoppalevyformaatissa toimivan seulontamenetelmän kehittäminen *E. colin* (BAA1161) efluksipumppuinhibiittorien seulomiseen, sekä kehitetyn menetelmän testaaminen.

Menetelmät: Absorbanssimittauksen riittävän herkkyyden varmistaminen bakteerikannan (BAA1161) kasvun seurantaan 384-kuoppalevyformaatissa. Seulontamenetelmässä käytettävän antibiootin (piperasilliini) ja positiivisena kontrollina käytettävän efluksipumppuinhibiittorin (meflokiini) BAA1161 kasvua estävän konsentraation (MIC) määrittäminen sekä 96- että 384-kuoppalevyformaatissa. Piperasilliinin ja meflokiinin BAA1161:n kasvua estävän synergian varmistaminen 96- ja 384-kuoppalevyformaateissa checkerboard-menetelmällä. Sijainnin vaikutuksen selvittäminen 384-kuoppalevyllä. Korkeimman BAA1161:n kasvuun vaikuttamattoman DMSO-konsentraation määrittäminen 384-kuoppalevyformaatissa. 126 luontoperäisen yhdisteen seulominen 384-kuoppalevyillä kehitetyn menetelmän testaamiseksi. Seulonta suoritettiin neljällä rinnakkaisella näytteellä perustuen seulottavien yhdisteiden bakteerin kasvua estävään vaikutukseen piperasilliinin kanssa. Yhdisteille, jotka osoittivat seulonnassa BAA1161:n kasvua estävää vaikutusta, suoritettiin annos-vaste -kokeet sekä piperasilliinin kanssa että ilman 384-kuoppalevyllä.

Tulokset ja pohdinta: Absorbanssimittaus osoittautui riittävän herkäksi menetelmäksi BAA1161:n kasvun mittaamiseen 384-kuoppalevyllä. 96- ja 384-kuoppalevyillä meflokiinin MIC-arvoksi saatiin 32 μg/ml. Piperasilliinin MIC-arvoksi saatiin 1024 μg/ml 96-kuoppalevyllä, mutta 384-kuoppalevyllä MIC-arvossa oli vaihtelua. Piperasilliini ja meflokiini osoittivat synergistista BAA1161:n kasvun estoa checkerboard-kokeissa. Kuopan sijainnin mahdollista vaikutusta menetelmän tuloksiin ei voitu arvioida, koska piperasilliinin vaikutuksessa BAA1161:n kasvuun oli suurta sattumanvaraista vaihtelua. Tämä sattumanvaraisesti toistuva ilmiö, jossa piperasilliini esti osassa kuoppia kokonaan tai lähes kokonaan BAA1161:n kasvun pitoisuudella joka oli alle MIC:n, toistui myös kaikissa seuraavissa kokeissa 384-kuoppalevyllä. Yksi mahdollinen syy tähän 384-kuoppalevyformaatissa toistuvaan ilmiöön on BAA1161 kannan heterogeenisyys piperasilliiniresistenssin suhteen. Testiseulonnassa neljä yhdistettä, jotka kaikki sisälsivät gallushappoesterin, osoittivat lupaavaa aktiivisuutta. Nämä yhdisteet olivat: epigallokatekiinigallaatti, hamamelitanniini, isopropyyligallaatti ja oktyyligallaatti. Hamamelitanniinin ja oktyyligallaatin teho osoittautui synergistiseksi piperasilliinin kanssa annos-vaste-kokeessa.

Johtopäätökset: Kehitettyä menetelmää voidaan hyödyntää uusien efluksipumppuinhibiittorien seulontaan. Menetelmän jatkokehittäminen lienee kuitenkin järkevää piperasilliinin vaikutuksen vaihtelun poistamiseksi ja siten menetelmän luotettavuuden lisäämiseksi. Menetelmän kuoppalevyformaattia vaihdettaessa tulisi myös kiinnittää erityistä huomiota tekijöihin jotka saattavat vaikuttaa menetelmän toimivuuteen uudessa formaatissa. Testiseulonnan perusteella gallushappoesterit ovat kiinnostava yhdisteryhmä, joiden antibioottien tehoa lisäävää vaikutusta kannattanee tutkia lisää tulevaisuudessa.

Avainsanat – Nyckelord – Keywords
efflux pump, piperacillin, mefloquine, *E. coli*, RND, miniaturization, efflux pump inhibitor, 384-well plate

Säilytyspaikka – Förvaringställe – Where deposited
Helsinki

Muita tietoja – Övriga uppgifter – Additional information
Ohjaajat**:** Heidi Kidron, Cristina Durante Cruz, Päivi Tammela

HELSINGIN YLIOPISTO
HELSINGFORS UNIVERSITET
UNIVERSITY OF HELSINKI

Tiedekunta/Osasto Fakultet/Sektion – Faculty Faculty of Pharmacy	Osasto/Sektion– Department Division of Pharmaceutical Biosciences	
Tekijä/Författare – Author Sampo Kurvonen		
Työn nimi / Arbetets titel – Title Miniaturization of a screening method to find novel inhibitors of *E. coli* efflux pumps		
Oppiaine /Läroämne – Subject Biopharmacy		
Työn laji/Arbetets art – Level Master's thesis	Aika/Datum – Month and year May 2019	Sivumäärä/ Sidoantal – Number of pages 77

Tiivistelmä/Referat – Abstract

Background: Antibiotics have been an important factor in the dramatic decrease of infectious disease mortality in the 20th century. Bacteria are, however, very quick to respond to the changes in their environment because of their short life cycle. Thus, the development of bacterial antibiotic resistance is a natural consequence of the enormous worldwide antibiotic use. The current situation is that the antibiotic resistance develops faster than novel antibiotics are found and developed. The three main resistance strategies of Gram-negative bacteria are: modification of the antibiotic target, enzymatic inactivation of the antibiotic and reduce of the intracellular antibiotic concentration by changing the function of the outer membrane. To decrease the intracellular antibiotic concentration bacteria use efflux pumps. RND efflux pumps are the most important family of efflux pumps regarding antibiotic resistance. They typically function as a part of a tripartite structure which allows the efflux of antibiotics to the extracellular space. Multiple inhibitors have been developed against RND efflux pumps but none has reached the clinical stage of drug development.

Objectives: Development and testing of a 384-well plate method for screening efflux pump inhibitors for *E. coli* (BAA1161) efflux pumps.

Methods: Verifying that the absorbance measurement is a sensitive enough method for measuring the bacterial (BAA1161) growth in 384-well plate format. The antibiotic chosen to be used in the screening method was piperacillin and the positive control efflux pump inhibitor was mefloquine. Determining the minimum growth inhibiting concentrations (MICs) of piperacillin and mefloquine in 96- and 384-well plate formats. Verification of the synergistic growth inhibitory effect of piperacillin and mefloquine with the checkerboard method in 96- and 384-well plate formats. Determining the positional effect in the 384-well plate. Determining the highest DMSO concentration without effect on the growth of BAA1161. Screening of 126 natural compounds in 384-well plates to test the developed method. Screening was done in quadruplicates based on the growth inhibitory effect of the natural compounds when combined with piperacillin. Dose-response assay was conducted in combination with and without piperacillin with the compounds that showed growth inhibiting effect during screening.

Results and discussion: Absorbance measurement was sensitive enough method for measuring the BAA1161 growth in the 384-well plate. MIC value of mefloquine was 32 µg/ml in both plate formats. Piperacillin's MIC was 1024 µg/ml in the 96-well plate, but on the 384-well plate there was variation in the MIC. Piperacillin and mefloquine showed synergistic effect on BAA1161 growth inhibition in the checkerboard assays. Positional effect could not be determined, because of the variation in the BAA1161 growth inhibition effect of piperacillin. This randomly occurring phenomenon were piperacillin inhibited BAA1161 growth completely or almost completely with sub-MIC concentration was encountered in all the subsequent experiments in the 384-well plate format. One possible reason for this phenomenon, occuring in the 384-well plate format, could be piperacillin heteroresistance of BAA1161 strain. In the test screen, four compounds, which all included gallic acid ester, showed promising activity. These compounds were: epigallocatechin gallate, hamamelitannin, isopropyl gallate and octyl gallate. In the dose-response assay, hamamelitannin's and octyl gallate's effect was synergistic with piperacillin.

Conclusions: The developed method can be used to screen novel efflux pump inhibitors. However, to increase the reliability of the method, further optimization is required to eliminate the variability in the effect of piperacillin. When plate format of a method is changed, factors which could affect the functionality of the method in the new format should be carefully assessed. Based on the test screed, gallic acid esters are interesting compounds which combined effects with antibiotics should be studied in the future experiments.

Avainsanat – Nyckelord – Keywords
efflux pump, piperacillin, mefloquine, *E. coli*, RND, miniaturization, efflux pump inhibitor, 384-well plate

Säilytyspaikka – Förvaringställe – Where deposited
Helsinki

Muita tietoja – Övriga uppgifter – Additional information
Supervisors**:** Heidi Kidron, Cristina Durante Cruz, Päivi Tammela

TABLE OF CONTENTS

LIST OF ABBREVIATIONS

ABC = ATP-binding cassette

cfu = colony-forming units

CLSI = Clinical and Laboratory Standards Institute

CR MDR = carbapenem and multi drug resistant

DMSO = dimethyl sulfoxide

EGCG = epigallocatechin gallate

EPI = efflux pump inhibitor

GNB = Gram-negative bacteria

HT = hamamelitannin

H33342 = Hoechst 33342

IG = isopropyl gallate

ITC = isothermal titration calorimetry

LB = lysogenic broth

MATE = multidrug and toxic compound extrusion

MD = molecular dynamic

MFS = major facilitator superfamily

MEF = mefloquine

MHA = Mueller-Hinton agar

MHB = Mueller-Hinton broth

MIC = minimal inhibitory concentration

MWC = monthly working culture

NC = natural compound

NMP = 1-(1-Naphthylmethyl)-piperazine

OG = octyl gallate

ONC = over-night culture

PAβN = phenyl-argine-β-naphtylamide

PIP = piperacillin

RND = resistance nodulation division

SMR = small multidrug resistance

WHO = World Health Organization

WWC = weekly working culture

384WP = 384-well plate

96WP = 96-well plate

ACKNOWLEDGEMENTS

I would like to especially thank my supervisors Cristina Durante Cruz, Heidi Kidron and Päivi Tammela, for their help and guidance with this project. Cristina for her limitless helpfulness with the practical things in the laboratory and with the writing process of this thesis. Heidi for her essential support and assistance with the writing and composing of this thesis. And, Päivi for her shared expertise and guidance regarding the study process. I would also like to thank Cristina, Heidi and Päivi for your support and positive solution-focused attitude during the difficulties encountered in this project. In addition, I would like to thank the whole Bioactivity Screening Group for helpfulness, support and providing a positive working atmosphere.

1. INTRODUCTION

The era of modern antibiotics started in 1930s with sulfamidochrysoidine (Dodds 2017). And since then the role of infectious diseases as a cause of death has dropped dramatically. For instance in US in 1937 mortality of infectious diseases was 283 out of 100 000 persons which dropped to 59 by 1996 (Armstrong et al 1999). Antibiotics have played a prominent role in this development but it has to be remembered that also other factors like vaccination, sanitation and improved living conditions have supported this development. Antibiotics have had especially large impact on the decrease of childhood mortality (Piddock 2012).

However, along with the development of antibiotics a new problem evolved, bacterial antibiotic resistance. Antibiotic resistance is a natural consequence of increased use of antibiotics. Bacteria are very quick to respond to the changes in their environment and to evolve because of their short life cycle (Piddock et al 2012). Unfortunately, antibiotics in their environment are not an exception. Evolution of antibiotic resistance was also not a surprise as Alexander Fleming already warned about it in his Nobel lecture in 1945 (Fleming, 1945).

Antibiotic use by humans is not the only reason for the development of antibiotic resistance. Antibiotics are also used in massive amounts for animals, even for non-therapeutic purposes, such as increasing feeding efficacy of food producing animals (Dodds 2017). In fact, in US most of the antibiotics by mass were consumed by food-producing animals in 2011. This extensive use of antibiotics in animals is connected to the global problem of antibiotic resistance and for some bacterial species food-producing animals have even become reservoirs of resistant strains.

The present situation is that resistant strains of pathogenic bacteria are occurring with increasing frequency and antibiotics against which resistance has not evolved are

discovered with decreasing frequency (Dodds 2017). The big pharmaceutical companies have lost a lot of their interest in the development of novel antibiotics and the economic reasons for that are clear (Piddock 2012). Antibiotics are usually used only for short periods of time and use of new antibiotics is usually restricted if resistance has not evolved against them. Thus, the ability to respond to antibiotic resistance has not substantially improved since the carbapenems in 1985 (Theuretzbacher, 2017). To globally assess the magnitude of antibiotic resistance World Health Organization (WHO) composed the report called: Antimicrobial Resistance Global Report (2014) (WHO, 2014). In the report WHO concluded that antimicrobial resistance has reached alarming levels and there are serious shortcomings in its surveillance. For instance, *Escherichia. coli*, which is the most frequent cause of urinary tract and blood stream infections, was found to have at least 48% resistance level to third generation cephalosporins and fluoroquinolones in at least one country of each WHO region (WHO, 2014). The qualitative and quantitative differences in the antibiotic resistance are large between countries and regions. All thing considered the return of an era when common infections and small injuries possessed substantial risk of death is not impossible.

The objective of the following literature review is to give an overview of the different mechanisms which Gram-negative bacteria (GNB) have developed to resist antibiotics. A second objective is to give more detail information of the function of resistance nodulation division (RND) efflux pumps and molecules which have been developed to inhibit their function. First four antibiotic resistance strategies of GNB will be presented. Then structure and function of AcrB, the main efflux transporter of *E. coli*, is reviewed. And finally, molecules which have been developed to inhibit AcrB and antibiotic resistance it causes are presented. The objective of the experimental part was to develop and miniaturize a screening assay for finding new molecules that could inhibit the antibiotic resistance mediated by efflux pumps of *E. coli*.

2. LITERATURE REVIEW

2.1 Antibiotic resistance mechanisms of Gram-negative bacteria

Antibiotic resistance mechanisms of GNB can be divided in at least three main strategies. These are: modification of the antibiotic target which results in hindered antibiotic binding, enzymatic inactivation of the antibiotic and decreased intracellular antibiotic concentration by altered outer membrane function. These resistance mechanisms differ for instance in specificity, efficacy, dissemination and origin. Bacteria often use multiple of these mechanisms concurrently and sometimes it is even required for clinically relevant resistance (Piddock 2006; Rodriguez-Martinez et al. 2016). Multiple resistance mechanisms utilize specific bacterium expressed proteins like efflux pumps and enzymes. Genes of these proteins can be chromosomally or plasmid encoded (Cag et al. 2016; Li et al. 2015). Plasmids allow horizontal gene transfer between different bacterial strains and species resulting in dissemination of the resistance mechanism. The level of antibiotic resistance and bacterial susceptibility to antibiotics is often measured with minimal inhibitory concentration (MIC). Clinical and Laboratory Standards Institute (CLSI) defines the MIC as "the lowest concentration of an antimicrobial agent that prevents visible growth of a microorganism in an agar or broth dilution susceptibility test" (CLSI, 2012).

2.1.1Antibiotic target structure modification

Modification of the antibiotic target structure is a common strategy for pathogenic bacteria to prevent the effect of antibiotic and to induce resistance against it. However, as the antibiotic targets have been selected based on their vital role for either survival or growth of the bacteria the modification has to be such that it prevents antibiotic binding without inactivating the target. The modification of the antibiotic target can occur by different mechanisms. Resistance causing target modification mechanisms include

mutations in the gene of the target protein, enzymatic modification of the target structure and expression of target structure binding proteins that inhibit antibiotic binding.

Mutations in the quinolone target enzymes gyrase and topoisomerase IV are the most common mechanism for fluoroquinolone resistance (Aldred et al. 2014). Location, type and quantity of gyrase and topoisomerase IV mutations affect the resulting resistance level. (Hopkins et al. 2005). Similar mutations can also result in different level of resistance depending on the bacterial species. Usually mutation in one target enzyme gene results in only low level of resistance to fluoroquinolones while selection for high level of resistance normally results in mutations in the genes of both quinolone target enzymes (Price et al. 2003; Aldred et al. 2014). Mutations in clinically found fluoroquinolone resistant strains are usually located in specific areas of the gyrase and topoisomerase IV genes, called quinolone resistant determining regions (Hopkins et al. 2005).

Modification of antibiotic target structure can also be enzymatic. In fact, posttranslational enzymatic antibiotic target modification is a common mechanism for resistance to bacterial ribosome targeting antibiotics like aminoglycosides, macrolides, lincosamides and streptogramin Bs (Wright 2011). For instance, aminoglycoside and macrolide resistance is mediated by 16s and 23s rRNA methyltransferases. Site-specific rRNA methylation by 16s methyltransferases inhibits aminoglycoside binding to 30S ribosomal subunit and prevents the following obstruction of protein synthesis (Doi et al. 2016). Also the binding of macrolides to 50S subunit of bacterial ribosome can be blocked by enzymatic methylation of rRNA (Gomes et al. 2016). Macrolide resistance is caused by methyl transferases that target the 23s rRNA of the 50S ribosomal subunit. Both of these rRNA targeting methyltransferases disseminate between pathogenic bacteria by plasmids (Doi et al. 2016; Gomes et al. 2016). Both 16s and 23s rRNA methyltransferases are also found and probably originate from antibiotic producing bacteria (Roberts 2004; Doi et al. 2016).

The third mechanism of antibiotic target modification is the target protection by bacterium expressed proteins. Qnr-proteins are around 200 amino acids long fluoroquinolone resistance mediating proteins that spread between pathogenic bacteria in plasmids (Aldred et al. 2014; Rodriguez-Martinez et al. 2016). Qnr-proteins belong to the pentapeptide repeat protein family and contain tandemly repeating amino acid domains (Rodriguez-Martinez et al. 2016). Plasmids that carry *qnr*-genes typically carry other additional resistance genes, also against other antibiotics. Qnr-proteins inhibit fluoroquinolone effect by binding to the target enzymes gyrase and topoisomerase IV and by decreasing the binding of these target enzymes to DNA (Aldred et al. 2014; Rodriguez-Martinez et al. 2016). Qnr-proteins typically cause only a low level of resistance to quinolones (Rodriguez-Martinez et al. 2016). However, *qnr*-genes promote emergence of resistance mutations and may cause high level of resistance when combined with other mechanisms of resistance. Qnr-proteins protect bacteria also from other compounds with similar mechanism of action to quinolones. The origin of *qnr*-genes is in the days before medical use of quinolones, supposedly in the water microbes of the environment.

2.1.2 Enzymatic inactivation of antibiotics

The second of the three main bacterial antibiotic resistance strategies is enzymatic inactivation of antibiotics. Multiple classes of antibiotic inactivating enzymes are expressed by pathogenic GNB. Some of these enzyme genes are chromosomal and some carried in plasmids (Cag et al. 2016). Seems likely that at least some of the resistance enzymes have evolved before the medical use of antibiotics. It is proposed that some β-lactamases have evolved even before the divergence of bacteria to Gram-positive and Gram-negative species (Hall and Barlow, 2003). Also findings of Bhullar et al. (2012) support the claim that the origin of antibiotic inactivating enzymes dates to the time before medical use of antibiotics. Bhullar et al. found bacteria capable of enzymatically inactivate β-lactams, macrolides and chloramphenicol from a cave that has been practically isolated from the outer world for over 4 million years. Bacterial strains from the cave were also less resistant to synthetic antibiotics ciprofloxacin and linezolid compared to natural product antibiotics.

The majority of enzymes that mediate antibiotic resistance catalyse either hydrolysis of the antibiotic or group transfer to the antibiotic (Wright 2005). Enzymes mediating hydrolysis of antibiotics include both amidases and esterases. Enzymes responsible for group transfer include acyltransferases, phosphotransferases, thioltransferases, nucleotidyltransferases and glycosyltransferases. Because amidases and esterases unlike the transferases require only water as a co-substrate they can be excreted to extracellular space, thus allowing inactivation of the antibiotic even before reaching the bacterium. To prevent the enzymatic inactivation of antibiotics, antibiotic structures have been modified and enzyme inhibitors have been developed.

β-lactamases are encoded by the *bla*-genes. They are the most common reason for β-lactam resistance in clinically relevant GNB (Bush and Jacoby 2010). β-lactamases are amidases that inactivate the β-lactams by hydrolysis of the β-lactam ring (Wright 2005). β-lactamases can be divided into two groups based on the hydrolysis mechanism. Metallo-β-lactamases catalyse the hydrolysis by activating the water molecule with a Zn^{2+}-ion. Serine-β-lactamases hydrolyse the β-lactams in a two-step reaction. First the active site serine causes the ring opening by nucleophilic attack, which is followed by hydrolysis of the covalent enzyme-antibiotic intermediate. Hydrolysis mechanisms of the two β-lactamase groups are shown in the figure 1. β-lactamases can also be classified to four groups (A-D) based on the protein structure and to three groups with multiple subgroups based on their functionality (Bush and Jacoby 2010). Other bacterial enzymes that hydrolyse antibiotics include macrolide esterases and fosfomycin inactivating epoxidases (Wright 2005).

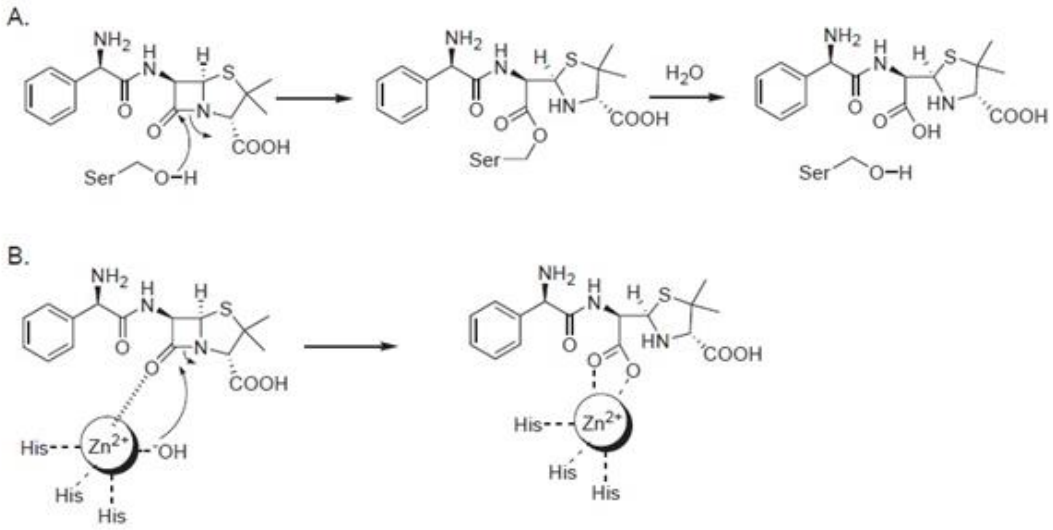

Figure 1. Mechanisms of β-lactam hydrolysis catalysed by β-lactamases (Wright 2005). A: Hydrolysis of ampicillin catalysed by serine β-lactamase. B: Hydrolysis of ampicillin catalysed by metallo-β-lactamase.

Transferases are larger and a more diverse group of resistance enzymes compared to hydrolysis catalysing enzymes (Wright 2005). For instance, aminoglycosides are inactivated by acetyltransferrases, phosphotransferases and nucleotidyltransferases. Other relevant group transfer enzymes include chloramphenicol acetyltransferases and lincosaminide nucleotidyltransferases. Covalent modification of the antibiotic by the transferase obstructs its binding to the target. Unlike the hydrolysing enzymes all the group transfer enzymes are only active in the bacterial cytosol.

In a retrospective observational cohort study conducted by Katchanov et al. (2018) 119 patients of German university medical centre were found to be colonized or infected by Gram-negative carbapenem and multi drug resistant (CR MDR) bacteria during the one year study period. The 119 patients with CR MDR bacteria accounted for 0.22% of the total patients of the hospital during the study period. The most often found species of the CR MDR bacteria were *Pseudomonas aeruginosa* (66 patients), *Klebsiella pneumoniae* (29 patients) and *Acinetobacter baumannii* (18 patients). Carbapenemase β-lactamase genes were assessed from the CR MDR bacterial isolates of the patients. 60 of the 102 isolates were found to carry a carbapenemase enzyme gene.

2.1.3 Membrane permeability in antibiotic resistance

The third antibiotic resistance strategy is to decrease the intracellular antibiotic concentration in bacterium by reducing the net flux through the outer membrane. GNB decrease the antibiotic outer membrane net flux by two mechanisms (Cag et al 2016). The penetration of antibiotics through the outer membrane can be reduced or the efflux of the antibiotics back to the extracellular space can be increased. Efflux pumps of the outer membrane play a key role in the antibiotic resistance mediated by antibiotic efflux. Porins are critical for the outer membrane permeability of many antibiotics.

Porins in antibiotic resistance

The outer membrane of GNB is normally only slightly or non-permeable to hydrophilic substances (Nikaido 2003). Thus, bacteria express multiple channel-forming proteins that allow the influx of important hydrophilic substances, like nutrients. Some of these channels are substrate-specific while some allow non-specific diffusion of hydrophilic solutes. These non-specific channels are called porins. The porins are likely important for outer membrane permeation of small antibiotics like β-lactams and fluoroquinolones, while large and hydrophobic antibiotics reach the intracellular space by diffusing across the lipid bilayer of the outer membrane.

The typical porin structure is a water filled β-barrel channel through the outer membrane to the periplasmic space (Patridge et al. 2015). Although porins are non-specific they often have general substrate preferences regarding size and charge of the substrate (Nikaido 2003). GNB often express multiple types of porins with different substrate preferences. For instance, *E. coli* expresses the following porins: OmpF, OmpC and PhoE. Porins and especially lack of them plays also an important role in the intrinsic antibiotic resistance of many Gram-negative species. For instance, high intrinsic resistance of *P. aeruginosa* to many antibiotics is partly mediated by the slow penetration of its main porin OprF.

Change in porin-mediated permeability can cause resistance to antibiotics for which porins are a relevant route across the outer membrane (Nikaido 2003). Three antibiotic resistance mechanisms concerning porins have been encountered clinically. Porin expression can be lost or reduced, expressed porin can be replaced by another one and porin function may be altered by mutation (Delcour 2009; Patridge et al. 2015). Mutations often occur in the L3 loop of the porin structure which folds into the channel and forms a narrowing (Nikaido 2003; Delcour 2009). GNB species for which altered porin function or expression mediated antibiotic resistance has been encountered include, for example, *E. coli, P. aeruginosa, Neisseria gonorrhoeae, Enterobacter aerogenes* and *K. pneumoniae.*

In the study conducted by Hasdemir et al. (2004) 18 different multi drug resistant *K. pneumoniae* strains were isolated from hospital patients in Turkey. The susceptibility of *K. pneumoniae* strains to 10 antibiotics with and without efflux pump inhibitor was measured and expression levels of efflux protein AcrA and porins OmpK35 and OmpK36 were determined. Interestingly 12 of 18 strains did not express OmpK35 in a low osmolarity medium unlike the reference strain ATCC 11296. Also, in two strains the expression level of OmpK35 was lower compared to the reference strain. However, OmpK36 was expressed in all multi drug resistant strains in both high and low osmolarity mediums in similar levels to reference strain. The absence of OmpK35 expression, one of the two major porins of *K. pneumoniae*, in the multi drug resistant strains and simultaneous normal expression of the OmpK36 may be explained by the results of Domenech-Sanchez et al. (2003). Domenech-Sanchez et al. found out that MIC values of five antibiotics, belonging to the cephalosporins and cephamycins, were at least four times lower in a *K. pneumoniae* strain that expressed only OmpK35 compared to strain that expressed only OmpK36. MIC values of the other tested antibiotics were the same or two times lower in the strain expressing only OmpK35 compared to the strain expressing only OmpK36. Thus, possibly the selective pressure by cephalosporins has caused the evolution of only OmpK36 expressing multi drug resistant *K. pneumoniae* strains.

A study by Clancy et al. (2013) shows the effect of porin mutations on antibiotic efficacy. 23 strains of sequence type 258 *K. pneumoniae* were isolated from bloodstream samples of different patients. All of the strains carried the KPC-2 β-lactamase gene and 18 of the 23 strains carried also an *ompK36* mutation. Seven of the 18 mutations were in the promoter and the rest were on the *ompK36* gene itself. The seven strains carrying promoter mutation and eight strains with similar six base pair insertion mutation (aa134-135 GD) had significantly higher MIC values of doripenem compared to other three strains with different mutations and five wild type strains. The KPC-2 β-lactamase expression level of the strains was not associated with the doripenem MIC values. The strains carrying the promoter mutation had significantly lower OmpK36 expression level compared to wild type strains and strains with other mutations. The strains with aa134-135 GD mutation did not show diminished expression of OmpK36. *OmpK36* mutations had no effect on MIC of the second tested antibiotic colistin. As these results show, porin mutations can affect antibiotic susceptibility of GNB by decreasing the porin expression or by mechanisms related to reduced porin function.

Efflux pumps and antibiotic resistance

The second mechanism of GNB to decrease the intracellular antibiotic concentration is the efflux, which is mediated by efflux pump proteins. Just like the porins, bacterial efflux pumps play a role in both intrinsic and acquired antibiotic resistance (Blair et al. 2014; Li et al. 2015). Most of the bacteria express a large number of different efflux pumps, however, usually only a few of those mediate antibiotic resistance (Piddock 2006). Substrate specificity of the bacterial efflux pumps varies from specific to broad (Blair et al. 2014). The origin of bacterial efflux pumps dates back to the time before medical use of antibiotics and it is thought that the original function of efflux pumps has been the efflux of intracellular metabolites and harmful compounds of the environment (Piddock 2006).

Resistance nodulation division (RND), multidrug and toxic compound extrusion (MATE), major facilitator superfamily (MFS), small multidrug resistance (SMR) and ATP-binding cassette (ABC) are all classes of bacterial efflux pumps with antibiotic efflux mediating members (Li et al. 2015) (Figure 2). These classes differ in structure, energy source of efflux, location in the bacteria and substrates. RND is clinically the most important antibiotic resistance mediating class of efflux pumps in GNB (Blair et al. 2014). ABC transporters use ATP as the energy source of the efflux while other classes are secondary transporters, most of which use proton motive force as the energy source (Li et al. 2015). RND transporters function as a part of a tripartite structure which spans from the inner membrane through the periplasmic space to the outer membrane allowing the extrusion of the substrate to the extracellular space. Most members of the other classes have a single-component structure and are located only in the inner membrane of the bacterium allowing only extrusion of substrate from the cytosol to the periplasmic space. This functional difference is probably one reason for the prominent role of the RND transporters in the antibiotic resistance.

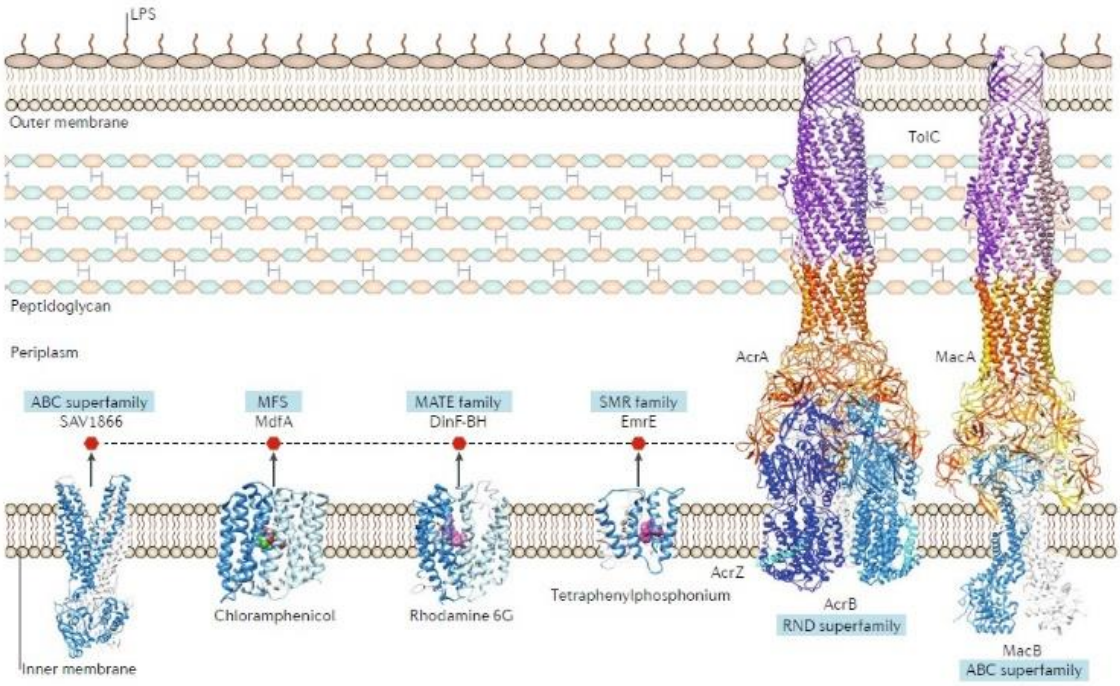

Figure 2. Schematic picture of structures and locations of different efflux pump classes in the membranes of Gram-negative bacteria (Du et al 2018). Members of ABC, MFS, MATE and SMR efflux pump families usually function as independent units and pump substrates (red hexagons) from the cytosol to the periplasmic space. Efflux pumps of the RND family usually function as a part of a tripartite efflux complex and pump substrates

from the periplasmic space to the extracellular space. Also more uncommon tripartite efflux complex with ABC-transporter is shown at the right.

RND pump mediated antibiotic resistance is heavily dependent on the antibiotic's outer membrane permeability (Li et al. 2015). Thus, the physicochemical properties of the antibiotic, the species of the bacteria and the porin profile of the outer membrane can affect the efficacy of efflux. If the antibiotic flux through the outer membrane is rapid the efflux pumps cannot outweigh the influx and therefore even the overexpression of efflux pumps will not generate significant resistance. However, if the antibiotic permeates the outer membrane of the bacterium slowly, overexpression of the efflux pumps can cause great increase in the resistance. Thus, overexpression of the efflux pumps generates higher level of resistance in bacterial species with low outer membrane permeability, like in *P. aeruginosa* and against antibiotics which penetrate the outer membrane slowly, like erythromycin.

Clinically relevant GNB species for which the antibiotic resistance caused by overexpression of efflux transporter is common include *P. aeruginosa, A. baumannii, Burkholderia pseudomallei, Salmonella, Campylobacter jejuni* and *E. coli* (Blair et al. 2014). Clinically relevant RND efflux pumps in Gram-negative species include AcrAB-TolC of *E. coli* and *Salmonella enterica*, MexAB-OrpM of *P. aeruginosa* and CmeABC of *C. jejuni* for example. Efflux pumps of RND family are mainly chromosomally encoded but there are also some clinically relevant plasmid encoded efflux proteins, like fluoroquinolone resistance mediating *qepA* of the MFS-family (Yamane et al. 2007, Li et al. 2015). Also increase in the prevalence of RND transporter carrying plasmids and the following dissemination is an unsettling future scenario (Li et al. 2015).

The overexpression of the efflux pump and the following antibiotic resistance can result from mutations in the efflux pump expression regulating genes, like in local repressor, global regulator and transcription factor genes (Piddock 2006; Blair et al. 2014). Also, mutations in the promoter area of the efflux pump gene can result in overexpression and antibiotic resistance. In a study conducted by Shigemura et al. (2015) 105 strains of *P. aeruginosa* were isolated from urinary tract infection patients of three hospitals in Japan.

26.7%, 11.4%, 41.9% and 38.1% of the *P. aeruginosa* strains were increasingly expressing *mexB*, *mexC*, *mexE* and *mexY* RND efflux pump genes, respectively, compared to the control strain PAO1. Significant association was found between levofloxacin resistance and overexpression of *mexC*. However, no other statistically significant associations were found with gene expressions of the four efflux pump genes and susceptibilities to nine antibiotics of different classes.

2.2 RND efflux pump structure and function

As mentioned earlier RND transporters are the most relevant antibiotic efflux-proteins of GNB (Blair et al. 2014). RND transporter complex AcrAB-TolC is the most effective antibiotic efflux complex of wild type *E. coli.* AcrAB-TolC has an extremely wide substrate range, including members from practically all classes of antibiotics with the exception of aminoglycosides (Sulavik et al. 2001; Li et al. 2015). In this chapter the structure and function of this most studied member of RND class of efflux transporters is shortly covered (Li et al. 2015).

RND transporters are located in the inner membrane of GNB and function as a part of a tripartite structure (Li et al. 2015). This three-part efflux complex spans from the bacterial cytosol through the periplasmic space to the extracellular space and is composed of the RND pump, a periplasmic adaptor protein and an outer membrane channel. All of these components of the RND pump complex are necessary for its efflux function (Ma et al. 1995; Fralick 1996; Anes et al. 2015). For instance, RND pump complex AcrAB-TolC is composed of the RND pump AcrB, periplasmic adaptor protein AcrA and outer membrane channel TolC (Li et al. 2015). The stoichiometry of these components is 3:6:3, thus, AcrB and TolC are homotrimers and AcrA is a hexamer in the AcrAB-TolC complex (Tikhonova et al. 2011; Du et al. 2014; Wang et al 2017).

AcrB, the RND pump of the complex, is mainly located in the inner membrane and in the periplasmic space, however, a small part of it spans also to the cytosol (Murakami et al. 2002; Du et al. 2018). The second part of the complex, AcrA is located in the periplasmic space where it surrounds and interacts with periplasmic parts of the AcrB and TolC (Hinchliffe 2013; Anes et al. 2015). The most peripheral part of the complex is TolC, which is located in the outer membrane. TolC connects the periplasmic part of the AcrAB-efflux complex to the extracellular space. Based on the results by Tikhonova et al (2011), AcrB binds to the TolC directly in the periplasmic space and AcrA is not required for the interaction. However, the periplasmic adaptor protein AcrA probably stabilizes the interaction between AcrB and TolC (Hinchliffe et al. 2013). AcrA is also required for sealing the periplasmic part of AcrAB-TolC (Wang et al 2017). In addition to the AcrAB-TolC complex, TolC functions as an exit duct also in other tripartite efflux pump complexes of *E. coli*, for instance in MacAB-TolC and EmrAB-TolC complexes (Hinchliffe et al. 2013). Simplified illustration of the AcrAB-TolC structure is shown in the Figure 3.

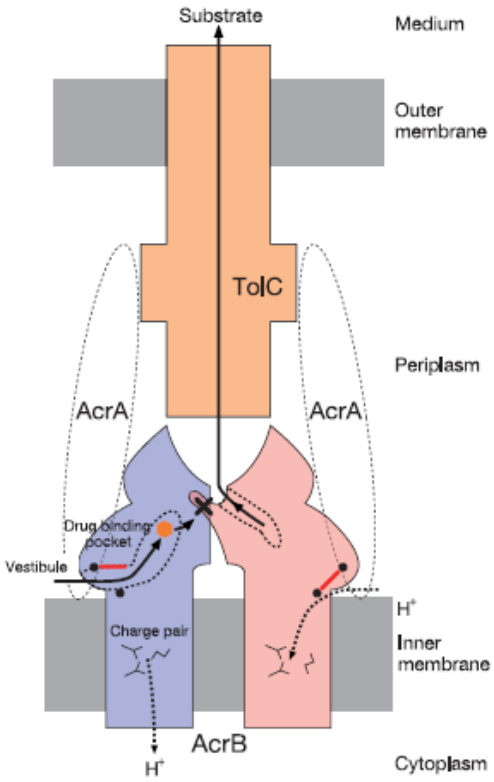

Figure 3. Simplified side view picture of the AcrAB-TolC efflux pump complex (Murakami et al 2006). In the picture blue AcrB proteomer is in the open conformation and the red proteomer is in the extrusion conformation. Orange hexagon represents the

substrate and solid arrows represent the efflux path of the substrate. Dotted arrows represent the proton influx.

AcrB is a homotrimer with the three proteomers in different conformations in the ligand binding state (Murakami et al. 2006). Rotation of the trimer conformers seems to mediate the efflux mechanism. The three proteomers of AcrB are in a ring-like formation and form a short tube looking protein (Murakami et al 2002). The three proteomers are linked to each other in the periplasmic end of the protein by long hairpin structures which presumably provide strong interaction. Compared to the periplasmic end the proteomers seem to be more loosely packed in the transmembrane part of AcrB. Inside the proximal periplasmic AcrB the three proteomers form a cavity with around 30Å diameter called the central cavity. The base of the central cavity is presumably formed by the inner membrane and the side walls and the top are formed by the three proteomers (Murakami et al 2002; Eicher el al. 2012). In the distal periplasmic AcrB the proteomers form a funnel structure (Murakami et al 2002). A close homolog transporter with very similar structure to AcrB is found in all members of *Enterobacteriaceae* and for instance in *P. aeruginosa* (MexB) (Li et al. 2015).

Inside each AcrB proteomer is a substrate tunnel which leads from the entrance channels on the proximal periplasmic surface of the proteomer to the inner surface of the funnel structure at the distal end of the AcrB (Murakami et al. 2006; Nakashima et al. 2011; Eicher el al. 2012). The different conformations of the proteomer change the diameter of this substrate tunnel at different parts of it. The tunnel is not thoroughly open at any conformation, thus conformation changes are needed for substrate to traverse the whole tunnel.

Substrates have access to inside of the AcrB proteomer from at least two entrance channels, possibly three, when the proteomer is in the open conformation (O-conformation, or also called access conformation) (Nakashima et al. 2011). One of the two entrance channels is just above the inner membrane while the second one is further away in the periplasmic part of the AcrB. The third putative entrance channel is located

on the surface of the central cavity. Substrate entrance channels lead to the two substrate binding sites (Nakashima et al. 2011; Eicher el al. 2012). These two binding sites are close to each other separated by the switch loop structure. The diameter and shape of these two binding sites and the conformation of the switch loop between them changes at the different conformations of the proteomer. Both polar and hydrophobic amino acids are located at both binding sites, thus allowing multiple types of interactions with substrates (Murakami et al. 2006; Nakashima et al. 2011). However, at least in the distal binding site most of the amino acids are hydrophobic (Murakami et al. 2006). From the proximal binding site through the distal binding site the substrate tunnel leads to the extrusion channel which connects the binding sites to the funnel (Nakashima et al. 2011; Eicher el al. 2012). The funnel eventually leads to the extra cellular space through the TolC pore.

The prevailing theory of AcrB efflux mechanism is based on the three conformations of the proteomers (Murakami et al. 2006; Nakashima et al. 2011; Eicher el al. 2012). The conformations are open conformation, binding conformation (also called tight or T-conformation) and extrusion conformation (also called loose or L-conformation). Each of these conformations mediates one of the three steps in the efflux mechanism. These three conformations are concertedly rotating in the trimer so that every proteomer is in a different conformation and phase of the efflux mechanism. Simplified illustrations of the conformations and efflux mechanism of AcrB proteomer and trimer are shown in the Figures 4 and 5.

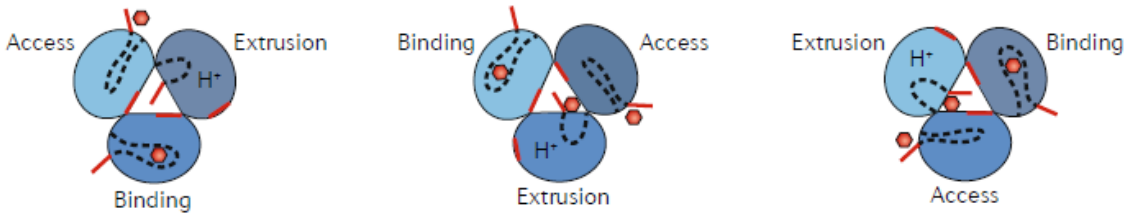

Figure 4. Top-view illustration of the concerted efflux mechanism of AcrB protein (Du et al 2018). The three proteomers are in different tints of blue and the substrates are represented by the orange hexagons. AcrB transfers the substrates from the periplasmic space (outside the protein) to the funnel structure (in middle of the proteomers) which connects the substrate extrusion pathway to the TolC component of the AcrAB-TolC efflux complex.

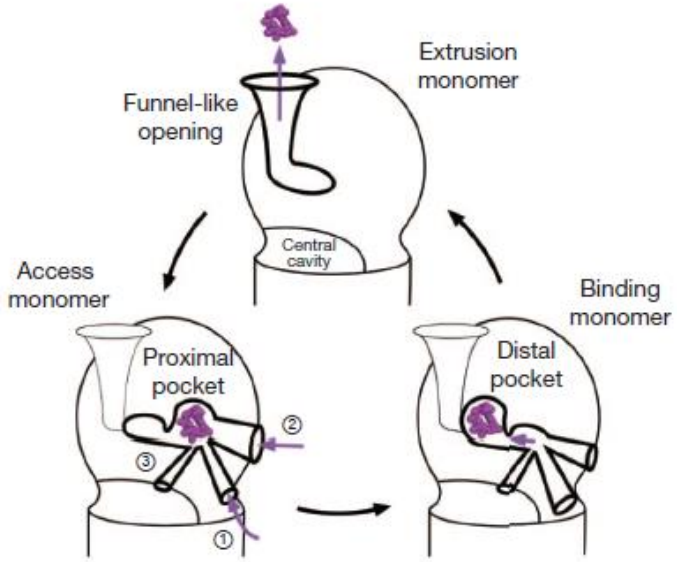

Figure 5. Illustration of the three different conformations of the AcrB proteomer mediating the efflux process (Nakashima et al 2011). AcrB substrate is represented as violet molecule. On the left, the access (open) conformation in which the substrate moves from the periplasmic space to the proximal binding site through one of the three entrance channels. Next, on the right, the binding conformation in which the substrate moves to the distal binding site. Movement is caused by the conformation changes of the switch loop and proximal and distal binding sites. Switch loop is located between the two binding sites. On the top is the extrusion conformation which mediates the last step of the efflux process. In the extrusion conformation distal binding site shrinks and squeezes the substrate out of the proteomer to the funnel-like opening on the top of the AcrB protein.

In the open conformation the substrate enters to the proteomer from an entrance channel (Murakami et al. 2006; Nakashima et al. 2011; Eicher el al. 2012). In this conformation the distant binding site is shrinked and the switch loop provides a steric hindrance to distant binding site access (Nakashima et al. 2011; Eicher el al. 2012). Thus, in the open conformation only low molecular mass substrates have an access to the distant binding site and the high molecular mass substrates bind to the proximal binding site. In the binding conformation the distant binding site expands enhancing the substrate binding. Also the switch loop conformation changes forcing the high molecular mass substrates to the distant binding site from the proximal binding site. In the extrusion conformation the extrusion channel to the funnel opens and the channel to the entrance channels closes (Murakami et al. 2006; Nakashima et al. 2011; Eicher el al. 2012). Also the conformation of distant binding site shrinks pushing the substrates to the extrusion channel. These changes squeeze the substrate from the distant binding site to the AcrB funnel structure

in the distant head of the protein. From the funnel through the TolC pore to the extracellular space the path is common to substrates of the all three proteomers (Murakami et al. 2006). It is speculated that AcrA mediates the conformation changes of AcrB proteomers to the TolC and causes the synchronized opening of the TolC pore (Wang et al 2017; Murakami et al. 2006). Energy for the substrate efflux by AcrB is derived from proton influx from the periplasmic space to the cytosol (Li et al. 2015).

In addition to the three necessary components of the AcrAB-TolC, more recently a fourth component of the efflux complex was found by Hobbs et al. (2012). It was named as AcrZ. AcrZ seems to interact with the RND pump AcrB of the complex. This small 49 amino acids protein affects only efflux of some substrates by AcrAB-TolC. It is suggested that the AcrZ adjusts recognition and binding of certain substrates by AcrB by conformation modulation.

The large volume of AcrB binding sites and the high quantity of interaction mediating residues in the binding sites are likely important factors for the wide substrate range of AcrAB-TolC complex (Murakami et al. 2006). This allows different substrates to bind to different residues in the binding sites (Murakami et al. 2006; Nakashima et al. 2011). In fact, in molecular dynamic simulations (MD) conducted by Vargiu and Nikaido (2012) the nine simulated substrates were found to interact with 25 different amino acids in the distal binding site. One or multiple hydrophobic groups in the molecular structure is a common property of AcrB substrates (Nikaido et al. 1998, Li et al. 2015). This common property of substrates might be key for wide substrate range of multidrug efflux pumps as suggested by Neyfakh (2002). Because of the hydrophobic groups, the substrate antibiotics are not strongly stabilized by the water molecules of the cytosol, thus the energy barrier to overcome in the efflux pump binding is relatively low compared to binding of hydrophilic substrates to enzymes (Neyfakh 2002; Li et al. 2015). Because of this relatively low energy barrier of binding the binding sites of AcrB can be large and polyspecific.

2.3 Inhibitors of RND efflux pumps

One strategy to obstruct the function of above described RND transporters of Gram-negative pathogens is small molecule efflux pump inhibitors (EPIs), which would be used as a combination therapy with antibiotics. EPIs could restore the effectivity of antibiotics, which RND transporter mediated resistance has made clinically non-useful. EPIs could possibly even make some of the antibiotics currently used only against Gram-positive species effective also against Gram-negative pathogens (Li et al 2015; Mahmood et al 2016). In addition to the antibiotic potentiating effect, EPIs could possibly prevent occurrence of bacterial resistance mutations, biofilm formation and even inhibit toxin mediated virulence of some enteropathogenic species (Opperman and Nguyen 2015). However, despite multiple efforts still no EPI against bacterial RND efflux pumps has reached the clinical phase of drug development. Multiple EPI drug candidates have been studied *in vivo*, *in vitr*o and *in silico* by using for instance efflux pump deleted mutant strains, substrate competition assays, RND substrate dye accumulation, isothermal titration calorimetry (ITC), X-ray crystallography, docking and MD simulations (Li et al 2015; Opperman and Nguyen 2015; Mahmood et al 2016). Still toxicity, pharmacokinetics, spectrum of activity, potency and outer membrane permeability related problems have prevented progress of candidates to the clinical phase (Opperman and Nguyen 2015). Also, the wide substrate range and extensiveness of the substrate binding site of RND transporters add difficulty to EPI development because there are no clear limits for the physiochemical properties of EPIs or RND substrates (Mahmood et al 2016). In the following paragraphs four known inhibitors of the AcrB RND efflux pump of *E. coli* will be presented in chronological order of discovery, which is followed by broader group of quinolone derivates with documented EPI activity.

2.3.1 Phenyl-argine-β-naphtylamide

The first notable effort to develop an EPI against RND efflux pumps reaching the preclinical drug development phase was phenyl-argine-β-naphtylamide (PAβN) (Figure 6) (Aron and Oppermann 2018). PAβN, also known as MC-207,101, was found as a result

of compound collection screening against *P. aeruginosa* strains overexpressing Mex RND efflux pumps (Renau et al 1999). Later it was found out that PAβN also inhibits AcrAB-TolC of *E. coli* in addition to MexAB-OrpM, MexCD-OrpJ and MexEF-OrpN RND pumps of *P. aeruginosa* (Lomovskaya et al 2001). Intrinsic MIC values of 400 and 256 μg/ml have been obtained for PAβN in wild type *E. coli* strains and the MIC value has been found to be dependent on the expression level of *acrAB* in *E. coli* (Kern et al 2006; Matsumoto et al 2011). PAβN has no effect on the proton gradient of the inner membrane and thus the inhibition of RND efflux pumps is not based on de-energization (Lomovskaya et al 2001). However, it was found out that PAβN also increased the outer membrane permeation of *P. aeruginosa*, in addition to its EPI activity. Based on the results of Matsumoto et al (2011), PAβN may have similar permeabilizing effect also on *E. coli*. Thus, the experiments measuring the EPI activity of PAβN should be done in 1mM Mg^{2+} which minimizes the permeating effect (Opperman and Nguyen 2015). After all, it is not completely clear how significant the outer membrane effect of PAβN is regarding the increased antibiotic susceptibility, but it is likely strain and species dependent (Lomovskaya et al 2001; Matsumoto et al 2011).

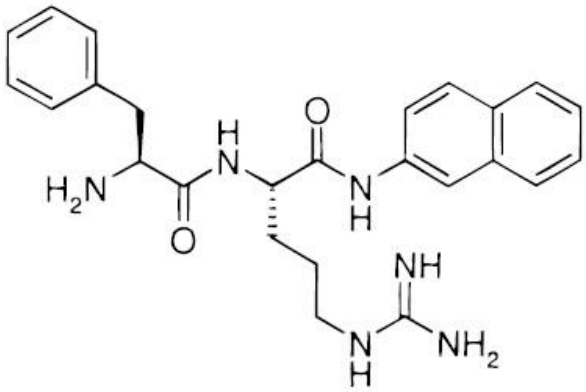

Figure 6. Molecular structure of efflux pump inhibitor Phenyl-Argine-β-naphtylamide (PAβN) (Renau et al 1999).

The initial *in vivo* experiments with a close homolog of the PAβN gave promising results (Renau et al 1999). An N-methyl derivate of PAβN was used in the *in vivo* experiments because PAβN is not stable in mouse, rat or human serum. In a murine neutropenic thigh model, combination of PAβN derivate with levofloxacin resulted in 3-log reduction in *P. aeruginosa* colony-forming units (cfu) compared to the no treatment controls and only

levofloxacin or N-methyl PAβN treated mice. 30 mg/kg dose was used for both levofloxacin and PAβN derivate in the experiment. However, in pharmacokinetic experiments done with rats, the active PAβN derivates were found to accumulate to kidney increasing the possibility for toxicity (Watkins et al 2003). It was found out that the dicationic nature of the PAβN derivates was likely causing the accumulation. Unfortunately, the dicationic structure was also essential for the EPI activity of the derivates. Because of these pharmacokinetic and toxicity problems development of PAβN as a drug candidate was suspended (Lomovskaya and Bostian 2006). Nevertheless, PAβN is still used as a laboratory reagent to study RND pump mediated bacterial efflux.

Based on the results of Lomovskaya et al. (2001), it seems likely that PAβN is both substrate and inhibitor of RND efflux pumps. PAβN inhibits the efflux of different RND substrates to different extent. This may be related to substrates binding to the different subsites within the substrate binding site. The mechanism of AcrB efflux inhibition by PAβN has been studied with computational methods by Vargiu and Nikaido (2012). Based on their MD-simulations, PAβN binds to substrate binding site of AcrB with higher affinity than average substrate. However, the affinities of simulated substrates are still quite similar to affinity of PAβN and some substrates like nitrocefin bind with even higher affinity than PAβN. These findings suggest that inhibition mechanism of PAβN is not based on high affinity binding resulting in hindrance to substrate binding and AcrB conformation changes. Nevertheless, in the simulations there was one clear difference in the AcrB binding of normal substrates compared to PAβN. Unlike the other substrates PAβN interacted with the switch loop in addition to the moieties of the distal binding site. These results suggest that inhibition mechanism of PAβN may be related to the straddling of the switch loop.

As described above PAβN inhibits the function of *E. coli* and *P. aeruginosa* RND efflux pumps. The effect of PAβN on antibiotic efflux of other pathogenic bacteria has also been studied. Based on the results of Panek et al. (2006), PAβN had very limited effect on *A. baumannii* RND efflux pump AdeABC. However, PAβN had also an AdeABC independent effect on clarithromycin and rifampicin susceptibility of *A. baumannii*,

which was probably based on the increased outer membrane permeability. In a study conducted by Hannula and Hänninen (2008) PAβN increased susceptibility of *C. jejuni* and *Campylobacter coli* to erythromycin and rifampicin but not to other CmeABC efflux pump substrates. Unfortunately, the outer membrane effect of PAβN was not taken in to consideration by Hannula and Hänninen, which reduces reliability of the conclusions regarding the effect of PAβN on CmeABC. PAβN increased also susceptibility of *Vibrio cholerae* to the antibiotics which are RND pump substrates (Bina et al 2009).

2.3.2 1-(1-Naphthylmethyl)-piperazine

EPI 1-(1-Naphthylmethyl)-piperazine (NMP) (Figure 7) was found by screening aryl piperazines with levofloxacin against AcrAB and AcrEF overexpressing *E. coli* strains (Bohnert and Kern 2005). With 100 μg/ml concentration NMP was found to reduce MIC values of levofloxacin, linezolid, clarithromycin and chloramphenicol for four times or more in AcrAB and AcrEF overexpressing *E. coli* strains but not in the AcrAB and AcrEF deficient strain. Also in a following study with clinical *E. coli* isolates, NMP was found to reduce MIC_{50}-values of levofloxacin, linezolid, rifampicin and ethidium bromide by four times or over in most of the studied isolates (Kern et al 2006). The intrinsic MIC value of NMP is 400 μg/ml with *E. coli* (Bohnert and Kern 2005). Unlike PAβN the intrinsic MIC value of NMP is not affected by expression of efflux pumps, suggesting that NMP is not a substrate of RND pumps like PAβN. Also results from Schuster et al (2014) suggest that NMP itself is not a substrate of AcrB or it is a very poor one.

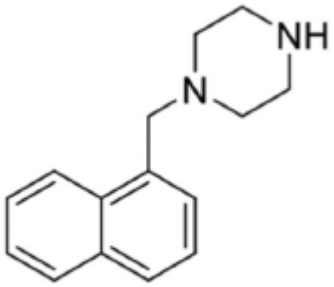

Figure 7. Molecular structure of efflux pump inhibitor 1-(1-Naphthylmethyl)-piperazine (NMP) (Vargiu et al 2014).

AcrB inhibition mechanism of NMP has been studied with MD-simulations in the same study by Vargiu and Nikaido (2012) as the PAβN inhibition mechanism. Based on the MD-simulations, the binding site and proposed inhibition mechanism of NMP were found to be relatively similar to those of PAβN. In one simulation NMP bound to the proximal binding site of AcrB, however, in most simulations NMP interacted with the distal binding site of AcrB as expected. Nevertheless, in all simulations NMP interacted with the tip of the switch loop and straddled it, thus suggesting impaired switch loop movement based inhibition mechanism similar to PAβN. If both NMP and PAβN inhibit the AcrB function by the same switch loop straddling mechanism, it is interesting how there are so evident differences in their effect on the efflux of AcrB substrates. Also, the results of random mutagenesis study done with AcrB overexpressing *E. coli* suggests different binding site for NMP (Schuster et al 2014). The G141D N282Y double mutation in the distal part of the AcrB distal binding site was the only mutation found to reverse the EPI activity of NMP. This double mutation was able to reverse the EPI activity of NMP with linezolid and in some assays with levofloxacin and Hoechst 33342 (H33342) but not with other AcrB substrates. However, none of the mutations was found to reverse the EPI activity of PAβN, indicating difference in the AcrB inhibition mechanisms of these EPIs. All in all, these results by Schuster et al 2014 and Vargiu and Nikaido (2012) seem to suggest different binding sites for these EPIs in the substrate binding sites of AcrB.

For its EPI-effect, NMP has been used at 100 μg/ml concentration while PAβN requires only 25μg/ml concentration (Bohnert and Kern 2005; Kern et al 2006). However, no efflux pump inhibition independent mechanisms, like the outer membrane effect of PAβN, has been found with NMP. The RND substrate specificities of NMP and PAβN differ. NMP increased susceptibility of *E. coli* clinical isolates to ethidium bromide much more effectively than PAβN (Kern et al 2006). On the other hand, PAβN increases susceptibility of *E. coli* more to pyronin Y, clarithromycin and rifampicin compared to NMP. However, the difference in effect on rifampicin and clarithromycin susceptibility may be related to the outer membrane effect of PAβN.

NMP has not been further developed towards use as an EPI-drug, probably because of its likely toxic serotonin agonist properties (Zechini and Versace 2009). It is still widely used as a reagent in RND efflux pump research, like PAβN (Opperman and Nguyen 2015). Thus, activity of NMP has been studied with multiple bacteria and efflux transporters in addition to *E. coli* and AcrB. Panek et al. (2006) showed that NMP had AdeB RND efflux pump dependent and independent effects on AdeB substrate antibiotic susceptibility of *A. baumannii*. NMP and PAβN had clearly different effects on the antibiotic susceptibility of *A. baumannii*. NMP increased susceptibility of *C. coli* and *C. jejuni* to same antibiotics as PAβN (erythromycin and rifampicin), but to lower extent (Hannula and Hänninen 2008). 100µg/ml and 50µg/ml concentrations of NMP and PAβN were used for determining the EPI-effect on the MIC values of antibiotics with *C. coli* and *C. jejuni.* In *V. cholerae* intrinsic MIC of NMP was found to be 600µg/ml and independent of RND pump expression level as in *E. coli* (Bina et al 2009). NMP also increased the susceptibility of *V. cholerae* to the same antibiotics as PAβN with some differences in the susceptibility levels.

2.3.3 D13-9001

Pyridopyrimidine EPI D13-9001 (Figure 8) has been developed by the same researchers as the previously presented PAβN (Nakayama et al 2003a). The initial hit compound leading to the development of D13-9001 was found by high-through put screening of levofloxacin-potentiating compounds in MexAB-OrpM overexpressing *P. aeruginosa* strain in 2003. The initial hit compound had poor physicochemical properties for a drug molecule, which led to optimization regarding its solubility, albumin binding, *in vitro* and *in vivo* efficacy and toxicity (Nakayama et al 2003a; 2003b; 2004a; 2004b; Yoshida et al 2006a; 2006b; 2007). This extensive optimization resulted D13-9001 (Yoshida et al 2007). In lethal pneumonia model with rats, D13-9001 was found to increase susceptibility of *P. aeruginosa* (PAM1020) to aztreonam. D13-9001 was also found to potentiate levofloxacin *in vitro* with MexAB-OrpM overexpressing strain. The lethal dose of D13-9001 for mouse was found to be over 100mg/kg. Later D13-9001 was found to also have EPI activity against AcrB of *E. coli* (Matsumoto et al 2011; Nakashima et al

2013). Unlike PAβN, D13-9001 is not substrate of AcrB or it is very poor one. The intrinsic MIC value of D13-9001 is over 64 μg/ml in wild type *E. coli* and with 32 μg/ml concentration it caused four-fold reduction of ciprofloxacin and erythromycin MICs (Matsumoto et al 2011). The decrease in ciprofloxacin and erythromycin MICs was not seen in *acrB* or *tolC* deleted mutants of *E. coli*.

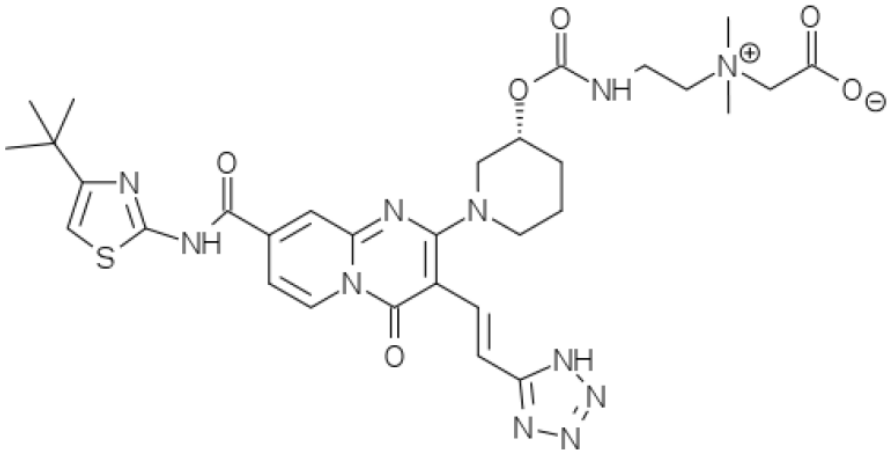

Figure 8. Molecular structure of efflux pump inhibitor D13-9001 (Nakashima et al 2013).

D13-9001 is the first EPI which has been cocrystallized with an RND efflux pump (Nakashima et al 2013). Structures of D13-9001 bound to the close homologs AcrB and MexB were obtained by Nakashima et al in 2013, six years after the development of D13-9001. Based on these X-ray crystallography results, Nakashima et al were able to determine that in both RND efflux pumps D13-9001 binds to the same area in close proximity of the distal binding site. The lipophilic part of D13-9001 binds to a cavity which branches off from the distal binding site (Figure 9). This cavity structure, also called hydrophobic trap, is formed by multiple phenylalanine residues and it doesn't form direct interactions with the efflux pump substrates. The volume of this hydrophobic trap was found to be critical for binding and efflux inhibition effect of D13-9001. The hydrophilic parts of the D13-9001 interact with the hydrophilic side chains of the distal binding site. Based on ITC measurements, D13-9001 binds to AcrB and MexB with high affinity. Binding energy of D13-9001 was found to be around twice the measured binding energies of substrates minocycline and doxorubicin. Based on these results Nakashima et

al (2013) propose that D13-9001 inhibits the efflux mechanism of AcrB by preventing the conformation changes related to the functional rotation mechanism of AcrB.

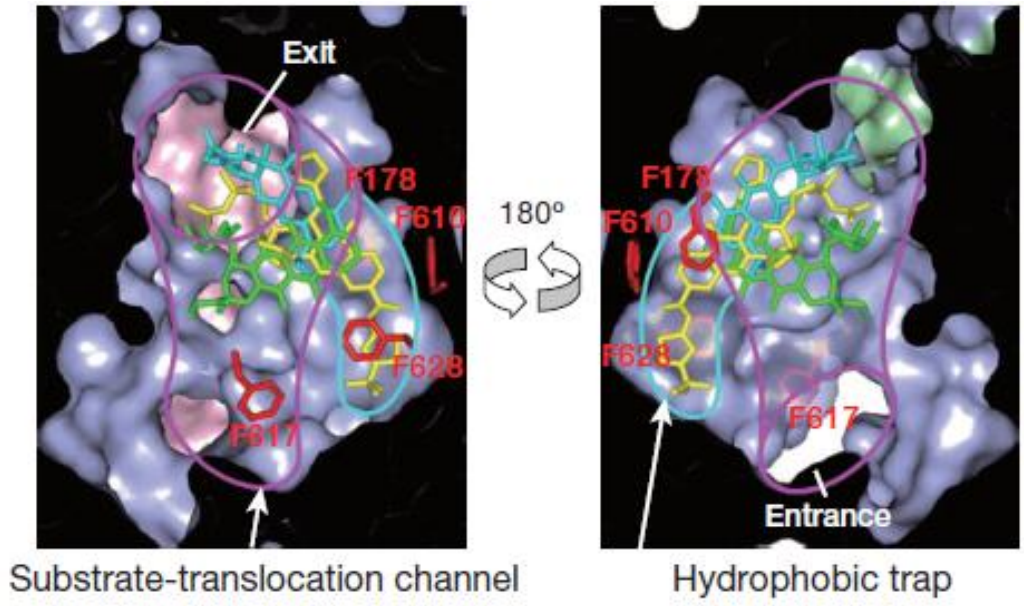

Figure 9. Cutaway view of the distal binding site of AcrB (Nakashima et al 2013). Distal binding site is defined by the violet line and the hydrophobic trap, which branches off from the binding site, is defined by the cyan line. Binding sites of two substrate molecules minocycline (blue) and doxorubicin (green) and inhibitor D13-9001 (yellow) are also shown in the picture.

Although preclinical development of D13-9001 advanced to as far as determination of pharmacokinetic properties with monkeys, this project was still eventually terminated before the clinical stage (Yoshida et al 2007, Aron and Opperman 2018). Reason for the discontinuation was probably the lack of EPI activity against MexY RND efflux pump of *P. aeruginosa* (Yoshida et al 2007). Inactivity against MexY limits the usefulness of this EPI against its original target *P. aeruginosa* (Yaguchi et al 2015). The reason for the inactivity against MexY is the narrower hydrophobic trap of this efflux pump, which causes steric hindrance to D13-9001 binding (Nakashima et al 2013).

2.3.4 MBX2319

Pyranopyridine EPI MBX2319 (Figure 10) was found by screening compounds that act synergistically with ciprofloxacin against *E. coli* (Opperman et al 2014). In the follow-up studies the mechanism turned out to be based on AcrB inhibition. It is clearly the most potent of the EPIs presented by far. In wild type *E. coli* MBX2319 decreased MIC values of ciprofloxacin, levofloxacin and piperacillin 2, 4 and 8 fold with 12.5μM (5.1 μg/ml) concentration. In *tolC* and *acrB* deleted mutants it had no effect at all on ciprofloxacin´s MIC and no over two-fold changes were observed with levofloxacin and piperacillin. The intrinsic MIC value of MBX2319 is over 100 μM (40.95 μg/ml) in wild type and AcrAB-TolC deficient *E. coli* strains. MBX2319 has neither effect on the inner membrane proton gradient nor on the outer membrane permeability of *E. coli*. MBX2319 shows EPI activity also in other members of the *Enterobacteriaceae* family and to some extend in *P. aeruginosa.*

MBX2319 has good drug-like properties regarding molecular weight (409,54), calculated logP (4,03), number of hydrogen bond donors and acceptors (0 and 5), polar surface area (45.49 $Å^2$) and number of rotatable bonds (2) (Opperman et al 2014). However, MBX2319 is very unstable in *in vitro* metabolic assays with human and murine liver microsomes (Nguyen et al 2015). To study the structure-activity relationship and to further optimize the properties of the molecule regarding potency, metabolic stability and water solubility Nguyen et al (2015) prepared a collection of close MBX2319 analogues. One of the synthesized analogues, MBX3135 (Figure 11) shows four-fold reduction in MIC values of levofloxacin and piperacillin in *E. coli* with 0.1 and 0.05 μM concentrations making it over 10 times more potent than MBX2319 and around 500 times more potent than PAβN (Nguyen et 2015; Sjuts et al 2016). MBX3135 also has improved water solubility and metabolic stability *in vitro* compared to the parent compound MBX2319 (Nguyen et 2015). Like MX2319, MBX3135 has no effect on the inner membrane proton gradient and it does not increase outer membrane permeability. Still, results of Sjuts et al (2016) indicate that MBX3135 causes bacterial RND substrate

accumulation also with other mechanism in addition to AcrB inhibition. They suggest that MBX3135 inhibits also other RND pumps of *E. coli*.

AcrB inhibition mechanism of pyranopyridine EPIs has been studied with *in silico* docking, MD-simulations, X-ray crystallography and cryogenic electron microscopy methods (Vargiu et al 2014; Sjuts et al 2016; Wang et al 2017). MD-simulations by Vargiu et al. (2014) predicted that MBX2319 would bind to the hydrophobic trap similarly to D13-9001. However, MBX2319 is a much smaller molecule than D13-9001 and thus it does not reach the distal binding site, like D13-9001, from the hydrophobic trap. Based on the MD-simulations, MBX2319 binds to AcrB with high affinity with the interactions to the residues in the hydrophobic trap forming almost 70% of the affinity. Based on the simulated affinities, MBX2319 binds to AcrB with slightly lower affinity than D13-9001 but with higher affinity than NMP and PAβN. Simulations also suggest that at least one of the inhibition mechanisms of MBX2319 would be based on conformation changes in the distal binding site caused by its high affinity binding to the hydrophobic trap.

In silico results of Vargiu et al (2014) were later confirmed by the X-ray crystallography results of Sjuts et al (2016). Sjuts et al (2016) engineered a soluble version of the periplasmic AcrB (AcrBper). In the AcrBper protein both MBX2319 and MBX3135 bind to the hydrophobic trap. MBX3135 binds to AcrB with even higher affinity compared to MBX2319, which likely explains its higher potency. The AcrAB-TolC inhibition mechanism of another MBX2319 analog MBX3132 (Figure 12) has been studied with cryogenic electron microscopy (Wang et al 2017). The results confirmed that this pyranopyridine EPI also binds to the hydrophobic trap. Interestingly, in the presence of MBX3132 none of the AcrB proteomers took the open conformation and it caused accumulation of the biding conformations in the AcrB trimers. In presence of MBX3132 over 70% of the AcrB trimers were in homological TTT-conformation making the AcrAB-TolC complex non-functional. These results suggest that pyranopyridine EPIs prevent the functional conformation rotation of AcrAB-TolC by trapping proteomers to

the binding conformation. While the pyranopyridine EPIs' inhibition mechanism and *in vitro* activity are relatively well studied they still lack results from *in vivo* experiments.

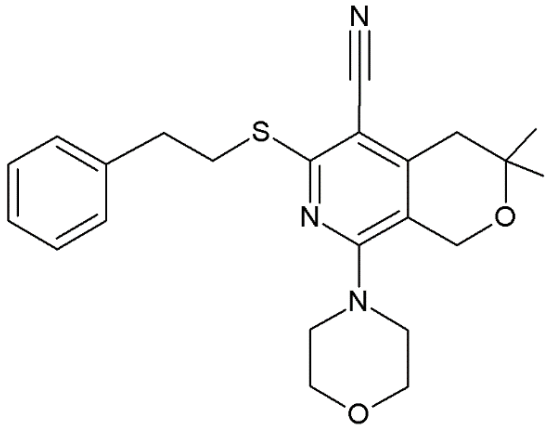

Figure 10. Molecular structure of efflux pump inhibitor MBX2319 (Opperman et al 2014).

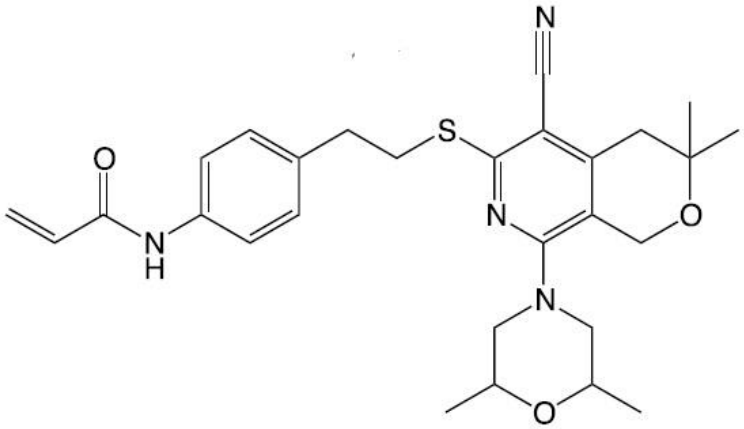

Figure 11. Molecular structure of efflux pump inhibitor MBX3135 (Sjuts et al 2016).

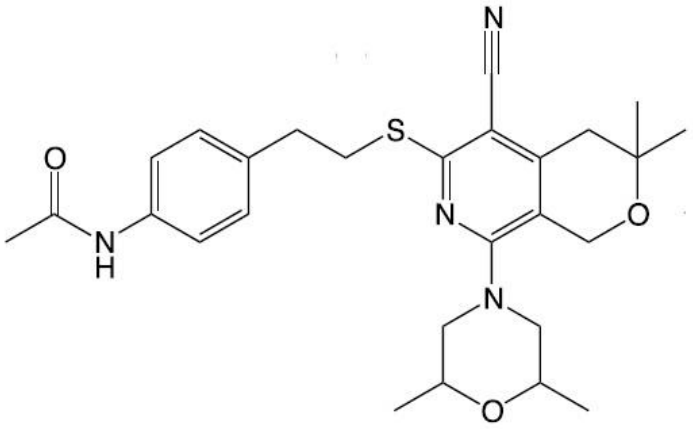

Figure 12. Molecular structure of efflux pump inhibitor MBX3132 (Sjuts et al 2016).

2.3.5 Quinolones

In addition to the above mentioned well characterized EPIs, multiple quinolone derivates have been reported to have EPI activity against the AcrAB-TolC efflux complex. However, the EPI mechanisms of these quinolone derivates have been less studied compared to the above presented EPIs and only by single studies. Results of Vidal-Aroca et al (2009) suggest that mefloquine (Figure 13) inhibits AcrB and MexB RND efflux pumps of *E. coli* and *P. aeruginosa*. Mefloquine causes dose dependent accumulation of AcrB substrate ethidium bromide to wild type *E. coli* with 25 (9.46 μg/ml) and 50 μM (18.92 μg/ml) concentrations.

Results by Mallea et al (2003) suggest that 4-alkylamino quinolones also inhibit AcrB function. The most potent of the studied 4-alkylamino quinolones, called compound 814 **(**Figure 14**)**, causes 16-fold decrease in the MIC value of the AcrB substrate chloramphenicol in *acrAB-tolC* overexpressing *E. aerogenes* strain. Compound 814 causes the 16-fold decrease of chloramphenicol MIC at 200 μM concentration which is one fifth of its intrinsic MIC. Compound 814 causes also chloramphenicol accumulation to *acrAB-tolC* overexpressing *E. aerogenes* strain and decreases MIC values of norfloxacin and tetracyclin.

The third quinolone derivate showing potential EPI activity against AcrB is 4-alkoxy quinolone, called compound 905 (Figure 15**)** by Chevalier et al (2004). Compound 905 is also able to decrease chloramphenicol MIC by 16-fold in *acrAB-tolC* overexpressing *E. aerogenes* strain. Like compound 814, compound 905 increases accumulation of chloramphenicol to *acrAB-tolC* overexpressing *E. aerogenes* strain. Compound 905 had no significant effect on the chloramphenicol MIC value in *tolC* and *acrA* deleted strains, supporting the AcrAB-TolC inhibition mediated mechanism. Unfortunately effects of mefloquine and 4-alkylamino quinolone compound 814 were not studied in AcrB-inactivated strains (Mallea et al 2003; Vidal-Aroca et al 2009). Chevalier et al (2004) studied the effect of compound 905 also on the outer membrane permeability of *E.*

aerogenes, finding out that it has no outer membrane permeabilizing effect. Unfortunately, neither mefloquine's nor compound 814's outer membrane permeabilizing effect and effect on the inner membrane proton gradient were not studied (Mallea et al 2003; Vidal-Aroca et al 2009).

All in all, these quinolone derivates seem to cause intracellular accumulation of AcrB substrate antibiotics and increase susceptibility to them. However, these compounds' exact cellular mechanisms are not clear. The role of different AcrAB-TolC components and other efflux pumps in addition to the possible outer membrane and proton gradient effects should be studied before further conclusions about AcrB inhibition.

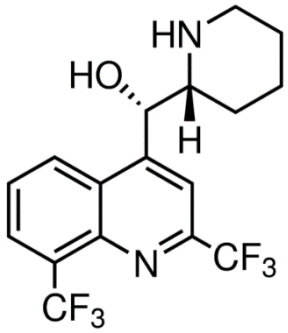

Figure 13. Molecular structure of mefloquine (Merck KGaA 2019a).

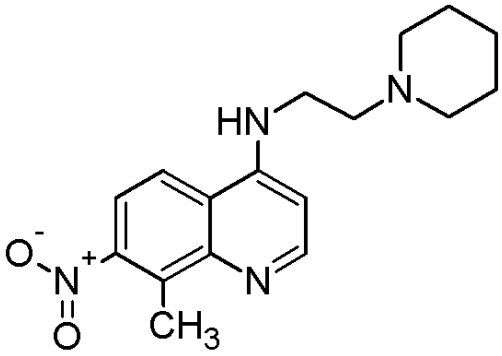

Figure 14. Molecular structure of compound 814 (Mallea et al 2003).

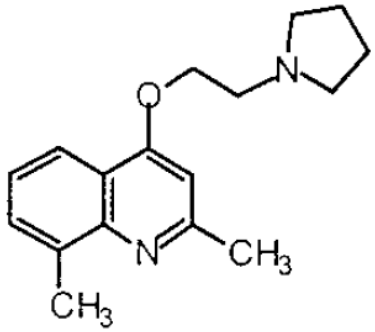

Figure 15. Molecular structure of compound 905 (Chevalier et al 2004).

2.4 Conclusions

Multiple inhibitors of the efflux pump AcrB have been explored and developed since 1999. These EPIs form a chemically diverse group of compounds with a common property of multiple hydrophobic ring structures. Based on *in silico* simulations and *in vitro* results, these EPIs also bind to different areas within the binding pocket of AcrB and have different antibiotic potentiating profiles. Potency of these EPIs has increased dramatically from the early EPIs like PAβN and NMP to the latest MBX-compounds. Still, despite the extensive optimization projects and promising *in vivo* efficacy results, none of these EPIs has reached the stage of drug development where it would have been tested in humans. Nevertheless, EPIs like PAβN and NMP have still turned out to be important tools for RND efflux pump research.

It has to be remembered that antibiotic resistance is a broad worldwide phenomenon mediated by multiple mechanisms. Thus, EPIs alone would not solve this problem as the bacteria have multiple other resistance mechanisms in their arsenal. Still, despite the antibiotic target site mutations, enzymatic inactivation of antibiotics and altered outer membrane porins the EPIs could be a remarkable way to fight the increasing antibiotic resistance among pathogenic GNB. As it is common for multiple antibiotics and antibiotic resistance mechanisms it is possible that effective EPIs created by evolution are still to be found from the nature.

3. OBJECTIVES OF THE EXPERIMENTAL PART

The objective of this thesis' experimental part was to develop and validate an EPI screening method in 384-well plate (384WP) format for screening new EPIs against efflux pumps of *E. coli*. The *E. coli* strain (BAA1161), the positive control EPI (mefloquine) and the antibiotic (piperacillin) for the screening assay were already determined in previous studies by Yrjänheikki (2018). The first objective was to validate and miniaturize the screening assay from the 96-well plate (96WP) to 384WP format. The

second objective was to conduct a few thousand compounds screen with the developed assay to test the newly developed assay and to identify novel EPIs. However, as constant difficulties in the miniaturization process were encountered the size of the EPI screen had to be reconsidered. The inconsistencies of bacterial growth encountered in the plate uniformity and DMSO compatibility assays made a large test screen unreasonable. Thus, it was decided that a dramatically smaller screen would be conducted to test the functionality of developed assay. Steps of the miniaturization process and development of the EPI screening assay are presented in the Figure 16.

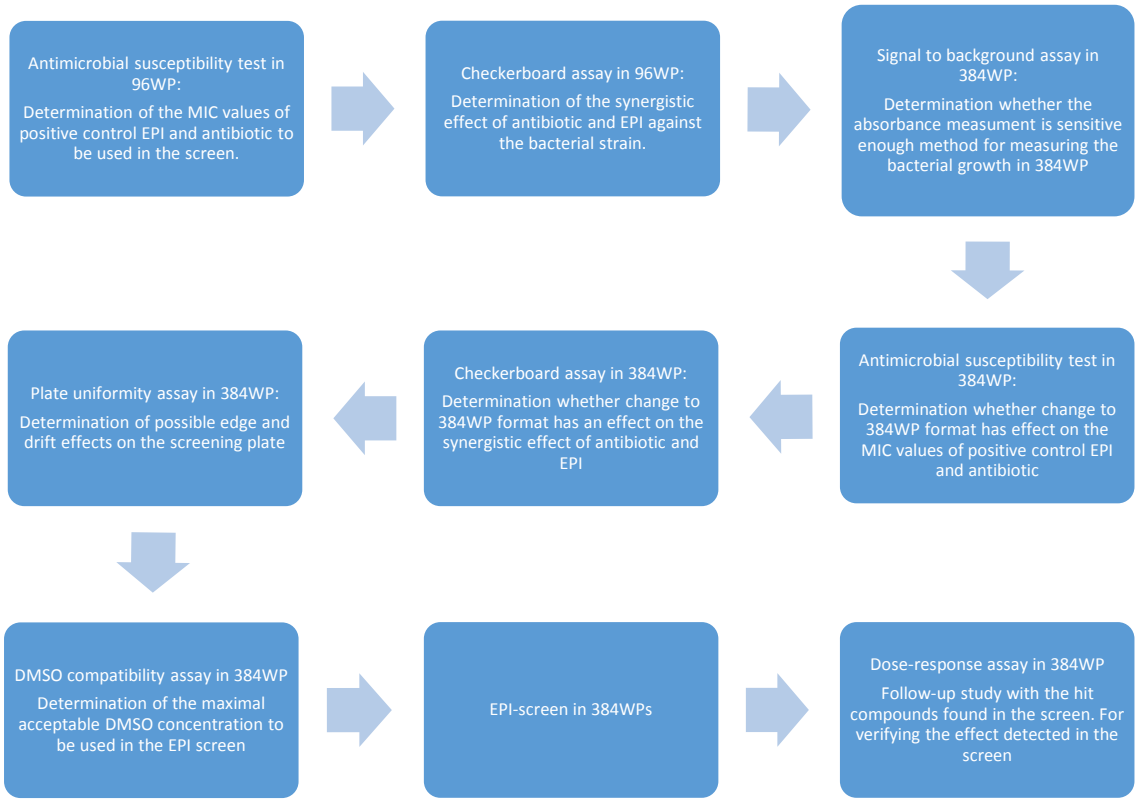

Figure 16. Flow chart of the EPI screening assay development and validation process. The test screen and follow-up assays with the hit molecules are also included.

4. MATERIALS AND METHODS

4.1 Bacterial strains and handling

E. coli BAA1161 was chosen as the bacterial strain to be used in the EPI screening based on the results of Yrjänheikki (2018). In her M. Sc. thesis Yrjänheikki conducted multiple assays including H33342 accumulation (Coldham et al 2010), antibacterial susceptibility (CLSI, 2012) and checkerboard assays (Lomovskaya et al 2001) to define an optimal *E. coli* strain, antibiotic and control EPI to be used in the EPI screening assay. *E. coli* strain BAA1161 was purchased from American Type Culture Collection (ATCC). In addition to BAA1161, *tolC* deleted *E. coli* strain JW5503 was used in the antimicrobial susceptibility assays. *E. coli* BAA1161 was the only bacterial strain used in the other assays. JW5503 was used for confirming the role of efflux pumps for tolerance of antibiotic used in the screening assay. *E. coli* strain JW5503 was obtained from National BioResource Project (Keio collection).

All the experiments and handling of bacteria was performed in level two laminar hoods following aseptic practices with the exception of automated source plate preparation for checkerboard assay with Biomek i7 automated workstation. In all the experiments passage number of bacteria was constant as following protocol of bacterial culture was followed in all the experiments. Main stocks of the bacteria were stored in -80 °C. At least once a month, a monthly bacterial working culture (MWC) was prepared from the main stock on a Mueller-Hinton agar (MHA) plate and was incubated overnight in 37 °C. After overnight incubation in 37 °C MWC was stored in +4 °C and it was used for preparation of weekly bacterial working cultures (WWC). WWC was also prepared on a MHA plate and was incubated overnight in 37 °C before storing in +4 °C. WWC cultures were used for maximum of one week for preparation bacterial overnight cultures (ONC). For the experiments only bacteria from ONCs were used. ONCs were prepared 20h before the experiment on a MHA plate and were incubated in 37 °C. MHA plates were prepared in house. Instead of MHA plates, lysogenic broth (LB) agar slants with 25 µg/ml kanamycin

were used for *E. coli* JW5503 MWCs. LB agar plates with 25 µg/ml kanamycin were purchased from Media Kitchen.

In all the experiments bacterial growth was quantitated by absorbance measurement. A similar protocol for measuring the absorbance was used in all the experiments. Absorbance was measured with Multiskan GO (Thermo Scientific) device at the wavelength of 620 nm and before each measurement 5 seconds agitation was applied to the plate. Experiments in the 96WP format were done in Nunclon Delta Surface (Thermo Scientific) plates and experiments in the 384WP format were done in clear Nunc 384-well polystyrene plates (Thermo Scientific). During the experiments the plates were incubated in a plate thermo-shaker (Biosan) in 37 °C. 96WPs were incubated with 500 rpm agitation and 384WPs without agitation.

In all experiments $5x10^5$ cfu/ml bacterial concentration was used. To do so initial bacterial suspension was prepared from ONC to 0.9% saline solution. Then bacterial concentration of this initial suspension was measured with DEN-1B McFarland Densitometer (Biosan). Based on the measured concentration of initial bacterial suspension, required volume of initial bacterial suspension was diluted with Mueller-Hinton broth (MHB) resulting in $1x10^6$ cfu/ml bacterial suspension. $1x10^6$ cfu/ml bacterial suspension was diluted to final bacterial concentration of $5x10^5$ cfu/ml in all experiments with the treatment solutions.

4.2 Chemicals

Piperacillin (PIP) was chosen to be used as the antibiotic and mefloquine (MEF) was chosen to be used as the positive control EPI in the EPI screening assay, based on the results of Yrjänheikki (2018). MEF and PIP were purchased from Sigma-Aldrich. Dimethyl sulfoxide (DMSO) was produced by VWR international. MHB and MHA were produced by LabM. Saline solution (0.9%) and ultrapure water were prepared in house. All MEF stock solutions were prepared in DMSO following aseptic techniques and stored in -20 °C. All PIP stock solutions were prepared following aseptic techniques in ultrapure

water and filter sterilized with polyether sulfone (VWR International) or cellulose acetate (VWR International) filter. PIP stock solutions were stored in -20 °C.

4.3 Absorbance signal strength assessment in 384-well plate

Absorbance signal strength assessment assay was conducted in 384WP after the antimicrobial susceptibility and checkerboard assays in 96WP format before other assays in 384WP format were conducted. Nevertheless, this assay is reviewed first as the antimicrobial susceptibility and checkerboard assays of both plate formats are reviewed in same sections. Absorbance signal level caused by maximal BAA1161 growth in 384WP was determined, to decide whether the absorbance measurement is sensitive enough method for quantifying the bacterial growth in the 384WP. The assay was performed as follows: to half of the 384WP only 50 µl of MHB with 5% of water and 1% of DMSO was added. These wells represented the background level of absorbance in the wells without bacterial growth. To the other half of the 384WP 25 µl of MHB with 10% of water and 2% of DMSO was added. Which was followed by the addition of 25 µl of $1x10^6$ cfu/ml bacterial suspension. This second half of the plate represented the maximal bacterial growth and absorbance to be measured in the 384WP. Absorbance of the wells was measured at the time points 0, 8 and 24h. From the 24h time point results signal to background and Z-factor were calculated.

4.4 Antimicrobial susceptibility assays for determining the MIC values

MIC values of the antibiotic PIP and EPI MEF were determined to quantitate the intrinsic antibacterial effects of these compounds. Intrinsic antibacterial effects of these compounds had to be determined before the synergistic effect of these compounds could be determined with the checkerboard assay. MIC values of PIP and MEF were determined in both 96 and 384WP formats to see whether the plate format has any effect on the antimicrobial effect of these compounds.

For determining the MIC values of PIP and MEF in 96WP and 384WP formats CLSI's broth microdilution method was followed (CLSI 2012). The concentration which on average caused at least 90% inhibition of bacterial growth, based on the absorbance measurements, was considered as the MIC value. The MIC value was confirmed by two independent experiments. MIC values of PIP and MEF were determined with BAA1161 strain in 96 and 384WP formats. With JW5503 strain only MIC value of PIP was determined in 96WP format. In 96WP format the final volume of well was 200 µl while in the 384WP format it was 50 µl. In both plate formats a total of eight two-fold concentrations were tested. In 96WP there were three replicates of each concentration and in 384WP eight replicates of each concentration. In addition to the test compound wells, maximum growth, absorbance background and edge wells with only MHB were included to the plate layouts. Only MHB was added to the edge wells to prevent an edge effect.

A 200-fold final concentration range stock of MEF in DMSO was prepared and stored in -20 °C on the previous day of the assay with both plate formats. With PIP a 20-fold final concentration range stock was prepared on the previous day of the experiment because of the limited solubility of PIP in water. Other than that, protocol was the same with PIP and MEF in both plate formats. Test compound concentrations and concentration of the bacterial suspension were diluted to the final concentration in the assay with MHB. The tested concentration ranges of the PIP and MEF are shown in Table 1. With 96WP format, absorbance was measured at 0, 4, 8 and 24h time points, however the MIC was determined only based on the time point 24h. With 384WP format, the absorbance was measured only at 0 and 24h time points. Between the time points, 96WPs and 384WPs were incubated in plate thermo-shaker (Biosan) in conditions described above.

Table 1. Concentration ranges used in the antimicrobial susceptibility assays in 96-well plate (96WP) and 384-well plate (384WP) formats for determining MIC values of piperacillin (PIP) and Mefloquine (MEF).

E. coli strain	Plate format	Compound	Concentration range (µg/ml)
JW5503	96WP	PIP	0.5 – 0.25 – 0.125 – 0.0625 – 0.0313 – 0.156 – 0.0078 – 0.0039
BAA1161	96WP	PIP	2048 – 1024 – 512 – 256 – 128 – 64 – 32 – 16
BAA1161	96WP	MEF	64 – 32 – 16 – 8 – 4 – 2 – 1 – 0.5
BAA1161	384WP	PIP	2048 – 1024 – 512 – 256 – 128 – 64 – 32 – 16
BAA1161	384WP	MEF	64 – 32 – 16 – 8 – 4 – 2 – 1 – 0.5

4.5 Checkerboard assays

Checkerboard assays were conducted in 96WP and 384WP formats to verify the synergistic growth inhibition effect of PIP and MEF on *E. coli* BAA1161, as reported by Yrjänheikki (2018). In the checkerboard assay, concentration ranges of two compounds are combined in the assay plate and the effect of concentration combinations on growth inhibition is measured. A total of five checkerboard assays were conducted in 96WP and three were conducted in 384WP. The results of checkerboard assays were also used for deciding the PIP concentration to be used in the EPI screening. In all checkerboard assays absorbance was measured at 0, 4, 8 and 24 hour time points.

In 96WP, two different checkerboard assay layouts with different PIP and MEF concentration ranges were studied. Different concentration ranges of PIP and MEF studied in checkerboard assays are presented in Table 2. Two checkerboard assays with

the same plate layout were conducted completely manually. Then the following three assays with the second layout were conducted partially automatically with Biomek i7. Biomek i7 was used for diluting and dispensing the PIP and MEF solutions on the 96WP. The same Biomek i7 protocol was used by Yrjänheikki (2018). Bacterial suspension was prepared and added to the wells manually in all the checkerboard assays. In the 96WP checkerboard assay there is only one well of each concentration combination. MEF and PIP source plates for the checkerboard assays were prepared on the previous day and were stored in -20°C. Source plates for completely manually conducted 96WP checkerboard assays constituted of 20-fold final concentration of PIP and 100-fold final concentration of MEF. For the partially automated checkerboard assays 40-fold final concentration of PIP and 100-fold final concentration of MEF source plate was prepared. To each well of the 96WP checkerboard assay plate 100 µl of MHB with PIP and MEF and 100 µl of $1x10^6$ cfu/ml bacterial suspension was added. To the edge wells only 200 µl of MHB was added.

In 384WP format, three checkerboard assays were conducted in different plate layouts. The concentration ranges of the assays are presented in the Table 2. Checkerboard assays were conducted in 384WP to find out whether the plate format affects the synergistic effect of PIP and MEF against *E. coli* BAA1161. 384WP checkerboard assay protocol followed 96WP checkerboard assay protocol with minor modifications. All checkerboard assays in 384WPs were conducted completely manually. Like with the 96WP, source plates for the 384WP checkerboard assays were prepared on the previous day to 96WP and were stored at -20°C. PIP and MEF concentrations of the source plates were 20 and 200-fold final concentration. However, unlike in the 96WP, each concentration combination had four replicates in the 384 well checkerboard assay plate, because PIP concentration changed every second column and MEF concentration changed every second row in the assay plate. An additional dilution step between the source plate and the assay plate called the dilution plate was included because of the lower volumes of 384WP. The dilution plate was a 96WP were PIP and MEF concentration combinations were prepared and diluted to two-fold final concentration with MHB. From each well of the dilution plate, 25µl of PIP and MEF combination was added to four wells in the 384 well checkerboard assay plate. Then 25µl of $1x10^6$ cfu/ml bacterial suspension was added

to all of those wells, resulting in a final volume of 50µl. To the edge wells only 50 µl of MHB was added.

Table 2. Summary of the checkerboard assays performed in the 96-well plate (96WP) and 384-well plate (384WP) formats with combination of piperacillin (PIP) and Mefloquine (MEF).

Number of replicate assays	Plate format	PIP concentration range (µg/ml)	MEF concentration range (µg/ml)	Partially automated	Final volume of wells (µl)
2	96WP	2048 – 1024 – 512 – 256 – 128 – 64 – 32 – 16 – 8 – 0	64 – 32 – 16 – 8 – 4 – 0	No	200
3	96WP	1024 – 512 – 256 – 128 – 64 – 32 – 16 – 8 – 4 – 0	16 – 12 – 8 – 6 – 4 – 0	Yes	200
1	384WP	1024 – 64 – 32 - 0	32 – 16 – 12 – 0	No	50
1	384WP	1024 – 64 – 32 – 16 – 0	32 – 16 – 12 – 0	No	50
1	384WP	256 – 0 – 256 – 0 – 256 – 0	16 – 12 – 8 – 6 – 0	No	50

4.6 Plate uniformity assay

After the checkerboard assays in 384WP, the next step in the miniaturization of the EPI screening method was the plate uniformity assay in 384WP. Plate uniformity assays were conducted according to Iversen et al (2012) with minor modifications. Plate uniformity assay was conducted to explore the possible effect of position in the plate on the bacterial growth and absorbance. By using the data of plate uniformity assay in scatter plots edge

and drift effects on the plate could be explored. Thus, the results of plate uniformity assay could be used for optimizing the plate layout for the EPI screen.

The plate uniformity assay is conducted with three types of treatments which result in different signal levels on the plate (Iversen et al 2012). These three treatments, called max, mid and min, should represent different signal levels expected to be measured in the actual screen. The max signal wells represent maximal bacterial growth and absorbance expected to be measured in the actual screen. Thus, only 256 μg/ml PIP and 0.5% DMSO were used for the max signal treatment. For mid signal treatment 256 μg/ml of PIP in combination with 6 or 8 μg/ml MEF was used. The mid signal wells represent bacterial growth and absorbance in presence of PIP and compound with low level of antibacterial or synergistic activity. For the min signal the combination of 256 μg/ml of PIP and 16 ug/ml of MEF was used as this combination was expected to completely inhibit bacterial growth. Thus, this min signal represents the minimal absorbance and complete inhibition of bacterial growth caused by the combination of PIP and compound with a strong antimicrobial or synergistic effect. PIP and MEF concentrations for the max, mid and min were determined based on the 384WP checkerboard assay results.

The plate uniformity assay was conducted using the interleaved signal format (Iversen et al 2012). In the interleaved-signal format the plate uniformity assay consists of three complete 384WPs. In those three assay plates all three treatments (max, mid and min) are tested in all wells of the plate once (Figure 17). However, in total nine plates were eventually prepared because of inconsistent results of mid and max signal. Experiments were carried with varying conditions regarding the bacteria culture time before the assay, MEF concentration in the mid treatment and also with different PIP and MEF stock solutions to track the cause of inconsistency. Absorbance of plates was measured at the time points 0 and 24h with the exception of last assay plate. The absorbance of the ninth plate was measured at eight time points between 0 and 28 hours to determine the lag time of bacterial growth and difference in it between the wells. All the plate uniformity assay plates were prepared at different days. Treatment solutions with two-fold final concentrations were prepared in MHB at the day of the assay. 25μl of two-fold treatment

solutions and 25µl of $1x10^6$ cfu/ml bacterial suspension was added to the wells of plate uniformity assay plate.

Plate 1

Row	C1	C2	C3	C4	C5	C6	C7	C8	C9	C10	C11	C12	C13	C14	C15	C16	C17	C18	C19	C20	C21	C22	C23	C24
1	H	M	L	H	M	L	H	M	L	H	M	L	H	M	L	H	M	L	H	M	L	H	M	L
2	H	M	L	H	M	L	H	M	L	H	M	L	H	M	L	H	M	L	H	M	L	H	M	L
3	H	M	L	H	M	L	H	M	L	H	M	L	H	M	L	H	M	L	H	M	L	H	M	L
4	H	M	L	H	M	L	H	M	L	H	M	L	H	M	L	H	M	L	H	M	L	H	M	L
5	H	M	L	H	M	L	H	M	L	H	M	L	H	M	L	H	M	L	H	M	L	H	M	L
6	H	M	L	H	M	L	H	M	L	H	M	L	H	M	L	H	M	L	H	M	L	H	M	L
7	H	M	L	H	M	L	H	M	L	H	M	L	H	M	L	H	M	L	H	M	L	H	M	L
8	H	M	L	H	M	L	H	M	L	H	M	L	H	M	L	H	M	L	H	M	L	H	M	L
9	H	M	L	H	M	L	H	M	L	H	M	L	H	M	L	H	M	L	H	M	L	H	M	L
10	H	M	L	H	M	L	H	M	L	H	M	L	H	M	L	H	M	L	H	M	L	H	M	L
11	H	M	L	H	M	L	H	M	L	H	M	L	H	M	L	H	M	L	H	M	L	H	M	L
12	H	M	L	H	M	L	H	M	L	H	M	L	H	M	L	H	M	L	H	M	L	H	M	L
13	H	M	L	H	M	L	H	M	L	H	M	L	H	M	L	H	M	L	H	M	L	H	M	L
14	H	M	L	H	M	L	H	M	L	H	M	L	H	M	L	H	M	L	H	M	L	H	M	L
15	H	M	L	H	M	L	H	M	L	H	M	L	H	M	L	H	M	L	H	M	L	H	M	L
16	H	M	L	H	M	L	H	M	L	H	M	L	H	M	L	H	M	L	H	M	L	H	M	L

Plate 2

Row	C1	C2	C3	C4	C5	C6	C7	C8	C9	C10	C11	C12	C13	C14	C15	C16	C17	C18	C19	C20	C21	C22	C23	C24
1	L	H	M	L	H	M	L	H	M	L	H	M	L	H	M	L	H	M	L	H	M	L	H	M
2	L	H	M	L	H	M	L	H	M	L	H	M	L	H	M	L	H	M	L	H	M	L	H	M
3	L	H	M	L	H	M	L	H	M	L	H	M	L	H	M	L	H	M	L	H	M	L	H	M
4	L	H	M	L	H	M	L	H	M	L	H	M	L	H	M	L	H	M	L	H	M	L	H	M
5	L	H	M	L	H	M	L	H	M	L	H	M	L	H	M	L	H	M	L	H	M	L	H	M
6	L	H	M	L	H	M	L	H	M	L	H	M	L	H	M	L	H	M	L	H	M	L	H	M
7	L	H	M	L	H	M	L	H	M	L	H	M	L	H	M	L	H	M	L	H	M	L	H	M
8	L	H	M	L	H	M	L	H	M	L	H	M	L	H	M	L	H	M	L	H	M	L	H	M
9	L	H	M	L	H	M	L	H	M	L	H	M	L	H	M	L	H	M	L	H	M	L	H	M
10	L	H	M	L	H	M	L	H	M	L	H	M	L	H	M	L	H	M	L	H	M	L	H	M
11	L	H	M	L	H	M	L	H	M	L	H	M	L	H	M	L	H	M	L	H	M	L	H	M
12	L	H	M	L	H	M	L	H	M	L	H	M	L	H	M	L	H	M	L	H	M	L	H	M
13	L	H	M	L	H	M	L	H	M	L	H	M	L	H	M	L	H	M	L	H	M	L	H	M
14	L	H	M	L	H	M	L	H	M	L	H	M	L	H	M	L	H	M	L	H	M	L	H	M
15	L	H	M	L	H	M	L	H	M	L	H	M	L	H	M	L	H	M	L	H	M	L	H	M
16	L	H	M	L	H	M	L	H	M	L	H	M	L	H	M	L	H	M	L	H	M	L	H	M

Plate 3

Row	C1	C2	C3	C4	C5	C6	C7	C8	C9	C10	C11	C12	C13	C14	C15	C16	C17	C18	C19	C20	C21	C22	C23	C24
1	M	L	H	M	L	H	M	L	H	M	L	H	M	L	H	M	L	H	M	L	H	M	L	H
2	M	L	H	M	L	H	M	L	H	M	L	H	M	L	H	M	L	H	M	L	H	M	L	H
3	M	L	H	M	L	H	M	L	H	M	L	H	M	L	H	M	L	H	M	L	H	M	L	H
4	M	L	H	M	L	H	M	L	H	M	L	H	M	L	H	M	L	H	M	L	H	M	L	H
5	M	L	H	M	L	H	M	L	H	M	L	H	M	L	H	M	L	H	M	L	H	M	L	H
6	M	L	H	M	L	H	M	L	H	M	L	H	M	L	H	M	L	H	M	L	H	M	L	H
7	M	L	H	M	L	H	M	L	H	M	L	H	M	L	H	M	L	H	M	L	H	M	L	H
8	M	L	H	M	L	H	M	L	H	M	L	H	M	L	H	M	L	H	M	L	H	M	L	H
9	M	L	H	M	L	H	M	L	H	M	L	H	M	L	H	M	L	H	M	L	H	M	L	H
10	M	L	H	M	L	H	M	L	H	M	L	H	M	L	H	M	L	H	M	L	H	M	L	H
11	M	L	H	M	L	H	M	L	H	M	L	H	M	L	H	M	L	H	M	L	H	M	L	H
12	M	L	H	M	L	H	M	L	H	M	L	H	M	L	H	M	L	H	M	L	H	M	L	H
13	M	L	H	M	L	H	M	L	H	M	L	H	M	L	H	M	L	H	M	L	H	M	L	H
14	M	L	H	M	L	H	M	L	H	M	L	H	M	L	H	M	L	H	M	L	H	M	L	H
15	M	L	H	M	L	H	M	L	H	M	L	H	M	L	H	M	L	H	M	L	H	M	L	H
16	M	L	H	M	L	H	M	L	H	M	L	H	M	L	H	M	L	H	M	L	H	M	L	H

Figure 17. Layouts of the plate uniformity assay interleaved-signal format 384-well assay plates (Iversen et al 2012). In the figure, H, M and L stand for max, mid and min absorbance signal levels, respectively.

4.7 DMSO compatibility assay

As the last step before the EPI screen, the DMSO compatibility assay was performed to verify the DMSO tolerance of the *E. coli* BAA1161 in 384WP. DMSO compatibility was tested because the compounds to be screened are dissolved in 100% DMSO. Thus, DMSO compatibility dictates the highest compound concentration that can be used in the screen without effect of DMSO interfering the results.

DMSO tolerance was tested in presence and in absence of 256 μg/ml PIP, because in the actual EPI screen compounds will be screened in combination with 256 μg/ml of PIP. 0; 0.5; 1; 2; 3; 4 and 5% DMSO concentrations were tested in two independent replicate assays. Four replicate wells of each DMSO concentration were included in the assays. The assays were performed as follows: First the solutions with two-fold final DMSO and PIP concentrations were prepared to 96WP. From the 96WP 25μl of each solution was transferred to four replicate wells on the 384WP. Then 25μl of $1x10^6$ cfu/ml bacterial suspension was added to the wells. Absorbance was measured at 0 and 24h time points to determine the effect of DMSO on bacterial growth.

4.8 Test screen

A library consisting of 126 natural compounds (NC) was chosen to be screened with the developed EPI screening assay. Compounds of the collection are presented in the appendix (Appendix 1). In the collection, the compounds are dissolved in DMSO at 10mM concentration. For the screen 50 μM concentration of NCs was used in combination with 256 μg/ml (0.47 μM) PIP. Thus, for the screen a 200-fold dilution from the source plates was needed. The screen was conducted in two 384WPs with four replicates of each NC + PIP combination (Figure 18). In addition to the actual screening wells, 134 control wells were included in both 384WPs. Five types of control wells were included. Control wells with only 50 μl of MHB were located to the plate edges. Maximum bacterial growth wells with final concentrations of 0.5% DMSO and 1.3%

water in MHB were also included. Maximum bacterial growth wells were used for following the bacterial viability and for determining the effect of PIP. PIP effect controls with final concentrations of 256 μg/ml PIP and 0,5% DMSO in MHB were included for determining the antibacterial effect of PIP alone at the screening concentration. As the positive control a combination of 256 μg/ml PIP and 16 μg/ml MEF was used. Based on the checkerboard assay results, this PIP and EPI combination was expected to cause over 90% inhibition of *E. coli* BAA1161 growth. MEF control with 16 μg/ml MEF and 1.3% water in MHB was included to quantify the effect of MEF in the positive controls. Eight replicate wells of each control were added to both screening plates with the exceptions of edge wells and PIP effect controls. In total, 32 PIP effect control wells were added to each plate because of the inconsistencies observed in the previous assays (i.e. plate uniformity and DMSO compatibility assays).

The preparation of screening plates and the actual screening process are described here briefly. Two-fold solution with water and DMSO in MHB was prepared and stored to +4°C on the previous day of the screen. Two-fold PIP effect control, MEF effect control and PIP+MEF positive control solutions were prepared on the screening day. 25 μl of two-fold control solutions were pipetted to the 384WPs according to the plate layout (Figure 18). Next, 50 μl of MHB was pipetted to the edge wells of the screening plates to minimize possible edge effect and as contamination controls. Then, the 200-fold dilution of NCs was done in two steps. First, a 100 fold dilution of NCs was done in two 96 well dilution plates with PIP in MHB, resulting two-fold final concentrations of NC and PIP in MHB. Then, 25 μl of each two-fold NC + PIP solution was pipetted from the dilution plate to four replicate wells in the screening 384WPs. Then, 25 μl of $1x10^6$ cfu/ml bacterial suspension was added to all wells in screening 384WPs with the exception of edge wells. This resulted in the final volume of 50 μl in all screening plate wells. Final concentrations of PIP and NC in the screening wells were 256 μg/ml (0.47 μM) and 50μM. Before the 0h absorbance measurement and incubation, the plates were centrifuged at 1000 rcf for 5min. Absorbance was measured at 0, 20, 24 and 28h time points.

	1	2	3	4	5	6	7	8	9	10	11	12	13	14	15	16	17	18	19	20	21	22	23	24
A	EW	EW	EW	EW	EW	EW	EW	EW	EW	EW	EW	EW	EW	EW	EW	EW	EW	EW	EW	EW	EW	EW	EW	EW
B	EW	MAX	MAX	SW	SW	SW	SW	SW	SW	SW	SW	SW	SW	SW	SW	SW	SW	SW	SW	SW	SW	MAX	MAX	EW
C	EW	MAX	MAX	SW	SW	SW	SW	SW	SW	SW	SW	SW	SW	SW	SW	SW	SW	SW	SW	SW	SW	MAX	MAX	EW
D	EW	MEFC	MEFC	SW	SW	SW	SW	SW	SW	SW	SW	SW	SW	SW	SW	SW	SW	SW	SW	SW	SW	MEFC	MEFC	EW
E	EW	MEFC	MEFC	SW	SW	SW	SW	SW	SW	SW	SW	SW	SW	SW	SW	SW	SW	SW	SW	SW	SW	MEFC	MEFC	EW
F	EW	PIPC	PIPC	SW	SW	SW	SW	SW	SW	SW	SW	SW	SW	SW	SW	SW	SW	SW	SW	SW	SW	PIPC	PIPC	EW
G	EW	PIPC	PIPC	SW	SW	SW	SW	SW	SW	SW	SW	SW	SW	SW	SW	SW	SW	SW	SW	SW	SW	PIPC	PIPC	EW
H	EW	PIPC	PIPC	SW	SW	SW	SW	SW	SW	SW	SW	SW	SW	SW	SW	SW	SW	SW	SW	SW	SW	PIPC	PIPC	EW
I	EW	PIPC	PIPC	SW	SW	SW	SW	SW	SW	SW	SW	SW	SW	SW	SW	SW	SW	SW	SW	SW	SW	PIPC	PIPC	EW
J	EW	PIPC	PIPC	SW	SW	SW	SW	SW	SW	SW	SW	SW	SW	SW	SW	SW	SW	SW	SW	SW	SW	PIPC	PIPC	EW
K	EW	PIPC	PIPC	SW	SW	SW	SW	SW	SW	SW	SW	SW	SW	SW	SW	SW	SW	SW	SW	SW	SW	PIPC	PIPC	EW
L	EW	PIPC	PIPC	SW	SW	SW	SW	SW	SW	SW	SW	SW	SW	SW	SW	SW	SW	SW	SW	SW	SW	PIPC	PIPC	EW
M	EW	PIPC	PIPC	SW	SW	SW	SW	SW	SW	SW	SW	SW	SW	SW	SW	SW	SW	SW	SW	SW	SW	PIPC	PIPC	EW
N	EW	PC	PC	SW	SW	SW	SW	SW	SW	SW	SW	SW	SW	SW	SW	SW	SW	SW	SW	SW	SW	PC	PC	EW
O	EW	PC	PC	SW	SW	SW	SW	SW	SW	SW	SW	SW	SW	SW	SW	SW	SW	SW	SW	SW	SW	PC	PC	EW
P	EW	EW	EW	EW	EW	EW	EW	EW	EW	EW	EW	EW	EW	EW	EW	EW	EW	EW	EW	EW	EW	EW	EW	EW

Figure 18. Layout of the 384-well screening plate used in the efflux pump inhibitor screen. EW stands for edge well, in which only Mueller-Hinton broth (MHB) was added. MAX stands for maximum growth well, in which MHB with 0.5% of DMSO and 1.3% of water was added. MEFC stands for Mefloquine effect (MEF) control well, in which 16 µg/ml of MEF and 1.3% of water in MHB was added. PIPC stands for piperacillin (PIP) effect control well, in which 256 µg/ml of PIP and 0.5% of DMSO in MHB was added. PC stands for positive control well, in which 256 µg/ml of PIP and 16 µg/ml of MEF in MHB was added. SW stands for screening well, in which 50 µM of natural compound and 256 µg/ml of PIP in MHB was added. SWs were in four replicates with the same natural compound. All the wells had the final volume of 50 µl and with the exception of edge wells had the initial *E. coli* BAA1161 concentration of $5x10^5$ cfu/ml.

4.9 Dose-response follow-up study

After the EPI screen with the NCs a dose-response follow-up study was conducted with the NCs that showed promising activity in the screen. Growth inhibition activity of these NCs was determined in combination with and without 256 μg/ml of PIP to verify the activity seen in the screen and to measure the intrinsic antimicrobial activity of NCs. Thus, the results could also be used to assess whether the antimicrobial activity of these NCs is synergistic when combined with PIP. Tested concentration range of the NCs was 0; 12,5; 25; 50; 75 and 100 μM. To each plate three replicate wells of each treatment were included and the assay was repeated once to verify the results.

Briefly, the dose-response assay was performed as follows: 50-fold concentration ranges of the NCs were prepared in DMSO at the previous day and were stored in -20 °C. On the day of the assay, 50μl of MHB was pipetted to the edge wells on the plate. Then, 24μl of MHB was added to the wells where effect of only NCs was studied. To the wells where the combined effect of NCs and PIP was studied, 24μl of MHB with 533.33 μg/ml PIP was added. Then 1μl of NCs was added from the previously prepared 50-fold concentration ranges. Finally, 25μl of $1x10^6$ cfu/ml *E. coli* BAA1161 suspension was added to all but edge wells, resulting in the final volume of 50μl in all the wells.

4.10 Data analysis

Bacterial growth was calculated by subtracting the absorbance of the well at time point 0h from the absorbance of the well at the time point in question. Inhibition of bacterial growth was calculated by dividing the bacterial growth in the well by the average bacterial growth of maximum growth wells and subtracting the quotient from one. Z-factors of antimicrobial activity assays, signal to background assay and the EPI screen were calculated to evaluate the quality of assays. Z-factor (Z) was calculated with the following formula: $Z = 1 - \frac{(3\sigma_{max} + 3\sigma_{min})}{|\mu_{max} - \mu_{min}|}$ (Inglese et al 2007). Signal to background (S:B) in the absorbance signal strength assessment assay was calculated with the following formula:

$S:B = \frac{\mu_{max}}{\mu_{min}}$ In the equations μ stands for mean absorbance and σ for standard deviation of absorbance. In the equations, max stands for maximum bacterial growth controls and min for minimum bacterial growth controls.

5. RESULTS

5.1 Absorbance signal strength assessment in 384-well plate format

Results of the absorbance signal strength assessment in 384WP are presented in the Figure 19. Average absorbance of the maximum bacterial growth wells was 1.00 while the average absorbance of the background absorbance wells was 0.08. The value of Z-factor was 0.88 and the signal to background was 12.77. Based on these results, it was concluded that absorbance measurement is a sensitive enough method for measuring the growth of *E. coli* BAA1161 in 384WP-format. Interestingly, as an indication of edge effect clearly lower *E. coli* growth was observed in the corner wells of the plate.

5.2 Antimicrobial susceptibility assays

MIC values determined in antimicrobial susceptibility assays in the 96WP and 384WP formats are presented in the Table 3. The MIC value of PIP was over 4000 times lower in the *tolC*-deleted JW5503 *E. coli* strain compared to the BAA1161 strain, which was used in the EPI screen. The MIC value of MEF was 32 μg/ml in all antimicrobial susceptibility assays done in both 96WP and 384WP formats. For PIP however, MIC values with four-fold difference were obtained in the replicate assays done in the 384WP format. The MIC value of PIP was also different in the 96WP format compared to the 384WP format results. The Z-factors of the antimicrobial susceptibility assays in the 96WP format were between 0.94 and 0.99. For the assays done in the 384WP format Z-factors were between 0.83 and 0.89.

Background absorbance wells												Maximum bacterial growth wells											
0.07	0.07	0.07	0.08	0.07	0.07	0.08	0.07	0.07	0.07	0.07	0.08	1.09	1.05	1.02	1.00	1.01	1.02	1.00	0.99	1.00	0.98	0.94	0.85
0.07	0.07	0.08	0.08	0.08	0.08	0.08	0.08	0.08	0.08	0.08	0.08	1.08	1.06	1.02	1.01	1.01	1.03	1.02	1.03	1.04	1.04	1.04	0.93
0.08	0.07	0.07	0.07	0.08	0.08	0.08	0.08	0.08	0.07	0.07	0.08	1.06	1.02	0.98	0.99	0.98	0.98	0.98	1.00	0.99	1.00	1.02	0.97
0.08	0.08	0.07	0.08	0.08	0.08	0.08	0.09	0.08	0.07	0.08	0.08	1.03	1.01	0.99	0.98	0.99	0.97	0.99	0.97	1.00	0.99	1.01	1.01
0.08	0.08	0.07	0.08	0.08	0.08	0.09	0.08	0.08	0.08	0.07	0.08	1.03	0.99	0.97	0.98	0.98	0.97	0.96	0.99	0.98	1.00	1.01	1.01
0.08	0.08	0.08	0.08	0.08	0.08	0.08	0.08	0.08	0.07	0.07	0.08	1.03	1.01	0.99	0.98	0.97	0.98	0.98	0.96	0.98	0.99	1.02	1.02
0.08	0.08	0.08	0.08	0.08	0.08	0.08	0.08	0.08	0.07	0.07	0.08	1.04	1.00	0.97	0.98	0.98	0.97	0.98	1.01	0.99	0.97	1.01	1.03
0.08	0.08	0.08	0.08	0.08	0.08	0.08	0.08	0.08	0.07	0.07	0.08	1.04	1.02	1.00	0.98	0.99	0.98	0.99	0.99	0.99	1.00	1.00	1.03
0.08	0.08	0.08	0.08	0.08	0.08	0.08	0.08	0.08	0.08	0.08	0.08	1.05	1.01	0.99	0.98	1.01	0.98	0.97	0.98	0.98	0.99	1.01	1.02
0.08	0.08	0.07	0.08	0.08	0.08	0.08	0.08	0.08	0.08	0.08	0.08	1.05	1.03	1.00	1.00	0.98	1.00	0.98	0.98	0.99	1.00	1.00	1.03
0.08	0.08	0.07	0.08	0.08	0.08	0.08	0.08	0.08	0.08	0.08	0.08	1.07	0.99	0.99	0.99	0.99	0.95	0.95	1.02	0.98	1.00	0.99	1.00
0.09	0.08	0.08	0.07	0.08	0.08	0.08	0.08	0.08	0.07	0.08	0.08	1.05	1.01	0.98	1.00	0.98	0.96	0.99	1.00	1.01	0.98	0.99	0.99
0.08	0.08	0.08	0.08	0.08	0.08	0.09	0.08	0.08	0.07	0.08	0.09	1.07	1.03	1.02	1.01	1.01	0.99	0.98	1.00	1.01	1.00	1.00	0.99
0.08	0.08	0.08	0.08	0.08	0.08	0.08	0.08	0.09	0.08	0.08	0.08	1.09	1.04	1.02	1.03	1.01	1.02	1.02	1.01	1.00	1.00	1.03	0.96
0.08	0.08	0.08	0.08	0.08	0.09	0.08	0.08	0.09	0.08	0.08	0.08	1.12	1.06	1.05	1.04	1.07	1.03	1.03	1.03	1.03	1.04	1.01	0.93
0.08	0.07	0.07	0.07	0.09	0.08	0.08	0.08	0.08	0.07	0.07	0.08	1.07	1.02	1.01	1.00	0.98	0.98	0.98	0.98	0.98	0.96	0.93	0.86

Figure 19. Heat map presentation of the absorbance signal strength assessment plate. Separate color scaling was used for the two halves of the plate because of the drastic signal strength difference. Values presented in the figure are raw absorbance (620nm) values of the 24h measurement. Background absorbance wells constituted of 50 µl of Mueller-Hinton broth with 5% of water and 1% of DMSO. Maximum bacterial growth wells had initial bacterial concentration of $5x10^5$ cfu/ml and constituted of 50 µl of Mueller-Hinton broth with 5% of water and 1% of DMSO.

Table 3. Determined MIC values of piperacillin (PIP) and mefloquine (MEF) in 96- (96WP) and 384-well plate (384WP) formats. Results are from two independent experiments in triplicate. With the exception of PIP's MIC value in 384WP format, the same MIC values were obtained with the replicate assays.

Strain	Plate format	Compound	MIC value (μg/ml)
JW5503	96WP	PIP	0.25
BAA1161	96WP	PIP	1024
	96WP	MEF	32
	384WP	PIP	512—2048*
	384WP	MEF	32

*Replicate assays' results were 2048 and 512 μg/ml.

5.3 Checkerboard assays

Results of the three replicate checkerboard assays done in the 96WP format are presented in the Tables 4A and B. Results of the two other checkerboard assays done in the 96WP format with different MEF concentration range (two-fold) are presented in Appendix 2. The synergistic effect of PIP and MEF on the *E. coli* BAA1161 growth inhibition can be seen in the results of 96WP checkerboard assays. However, high variation in the growth inhibition level is seen with the concentration combinations which are in MIC value threshold. High variation in the growth inhibition level was observed especially with the following combinations: 256 μg/ml PIP + 6, 8 and 12 μg/ml MEF (Appendix 2 and 3). Nevertheless, constant over 90% growth inhibition was observed with the 256 μg/ml PIP + 16 μg/ml MEF combination.

Results of the checkerboard assay done in the 384WP format with 256 μg/ml PIP concentration is presented in Figure 20. Results of the two other checkerboard assays done in the 384WP format are presented in the appendix (Appendix 4). Compared to the 96WP checkerboard assays growth inhibition caused by 256 μg/ml of PIP was constantly higher in 384WP. However, similar to the 96WP format, growth inhibition caused by 256 μg/ml PIP + 6 and 8 μg/ml MEF was inconsistent. Variation of growth inhibition with

those concentration combinations was polarized as either over 95% inhibition or similar inhibition levels as with only 256 µg/ml PIP were measured with those PIP + MEF concentration combinations. Growth inhibition caused by 256 µg/ml PIP and 256 µg/ml PIP + 16 µg/ml MEF combination was considered consistent enough to move to the next assays.

Table 4. Average (A) and standard deviation (B) of *E. coli* BAA1161 growth inhibition (%) measured in the three 96-well plate format replicate checkerboard assays. Results are from three independent experiments at time point 24h.

Growth inhibition (%)

A

Mefloquine (µg/ml) \ Piperacillin (µg/ml)	1024	512	256	128	64	32	16	8	4	0
0	95	41	9	6	5	3	3	4	4	0
4	99	48	16	9	6	12	5	8	7	4
6	98	51	25	14	7	7	8	9	7	6
8	99	99	53	18	12	9	12	12	11	8
12	99	98	78	77	61	41	25	26	23	22
16	99	99	99	99	99	99	58	43	44	40

Standard deviation of growth inhibition

B

Mefloquine (µg/ml) \ Piperacillin (µg/ml)	1024	512	256	128	64	32	16	8	4	0
0	4.4	24.1	8.8	4.5	3.4	1.0	1.1	1.9	1.7	0.0
4	0.9	24.2	8.3	4.2	3.4	9.4	2.5	3.6	3.1	2.4
6	1.0	22.7	6.8	5.5	1.1	2.3	2.1	2.7	2.4	2.7
8	0.7	0.7	33.8	7.3	3.0	1.8	2.3	3.6	5.2	3.7
12	0.3	0.2	28.8	31.0	26.3	18.0	5.9	2.7	5.8	4.2
16	0.6	0.5	0.4	0.3	0.2	0.4	28.7	1.9	4.1	4.9

Piperacillin (µg/ml)

Mefloquine (µg/ml)	0	0	256	256	0	0	256	256	0	0	256	256	0	0
0	0	0	38	45	-1	-1	44	35	-2	-1	30	30	0	0
0	1	-1	57	43	1	1	53	41	3	0	42	41	1	-1
6	8	8	99	45	9	9	100	42	10	8	32	100	8	8
6	9	8	100	49	12	11	96	100	11	12	100	44	9	8
8	16	18	100	100	16	18	100	51	17	15	100	100	16	18
8	12	11	100	48	15	13	100	49	16	13	100	100	12	11
12	12	11	100	100	12	13	100	100	13	10	100	100	12	11
12	11	15	100	100	15	18	100	100	13	18	100	100	11	15
16	34	28	100	100	14	12	100	100	17	22	100	100	34	28
16	22	10	100	100	13	11	100	100	12	13	100	100	22	10

Figure 20. *E. coli* BAA1161 growth inhibition (%) results at time point 24h of the checkerboard assay conducted in the 384-well plate format.

5.4 Plate uniformity assay

In the plate uniformity assay, inconsistent bacterial growth was measured in mid or in mid and max treatment wells of all the plates with the exception of one plate (Appendix 5, Figure 1). As an example of observed inconsistency, results of one plate uniformity assay plate are presented in the Figure 21. Results of the other plate uniformity assay plates are presented in Appendix 5. Inconsistent and drastic variation between complete inhibition of growth and similar growth level as observed in the max wells was observed in the mid wells. However, this was basically expected as similar phenomenon was already observed in the checkerboard assays. Surprisingly, complete inhibition of bacterial growth was observed also in few max growth wells. This randomly occurring over 90% growth inhibition caused by 256 µg/ml PIP had not been encountered in the previous assays. It was observed with varying frequency in seven of the nine plate uniformity assay plates. Change in the bacterial culture time before the assay, in MEF concentration of the mid treatment and new compound stock solutions did not eliminate the inconsistency regarding the bacterial growth in the mid and max treatment wells. In

the last plate uniformity assay plate it was observed that lag time of bacterial growth varied substantially between the wells of same treatment (Appendix 5, Figures 8a-8e).

Unlike the mid and max treatment wells, the results of min treatment wells were consistent throughout the nine plate uniformity assay plates. Thus, it was decided that screening assay development would be continued, as the observed inconsistency in the mid and max treatment wells indicates only increased risk of false positive hits in the screen. However, because of these inconsistencies it was decided that only a small collection of NCs would be screened with four replicate wells to test the developed screening method. Unfortunately, results of the plate uniformity assay could not be used for their original purpose of optimizing the screening plate layout because of the inconsistencies in results.

5.5 DMSO compatibility assay

The growth inhibition effect of DMSO on *E. coli* BAA1161 in absence of PIP is shown in the Figure 22. DMSO concentrations up to 3% had no inhibitory effect on growth of *E. coli* BAA1161. Thus, it was decided that the screen could be conducted with up to 3% DMSO concentration. Results regarding the growth inhibition effect of DMSO in presence of PIP could not be used because of the inconsistencies in results. Similar to the plate uniformity assay, over 90% inhibition of growth was observed in some random wells with 256 µg/ml PIP. Results of the two independent DMSO compatibility assays are presented in Appendix 6.

MID	MIN	MAX	MID	MIN	MAX	MID	MIN	MAX	MID	MIN	MAX	MID	MIN	MAX	MID	MIN	MAX	MID	MIN	MAX	MID	MIN	MAX
-0.01	-0.01	0.84	0.73	0.00	0.80	0.38	-0.01	0.81	0.00	0.00	0.78	0.00	0.00	0.85	0.00	0.00	0.78	0.78	0.00	0.00	0.49	0.00	0.85
0.00	0.00	0.77	0.00	0.00	0.78	0.76	0.00	0.73	0.74	0.00	0.76	0.71	0.00	0.73	0.00	0.00	0.64	0.00	0.00	0.74	0.00	0.00	0.82
0.66	0.00	0.00	0.00	0.00	0.62	0.09	0.00	0.69	0.00	0.00	0.70	0.00	0.00	0.00	0.59	0.00	0.75	0.44	0.00	0.30	0.67	0.00	0.80
0.00	0.00	0.66	0.72	0.00	0.76	0.72	0.00	0.63	0.57	0.00	0.67	0.00	0.00	0.79	0.42	0.00	0.73	0.62	0.00	0.74	0.78	0.00	0.80
0.00	0.00	0.00	0.52	0.00	0.77	0.65	0.00	0.71	0.69	0.00	0.71	0.72	0.00	0.82	0.73	0.00	0.65	0.51	0.00	0.80	0.75	0.00	0.79
0.71	0.00	0.72	0.00	0.00	0.70	0.68	0.00	0.71	0.00	0.00	0.75	0.00	0.00	0.76	0.00	0.00	0.76	0.68	0.00	0.74	0.00	0.00	0.85
0.73	0.00	0.71	0.00	0.00	0.55	0.67	0.00	0.73	0.00	0.00	0.76	0.70	0.00	0.69	0.64	0.00	0.80	0.00	0.00	0.62	0.00	0.00	0.74
0.68	0.00	0.72	0.02	0.00	0.74	0.00	0.00	0.74	0.74	0.00	0.68	0.68	0.00	0.59	0.00	0.00	0.63	0.00	0.00	0.77	0.00	0.02	0.72
0.00	0.00	0.71	0.00	0.00	0.75	0.74	0.00	0.90	0.73	0.00	0.76	0.73	0.00	0.81	0.68	0.00	0.71	0.78	0.00	0.85	0.63	0.00	0.85
0.57	0.00	0.78	0.75	0.00	0.76	0.71	0.00	0.76	0.73	0.00	0.72	0.00	0.00	0.94	0.64	0.00	0.67	0.68	0.00	0.80	0.00	0.00	0.76
0.57	0.00	0.77	0.00	0.00	0.75	0.00	0.00	0.80	0.69	0.00	0.78	0.69	0.00	0.77	0.79	0.00	0.76	0.00	0.00	0.78	0.65	0.00	0.83
0.00	0.00	0.77	0.72	0.00	0.78	0.00	0.00	0.74	0.45	0.00	0.68	0.69	0.01	0.89	0.45	0.00	0.67	0.00	0.00	0.76	0.62	0.00	0.80
0.91	0.00	0.78	0.00	0.00	0.71	0.00	0.00	0.84	0.00	0.00	0.80	0.00	0.00	0.80	0.00	0.00	0.46	0.00	0.00	0.79	0.00	0.00	0.71
0.66	0.00	0.44	0.73	0.00	0.74	0.67	0.00	0.77	0.00	0.00	0.71	0.62	0.00	0.75	0.67	0.00	0.77	0.00	0.00	0.66	0.53	0.00	0.80
0.00	0.00	0.95	0.54	0.00	0.66	0.00	0.00	0.76	0.00	0.00	0.74	0.70	0.00	0.78	0.00	0.00	0.73	0.00	0.00	0.79	0.30	0.00	0.66
0.00	0.00	0.74	0.40	0.00	0.80	0.75	0.00	1.00	0.56	0.00	0.78	0.74	0.00	0.73	0.00	0.00	0.81	0.00	0.00	0.72	0.00	0.00	0.86

Figure 21. Heat map presentation of the bacterial (*E. coli* BAA1161) growth in the sixth plate uniformity assay plate at 24h measurement. The treatment of each column is presented above it in the figure. The treatments were: MAX: 256 µg/ml piperacillin, MID: 256 µg/ml piperacillin + 6 µg/ml mefloquine, MIN: 256 µg/ml piperacillin + 16 µg/ml mefloquine. Initial bacterial concentration of all the wells was $5x10^5$ cfu/ml. Inconsistency of mid and max treatment wells is well represented in this plate. There are four max treatment wells without bacterial growth and growth in the mid treatment wells is varying between zero and max level growth.

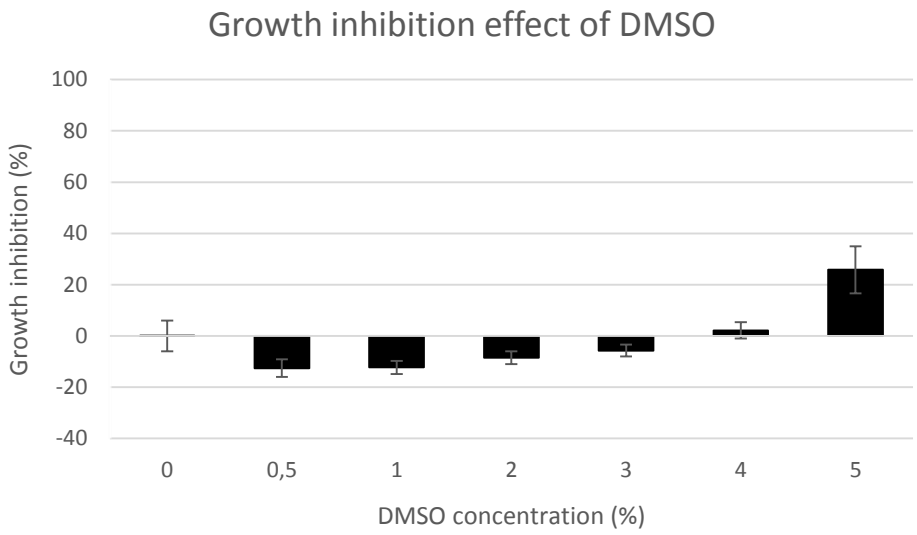

Figure 22. Average bacterial growth inhibition effect (± standard deviation) of the seven DMSO concentrations. Data was obtained from two individual assays with four replicates of each treatment in both.

5.6 Efflux pump inhibitor screen

The growth inhibition levels of NCs, presented in this section, were derived by subtracting the growth inhibition effect of PIP from the growth inhibition caused by NC + PIP combination, based on the PIP effect controls. Complete growth inhibition results of both screening plates at time point 24h are presented in Appendix 7. Of the 126 screened NCs four were found to have promising growth inhibition effect and were considered as hits. Properties and screening results of those four NCs are presented in the Table 5. Molecular structures of the four hit compounds are presented in Figures 23-26. Three of the four hit compounds had relatively consistent growth inhibition effect in all four replicate wells. However, the growth inhibition percentages of one hit compound, Isopropyl gallate (IG), were varying between -1.6 and 100% in the replicate wells, indicating possibility of false positive hit, resulting from the inconsistent growth inhibition caused by 256 µg/ml PIP. In the two screening plates total of seven wells (1.4% of the screening wells) with growth inhibition percentages between 75 and 100% were considered to be caused by the inconsistent effect of 256 µg/ml PIP. That conclusion was made based on the fact that in those seven wells multiple times higher growth inhibition was measured in one well compared to the three other replicate wells. Occurrence of

random extremely high growth inhibition values was expected because the same phenomenon was encountered in the plate uniformity and DMSO compatibility assays with PIP. Z-factors of the screening plates were 0.95 at the 24h time point.

Table 5. Summary of the screening results and properties of the four hit natural compounds found with the screen.

Code	Name	Inhibition (%)*	Standard deviation	Molecular weight (g/mol)	Concentration (µg/ml)
NC43	(-)-Epigallocatechin gallate	33	1.5	458.37	22.92
NC54	Hamamelitannin	30	5.8	484.37	24.20
NC66	Isopropyl gallate	52	37.5	212.21	10.61
NC84	Octyl gallate	45	4.2	282.34	14.12

*Growth inhibition effect of natural compound was calculated by subtracting piperacillin's effect from the growth inhibition effect of piperacillin + natural compound combination, based on the piperacillin effect controls of the screen.

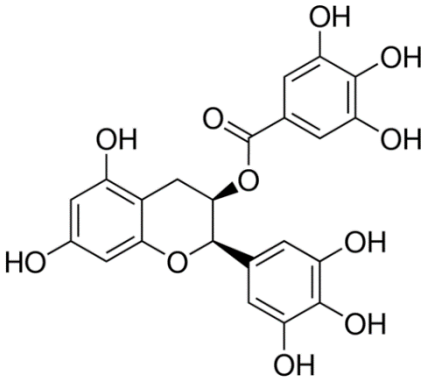

Figure 23. Molecular structure of the epigallocatechin gallate (Merck KGaA 2019b).

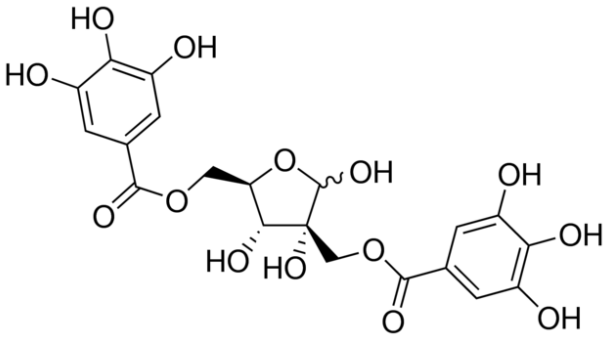

Figure 24. Molecular structure of hamamelitannin (Merck KGaA 2019c).

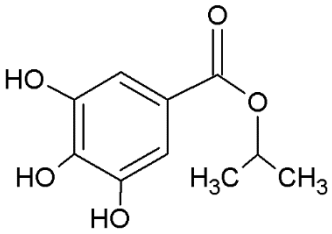

Figure 25. Molecular structure of isopropyl gallate (Narwal et al 2012).

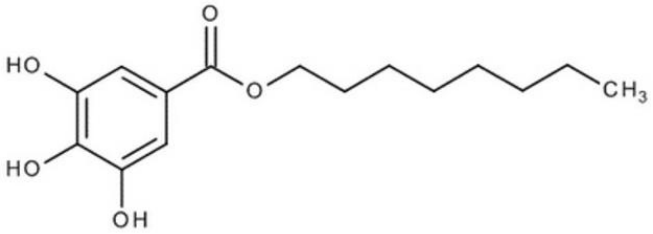

Figure 26. Molecular structure of octyl gallate (Merck KGaA 2019d)

5.7 Dose-response assay

Two of the four hit compounds, Hamamelitannin (HT) and Octyl gallate (OG) had promising results also in the first dose-response assay. Results of the first dose-response assay are presented in the Figure 27. When 100µM of HT was combined with 256 µg/ml PIP it resulted on average 94% growth inhibition. Separately the same concentrations of PIP and HT resulted growth inhibition levels of only 44% and 9%. OG caused an average growth inhibition of 100% with 75µM concentration when combined with 256 µg/ml PIP, but the growth inhibition caused by the 75µM OG alone was only 15%. Thus, these results indicate synergistic *E. coli* BAA1161 growth inhibition effect for HT and OG when combined with PIP.

Unfortunately, the results of the second dose-response assay could not be used for evaluating the effect of NCs when combined with PIP because of the similar inconsistencies as encountered in the plate uniformity assay, DMSO compatibility assay and in the EPI screen (Appendix 8). Random over 97% growth inhibition was measured only in the wells were effect of NC was studied in combination with 256 µg/ml PIP. Results of the wells with only NC were similar to the first assay's results. Based on these

assays, the four hit NCs possess only poor intrinsic antibacterial activities. The MIC values of Epigallocatechin gallate (EGCG), HT, IG and OG are all over 100µM. In fact, the highest measured intrinsic growth inhibition level of these NCs was 20% with 100µM concentration of OG.

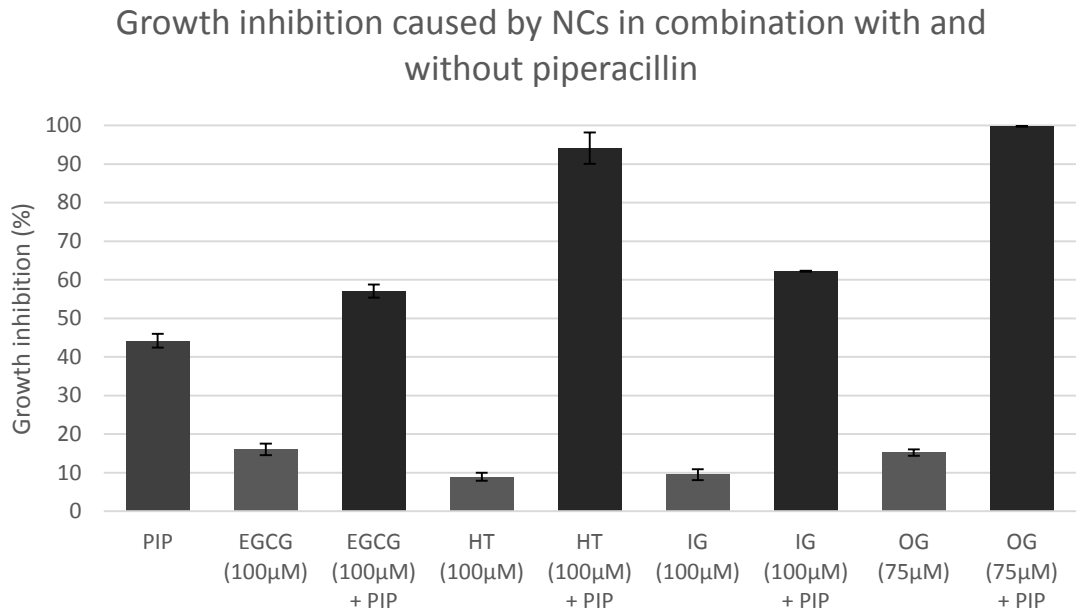

Figure 27. Average bacterial growth inhibition effect (± standard variation) of the natural compounds in combination with and without 256 µg/ml piperacillin (PIP). Experiment was performed once in triplicates. Natural compounds included in the experiment are Epigallocatechin gallate (EGCG), Hamamelitannin (HT), Isopropyl gallate (IG) and Octyl gallate (OG). Synergistic nature of HT's (100µM) and OG's (75µM) bacterial growth inhibition effect is observed when combined with piperacillin.

6. DISCUSSION

The experimental part of this thesis was a continuation of the EPI screening method development started by Yrjänheikki (2018) in her M. Sc. thesis. *E. coli* strain (BAA1161), antibiotic (piperacillin) and the positive control EPI (mefloquine) for the EPI screening assay were chosen based on her results. The *E. coli* strain BAA1161 was chosen based on H33342 accumulation assay results and its role as a clinically relevant uropathogenic strain. In the H33342 accumulation assay, median intracellular accumulation of H33342

was most increased in BAA1161 of the tested *E. coli* strains with all the EPIs tested, when the accumulation was compared to results without EPI. Thus, the results of H33342 accumulation assay suggest that *E. coli* strain BAA1161 has high efflux pump activity which can be suppressed with EPIs. PIP was chosen as the antibiotic for the screen as of the four tested antibiotics its MIC value decreased the most in the *tolC* deleted strain (JW5503) when compared to its parental strain (BW25113). PIP's MIC value for the BAA1161 strain was also above CLSI's MIC-breakpoint for resistance, which is 128 μg/ml, and in the checkerboard assay EPI MEF caused a two-fold reduction in PIP's MIC value with a sub-inhibitory concentration (CLSI 2018, Yrjänheikki 2018). All in all, results of Yrjänheikki (2018) indicate that efflux pumps play a substantial role in PIP resistance of BAA1161 making it good antibiotic for the EPI screening assay. MEF was chosen as the positive control EPI for the screen also based on the H33342 accumulation assay results (Yrjänheikki, 2018). MEF caused the highest median intracellular H33342 accumulation of the tested EPIs in all of the tested *E. coli* strains with the exception of JW5503.

Determined MIC values of MEF and PIP and the results of the checkerboard assays were mostly in line with the results of Yrjänheikki (2018), as expected. The determined MIC value of MEF was the same in both plate formats and the same as was determined by Yrjänheikki. In 96WP format, MIC value of PIP differed two-fold when compared to Yrjänheikki's results which, however, is still considered acceptable level of reproducibility by CLSI (Yrjänheikki, 2018; CLSI, 2012). The synergistic effect of PIP and MEF observed in the 96WP checkerboard assays was also relatively similar to results of Yrjänheikki (2018). Similarity in the results of these repeated assays verifies the determined susceptibility and synergy levels. It is important as the later stages of EPI screening method development are based on those results. Reproducibility by different persons is also important for the reliability of the method.

Based on the results of antimicrobial susceptibility and checkerboard assays, a PIP concentration of 256 μg/ml was chosen to be used in the screen in combination with the screen NCs. This concentration was also recommended by Yrjänheikki (2018) in her

thesis. 256 μg/ml was the highest PIP concentration which never caused MIC-level of growth inhibition in experiments done in 96WP format or in the experiments conducted by Yrjänheikki (2018). In the checkerboard assays, a MEF concentration two-fold lower than the MIC consistently caused a growth inhibition level of over 90% when combined with 256 μg/ml PIP. Thus, 256 μg/ml was considered as a PIP concentration which with also less potent EPIs could be detected without false positives.

However, persistent inconsistencies were later encountered with 256 μg/ml PIP. Inconsistency in bacterial growth inhibition effect of 256 μg/ml PIP was observed in all the assays conducted in 384WP format. In 384WP checkerboard assay the highly polarized variation in the growth inhibition was encountered for the first time. Only less than 51% and over 95% growth inhibition values were measured with 256 μg/ml PIP + 6 and 8 μg/ml MEF combinations. This polarized variation in the growth inhibition was then observed in all the following assays where growth inhibition effect of PIP was measured in 384WP format.

These inconsistent results with 256 μg/ml PIP could be resulting from hetero resistance of *E. coli* BAA1161 strain against PIP. Antimicrobial hetero resistance has been defined as a "phenomenon where subpopulations of seemingly isogenic bacteria exhibit a range of susceptibilities to a particular antibiotic" (El-Halfawy and Valvano 2015). Mechanisms causing the hetero resistance can be genetic, epigenetic and even non-genetic. Hetero resistance seems to usually result in bacterial subpopulations that can grow in antibiotic concentrations substantially above MIC. However, in this case the situation seemed to be the opposite as the sub-MIC PIP concentration was causing inconsistent over 90% bacterial growth inhibition in some wells. Nevertheless, a similar phenomenon has also been encountered when polymyxin B susceptibility of clinical *E. cloacae* and *E. aerogenes* isolates was studied (Landman et al 2013). In antimicrobial susceptibility assays some of the *E. clocae* and *E. aerogenes* isolates showed no visible growth in multiple wells with polymyxin B concentration lower than in wells where growth inhibition was not observed. *E. clocae* and *E. aerogenes* isolates contained subpopulations which were causing antibiotic hetero resistance.

But why the inconsistencies in growth inhibition effect of PIP were observed only in the 384WP format? This might be just because of the lower number of replicate wells in 96WP and lower number of assays conducted with 96WP format. However, as Yrjänheikki (2018) did not encounter similar inconsistencies in her experiments, which were all conducted in 96WP format, it seems more likely that inconsistencies are related to the 384WP format. Reason could be the size of bacterial inoculum. The same bacterial concentration was used in the experiments conducted in the 96WP and 384WP formats. Thus, the initial amount of bacterial cells in the wells was a four-fold lower in 384WP format compared to 96WP format. Possibly, in some wells of 384WP this smaller bacterial population did not survive the lag phase before start of bacterial growth in presence of 256 μg/ml. Substantial differences in the duration of lag phase were observed in wells with 256 μg/ml PIP in the plate uniformity assay (Appendix 5, Figures 8a-8e). The second theory is, that the used *E. coli* BAA1161 strain has a small subpopulation which is able to grow in presence of 256 μg/ml PIP while the main population is more susceptible to PIP. Then, when a four-fold lower initial amount of bacteria is used in higher number of replicate wells in 384WP format the probability of not adding bacteria belonging to the subpopulation to some of the wells is increased. These wells would then be seen as random wells without bacterial growth. The possibility of subpopulations could be studied by growing of BAA1161 cells on agar plates with 256 μg/ml PIP.

The latest experiments performed in the laboratory also support the hypothesis that the lower initial amount of bacteria in the wells is related to the inconsistent growth inhibition effect of PIP in the 384WP format (data not shown). No random over 90% growth inhibition values were measured when the effect of 256 μg/ml PIP on growth of *E. coli* BAA1161 was studied in 384WP format with the initial bacterial concentration of $2x10^6$ cfu/ml. However, when the same initial bacterial concentration ($5x10^5$ cfu/ml) was used as in the 96WP format similar inconsistencies in the bacterial growth inhibition were observed as in the plate uniformity assay, DMSO compatibility assay, dose-response assay and EPI screen of this thesis.

The screening method was miniaturized to 384WP format despite the additional work that the miniaturization process causes, because of the multiple benefits of the 384WP format. Compared to a similar assay in 96WP format lower volumes of reagents can be used in the 384WP format. Also more compounds can be screened in one plate with the miniaturized assay. Thus, the miniaturization of an assay can result in lower reagent costs, increased throughput and decreased requirement for plate incubation space. However, in this case optimization of bacterial inoculum size should have been included in the miniaturization process of the screening assay. Inoculum size optimization was neglected as CLSI's standard concentration of $5x10^5$ cfu/ml has been used in similar previously conducted assays. For instance, Chase et al (2016) used $5x10^5$ cfu/ml concentration of *E. cloacae* and *Acinetobacter* species in antimicrobial synergy assay in 384WP format with the final volume of 60µl. Also Miyasaki et al. (2013) used $5x10^5$ cfu/ml concentration of *E. coli* in 384WP format with the final volume of 40 µl per well, when determining the growth inhibition effect of combined antimicrobial compounds. On the other hand, the difficulties in 384WP format resulting from the inconsistent growth of BAA1161 in presence of PIP, could possibly have been avoided if completely different strategy for screening method development had been chosen. If the EPI screening method had been developed directly into 384WP format, instead of miniaturization, possibly the inconsistency in growth inhibition effect of PIP on BAA1161 would have been encountered earlier. As a result, an antibiotic and an *E. coli* strain which would have been more suitable for this method in 384WP format could have been chosen.

Despite the above mentioned difficulties, objectives of developing an EPI screening method and using the developed method for a test screen were reached. Inconsistent and random over 90% growth inhibition values, likely caused by PIP, were observed in the screen. However, the frequency of this phenomenon was low enough that with four replicate wells it did not lead to difficulties in interpreting the screening results. Still, the mechanism behind the inconsistent growth inhibition caused by PIP in 384WP should be explored and the effect of higher initial bacterial concentration on the reproducibility of the assay should be studied in the future experiments. If the higher inoculum size does not prevent the inconsistencies, change of the antibiotic or bacterial strain should be considered.

Hit compounds leading to development of EPIs D13-9001 and NMP were found by using a screening strategy similar to ours (Nakayama et al. 2003a; Bohnert and Kern 2005). Similarly, compound collections were screened in combination with antibiotic against an efflux pump overexpressing bacterial strain. However, also different screening methods have been developed to find novel EPIs against bacterial efflux pumps. Haynes et al (2018) have developed a fluorochrome retention based high-throughput flow cytometry EPI screening assay. In this method, intracellular retention of diacetyl fluorescein is measured in presence of screen compounds. Diacetyl fluorescein is a fluorescent RND efflux pump substrate whose intracellular retention time is increased by EPIs. With this method the known EPIs PAβN and NMP were found active, supporting the reliability of the method. *In silico* methods have also been used for screening EPIs against bacterial efflux pumps. For instance, Verma and Tiwari (2018) conducted a multiple step virtual high through put screen to find novel inhibitors of AdeC. AdeC is the outer membrane protein of AdeABC RND transporter complex of *A. baumannii*. Before the screen a 3D model of AdeC was prepared. The *in silico* screen was comprised of ADMET filter (absorbance, distribution, metabolism, excretion and toxicity), three docking assays of increasing precision and MD-simulation. This method was used to find the most promising AdeC inhibitor of 2 737 560 compounds included in the screen.

All the four NCs which showed promising growth inhibition in the test EPI screen were gallic acid esters. Three of those were gallates: epigallocatechin gallate (EGCG) (Figure 23), isopropyl gallate (IG) (Figure 25) and octyl gallate (OG) (Figure 26). In addition to these three gallates, there was one more gallate, called epicatechin gallate, included in the screened NC collection. Surprisingly, epicatechin gallate showed substantially lower growth inhibition activity in the test screen (average growth inhibition of 17% at 24h) and, thus, was not considered as hit. The fourth NC that showed promising EPI activity in the screen was hamamelitannin (HT) (Figure 24). HT is a tannin with two gallic acid esters in its molecular structure. Because of the gallic acids, all the four NCs that showed promising bacterial growth inhibition activity in the test screen possess multiple phenol groups in their structure. Multiple hydrophobic ring systems in the molecular structure is

typical for known bacterial RND EPIs. The four promising NCs have multiple aromatic ring systems or a ring system and an alkyl chain in their structure but the hydrophobicity of these aromatic ring systems is reduced because of the multiple phenol groups. Of these four NCs HT and OG showed especially interesting activity in follow-up dose-response assay. Growth inhibition effect of HT and OG with 256 μg/ml PIP was substantially greater than the combined growth inhibition caused by these NCs and 256 μg/ml PIP separately, suggesting synergistic effect.

Based on the literature, EGCG is the most studied of the four NCs, which showed promising activity in the test EPI screen. EGCG is the most abundant of the four main catechins in green tea (Reygaert 2014). Green tea catechins have been shown to have synergistic and intrinsic antibacterial activity, based on cell wall damaging and fatty acid synthesis inhibiting mechanisms. In *E. coli* EGCG's MIC value is 400 μg/ml, based on a study conducted with ten *E. coli* strains (Jeon et al 2014). The *E. coli* strains of the study included clinical multi drug resistant isolates. Results of Kanagaratnam et al (2017) show that RND efflux pumps play a role in EGCG's antibacterial mechanism of action in *P. aeruginosa*. Impairment of MexAB-OprM efflux pump complex enhanced the synergistic antimicrobial effect of EGCG with chloramphenicol and tetracyclines. Also, the combination of EGCG with the EPI PAβN resulted in synergistic antibiotic potentiating effect in wild type *P. aeruginosa.* In *Campylobecter* species EGCG increased susceptibility to macrolides with sub-MIC concentration (Kurincic et al 2012). Macrolide potentiating effect of EGCG had correlation with the effects of EPIs PABN and NMP, included in the study. All in all, the antibiotic potentiating effect of EGCG, observed in the EPI screen, has been detected in multiple bacterial species with multiple types of antibiotics. It is also recognized, that RND efflux pumps affect the antibiotic potentiating effect of EGCG.

HT is found from bark and leaves of the tree *Hamamelis virginiana* (Kiran et al 2008). Based on the literature, research regarding the antibacterial activity of HT has mainly been focused on its effects against *Staphylococcus aureus*. HT affects biofilm formation of *S. aureus* by affecting its quorum sensing (Kiran et al 2008; Brackman et al 2016). *In*

vitro HT decreases *S. aureus* biofilm formation and increases the susceptibility of biofilms to multiple classes of antibiotics (Cobrado et al 2012; Brackman et al 2016). It has also been shown that HT prevents biofilm formation on surface of medical devices *in vivo* (Kiran et al 2008; Cobrado et al 2013; Brackman et al 2016). Biofilm formation reducing activity of HT has also been shown with GNB *A. baumannii in vitro* (Cobrado et al 2012). No research was found regarding HT's antimicrobial activity against *E. coli* or regarding effux pump inhibition. The results presented in literature, however, suggest that a very high concentration of HT is required to reach the MIC in Gram-negative and positive bacterial species (Kiran et al 2008; Cobrado et al 2012). It is possible, that the activity of HT determined in our experiments is related to the anti-biofilm effect, as the 384WPs were incubated without agitation in our experiments. All in all, similar results regarding the observed HT's *E. coli* growth inhibition effect in combination with antibiotic, were not found from the literature.

No articles were found regarding the antibacterial activity of IG. In the test EPI screen it had the highest average growth inhibition effect of the screened NCs. There was, however, a very high variation in the measured growth inhibition levels of the replicate wells with IG. Bacterial growth inhibition levels of the replicate wells were between 100 and -1.6% (Appendix 7, Figure 1). On the other hand, in the dose-response study the growth inhibition effect of IG was relatively constant but lower than HT's and OG's. Thus, it seems likely that the high growth inhibition effect of IG observed in the EPI screen was resulting partially from the inconsistent growth inhibition effect of PIP.

In the dose-response assay, OG showed highest bacterial growth inhibition activity of the four NCs, when combined with PIP. It caused an average growth inhibition of 100% at 75μM concentration when combined with 256 μg/ml PIP, while the growth inhibition levels of OG and PIP separately were only 15 and 44%, indicating synergism. OG is used in food industry as an antioxidant (Rua et al 2011). Based on the results of Kubo et al (2003), it has a low antimicrobial activity against GNB species of *E. coli*, *P. aeruginosa* and *E. aerogenes* with MIC values of over 800 μg/ml (2.8 mM). On the other hand, it has substantially lower MIC values, ranging from 12.5 to 50 μg/ml (44 to 177 μM), against

GNB species of *Proteus vulgaris* and *Salmonella choleraesuis* and against all Gram-positive bacterial species and fungi that were included in the study. Possibilities of using OG against *Helicobacter pylori* infections have also been studied *in vitro* because of its antioxidant and antimicrobial properties (Wolf et al 2017). MIC value of 125 μg/ml (443 μM) was determined for OG against *H. pylori*. Alkyl gallates included in the study showed increasing bacterial growth inhibition with increasing alkyl chain length, suggesting cell membrane destabilization related mechanism. The antifungal mechanism of OG is also likely resulting from membrane destabilization (Kubo et al 2001). All in all, no results regarding a synergistic antibacterial activity of OG with antibiotics were found from the literature. Low intrinsic antimicrobial effect of OG against *E. coli* observed in the dose-response assay is in line with the previous studies. Based on the literature, it seems also possible that the observed synergistic antibacterial effect of OG with PIP, is resulting from increased membrane permeability.

Synergistic antibacterial effect of HT and OG with PIP against *E. coli* BAA1161 should be verified in the future experiments. It should also be studied whether the synergism is resulting from efflux pump inhibition or from other mechanisms, like outer membrane permeabilization. Synergistic effect of these NCs with PIP could be verified in checkerboard assays. The role of efflux pumps for the synergism could also be studied in the checkerboard assays by using both efflux pumps overexpressing *E. coli* strains and *E. coli* strains with impaired or deleted efflux pumps. Also H33342 accumulation assay could be used for studying the EPI activity of these NCs (Coldham et al 2010).

7. CONCLUSIONS

Bacterial antibiotic resistance is a global and progressive health threat. It is diminishing the effectivity of antibiotics by multiple mechanisms. One of these resistance mechanisms is mediated by bacterial efflux pumps which reduce the intracellular antibiotic concentration. Bacteria express multiple types of efflux pumps but the RND family of efflux pumps is especially important for the antibiotic resistance. In this thesis, an assay

for screening novel inhibitors against RND efflux pumps of *E. coli* was developed and tested with a small collection of natural compounds.

During the development of the EPI screening method, unexpected difficulties were encountered regarding the inconsistent growth inhibition effect of PIP against *E. coli* strain BAA1161 in 384WP format. These inconsistencies suggest that the strain may contain subpopulations which cause the encountered hetero resistance phenomenon. These results should be taken into consideration in future experiments with the *E. coli* strain BAA1161. It should also be carefully considered which factors should be optimized in the miniaturization process of an assay. For instance, it was apparently a mistake that the initial bacterial concentration was not optimized during the miniaturization process of this assay. Developing the assay directly to 384WP format instead of having a miniaturization process from 96WP to 384WP format could also help to avoid these kind of difficulties.

Despite the difficulties caused by the inconsistencies a test EPI screen was successfully conducted. Based on the screen, the developed method can be used in the future to find novel EPIs against *E. coli*. However, it would be beneficial to solve the issues regarding the inconsistent growth inhibition effect of PIP to increase the reliability of the method.

NCs with novel synergistic antimicrobial activity were found with the test screen of the developed method. All the compounds that showed promising activity in the screen contained gallic acid ester, indicating that gallates and other gallic acid esters may possess interesting antibiotic potentiating properties. Potential of gallic acid esters as antibiotic adjuvants should be determined in the future experiments. In the follow-up assay of the test EPI screen, two gallic acid esters showed synergistic antibacterial activity with PIP. Although the developed screening method is optimized to find compounds with EPI activity, the PIP potentiating activity of these NCs could also be resulting from outer membrane permeabilization, for instance. After all, it has to be remembered that relatively high concentrations of these gallic acid esters were required for the synergistic effects.

Gallic acid esters may, however, possess a scaffold that could be optimized towards more potent antibiotic adjuvants in the future.

8. REFERENCES

Armstrong GL, Conn LA, Pinner RW: Trends in Infectious Disease Mortality in the United States During the 20th Century. JAMA 281: 61–66, 1999.

Aron Z, Opperman TJ: The hydrophobic trap - the Achilles heel of RND efflux pumps. Research in Microbiology 169: 393–400 ,2018.

Aldred KJ, Kerns RJ, Osheroff N: Mechanism of Quinolone Action and Resistance. Biochemistry 53: 1565−1574, 2014.

Anes J, McCusker MP, Fanningand S, Martins M: The ins and outs of RND efflux pumps in *Escherichia coli*. Frontiers in Microbiology 6: 1-14, 2015.

Bhullar K, Waglechner N, Pawlowski A, Koteva K, Banks ED, Johnston MD, Barton HA, Wright GD: Antibiotic Resistance Is Prevalent in an Isolated Cave Microbiome. PLOS ONE 7: 2012.

Bina XR, Philippart JA, Bina JE: Effect of the efflux inhibitors 1-(1-naphthylmethyl)-piperazine and phenyl-arginine-b-naphthylamide on antimicrobial susceptibility and virulence factor production in *Vibrio cholerae*. Journal of Antimicrobial Chemotherapy 63: 103–108, 2009.

Blair JMA, Richmond GE, Piddock LJV: Multidrug efflux pumps in Gram-negative bacteria and their role in antibiotic resistance. Future Microbiology 10: 1165–1177¸ 2014.

Bohnert JA, Kern WV: Selected Arylpiperazines Are Capable of Reversing Multidrug Resistance in *Escherichia coli* Overexpressing RND Efflux Pumps. Antimicrobial Agents and Chemoterapy 49: 849–852, 2005.

Brackman G, Breyne K, De Rycke R, Vermote A, Van Nieuwerburgh F, Meyer E, Van Calenbergh S, Coenye T: The Quorum Sensing Inhibitor Hamamelitannin Increases Antibiotic Susceptibility of Staphylococcus aureus Biofilms by Affecting Peptidoglycan Biosynthesis and eDNA Release. Scientific Reports 6: 1-14, 2016.

Bush K, Jacoby GA: Updated Functional Classification of β-Lactamases. Antimicrobial Agents and Chemoterapy 54: 969–976, 2010.

Cag Y, Caskurlu H, Fan Y, Cao B, Vahaboglu H: Resistance mechanisms. Ann Transl Med 17: 326, 2016.

Chase P, Enogieru I, Madoux F, Bishop E, Beer J, Scampavia L, Spicer T: An Automated Miniaturized Method to Perform and Analyze Antimicrobial Drug Synergy Assays. ASSAY and Drug Development Technologies 14: 58-664, 2016.

Chevalier J, Bredin J, Mahamoud A, Mallea M, Barbe J, Pages JM: Inhibitors of Antibiotic Efflux in Resistant *Enterobacter aerogenes* and *Klebsiella pneumoniae* Strains. Antimicrobial Agents and Chemotherapy 48: 1043–1046, 2004.

Clancy C J, Chen L, Hong JH, Cheng S, Hao B, Shields RK, Farrell AN, Doi Y, Zhao Y, Perlin DS, Kreiswirth BN, Nguyen H: Mutations of the *ompK36* Porin Gene and Promoter Impact Responses of Sequence Type 258, KPC-2-Producing *Klebsiella pneumoniae* Strains to Doripenem and Doripenem-Colistin. Antimicrobial Agents and Chemotherapy 57:5258–5265, 2013.

Clinical and Laboratory Standards Institute (CLSI): Methods for Dilution Antimicrobial Susceptibility Tests for Bacteria That Grow Aerobically; Approved Standard—Ninth Edition. CLSI document M07-A9. Wayne, PA: Clinical and Laboratory Standards Institute: 2012.

Clinical and Laboratory Standards Institute (CLSI): Performance Standards for Antimicrobial Susceptibility Testing 28th edition. CLSI supplement M100. Wayne, PA: Clinical and Laboratory Standards Institute: 2018.

Cobrado L, Azevedo MM, Silva-Dias A, Ramos JP, Pina-Vaz C, Rodrigues AG: Cerium, chitosan and hamamelitannin as novel biofilm inhibitors? Journal of Antimicrobial Chemotherapy 67: 1159–1162, 2012.

Cobrado L, Silva-Dias A, Azevedo MM, Pina-Vaz C, Rodrigues AG: In vivo antibiofilm effect of cerium, chitosan and hamamelitannin against usual agents of catheter-related bloodstream infections. Journal of Antimicrobial Chemotherapy 68: 126–130, 2013.

Coldham NG, Webber M, Woodward MJ and Piddock LJV: A 96-well plate fluorescence assay for assessment of cellular permeability and active efflux in *Salmonella enterica* serovar *Typhimurium* and *Escherichia coli*. Journal of Antimicrobial Chemotherapy. 65: 1655–1663, 2010.

Delcour AH: Outer membrane permeability and antibiotic resistance. Biochimica et Biophysica Acta 1794: 808–816, 2009.

Dodds DR: Antibiotic resistance: A current epilogue. Biochemical Pharmacology 134: 139–146, 2017.

Doi Y, Wachino J, Arakawa Y: Aminoglycoside Resistance The Emergence of Acquired 16S Ribosomal RNA Methyltransferases. Infectious Disease Clinics of North America 30: 523–537, 2016.

Domenech-Sanchez A, Martínez-Martínez L, Hernandez-Alles S, Conejo MC, Pascual A, Tomas JM, Albertí S, Javier BV: Role of *Klebsiella pneumoniae* OmpK35 Porin in Antimicrobial Resistance. Antimicrobial Agents and Chemoterapy 47: 3332–3335, 2003.

Du D, Wang Z, James NR, Voss JE, Klimont E, Ohene-Agyei T, Venter H, Chiu W, Luisi BF: Structure of the AcrAB–TolC multidrug efflux pump. Nature 509: 512–515, 2014.

Du D, Wang-Kan X, Neuberger A, van Veen HW, Pos KM, Piddock LJV, Luisi BF: Multidrug efflux pumps: structure, function and regulation. Nature Reviews Microbiology 16: 523–539, 2018.

Eicher T, Cha H, Seeger MA, Brandstätter L, El-Delik J, Bohnert JA, Kern WV, Verrey F, Grütter MG, Diederichs K, Pos KM: Transport of drugs by the multidrug transporter AcrB involves an access and a deep binding pocket that are separated by a switch-loop. Proceedings of the National Academy of Sciences 109: 5687–5692, 2012.

Fleming A: Penicillin. Nobel Lecture, 1945. Available online: www.nobelprize.org/uploads/2018/06/fleming-lecture.pdf

Fralick JA: Evidence that TolC Is Required for Functioning of the Mar/AcrAB Efflux Pump of *Escherichia coli*. Journal of Bacteriology 178: 5803–5805, 1996.

Gomes C, Martínez-Puchol S, Palma N, Horna G, Ruiz-Roldán L, Pons MJ, Ruiz J: Macrolide resistance mechanisms in *Enterobacteriaceae*: Focus on azithromycin. Critical Reviews in Microbiology, 43: 1-30, 2017.

Hall BG, Barlow M: Structure-Based Phylogenies of the Serine b-Lactamases. Journal of Molecular Evolution 57: 255–260, 2003.

Hannula M, Hänninen ML: Effect of putative efflux pump inhibitors and inducers on the antimicrobial susceptibility of *Campylobacter jejuni* and *Campylobacter coli*. Journal of Medical Microbiology 57: 851–855, 2008.

Hasdemir UO, Chevalier J, Nordmann P, Pagès JM: Detection and Prevalence of Active Drug Efflux Mechanism in Various Multidrug-Resistant *Klebsiella pneumoniae* Strains from Turkey. Journal of Clinical Microbiology 42: 2701–2706, 2004.

Haynes MK, Garcia M, Peters R, Waller A, Tedesco P, Ursu O, Bologa CG, Santos RG, Pinilla C, Wu TH, Lovchik JA, Oprea TI, Sklar LA, Tegos GP: High-Throughput Flow Cytometry Screening of Multidrug Efflux Systems. Bacterial Multidrug Exporters Methods and Protocols: 293-318, 2018.

Hinchliffe P, Symmons MF, Hughes C, Koronakis V: Structure and Operation of Bacterial Tripartite Pumps. Annual Review of Microbiology 67: 221–42, 2013.

Hobbs EC, Yin X, Paul BJ, Astarita JL, Storz G: Conserved small protein associates with the multidrug efflux pump AcrB and differentially affects antibiotic resistance. Proceedings of the National Academy of Sciences 109: 16696–16701, 2012.

Hopkins KL, Davies RH, Threlfall J: Mechanisms of quinolone resistance in Escherichia coli and Salmonella: Recent developments. International Journal of Antimicrobial Agents 25: 358–373, 2005.

Inglese J, Johnson RL, Simeonov A, Xia M, Zheng W, Austin CP and Auld DS: High-throughput screening assays for the identification of chemical probes.Nature Chemical Biology 3: 466–479, 2007.

Iversen PW, Beck B, Chen YF, Dere W, Devanarayan V, Eastwood BJ, Farmen MW, Iturria SJ, Montrose C, Moore RA, Weidner JR and Sittampalam GS: HTS Assay Validation. Assay Guidance Manual: 1-31, 2012.

Jeon J, Kim JH, Lee CK, Oh CH,Song HJ:The Antimicrobial Activity of (－)-Epigallocatehin-3-Gallate and Green Tea Extracts against Pseudomonas aeruginosa and Escherichia coli Isolated from Skin Wounds. Annals of Dermatology 26: 565-569, 2014.

Kanagaratnama R, Sheikha R, Alharbia F, Kwona DH: An efflux pump (MexAB-OprM) of Pseudomonas aeruginosa is associated with antibacterial activity of Epigallocatechin-3-gallate (EGCG). Phytomedicine 36: 194–200, 2017.

Katchanov J, Asar L, Klupp EM, Both A, Rothe C, Koenig C, Rohde H, Kluge S, Maurer FP: Carbapenem-resistant Gram-negative pathogens in a German university medical center: Prevalence, clinical implications and the role of novel β-lactam/β-lactamase inhibitor combinations. PLOS ONE: 2018.

Kern WV, Steinke P, Schumacher A, Schuster S, von Baum H, Bohnert JA: Effect of 1-(1-naphthylmethyl)-piperazine, a novel putative efflux pump inhibitor, on antimicrobial drug susceptibility in clinical isolates of *Escherichia coli*. Journal of Antimicrobial Chemotherapy 57: 339–343, 2006.

Kiran MD, Adikesavan NV, Cirioni O, Giacometti A, Silvestri C, Scalise G, Ghiselli R, Saba V, Orlando F, Shoham M, Balaban N: Discovery of a Quorum-Sensing Inhibitor of Drug-Resistant Staphylococcal Infections by Structure-Based Virtual Screening. Molecular Pharmacology 73:1578–1586, 2008.

Kubo I, Fujita K, Nihei K, Masuoka N: Non-antibiotic Antibacterial Activity of Dodecyl Gallate. Bioorganic & Medicinal Chemistry 11: 573–580, 2003.

Kubo I, Xiao P, Fujita K: Antifungal Activity of Octyl Gallate: Structural Criteria and Mode of Action. Bioorganic & Medicinal Chemistry Letters 11: 347-350, 2001.

Kurincic M, Klancnik A, Mozina SS: Epigallocatechin gallate as a modulator of Campylobacter resistance to macrolide antibiotics. International Journal of Antimicrobial Agents 40: 467– 471, 2012.

Li XZ, Plésiat P, Nikaido H: The Challenge of Efflux-Mediated Antibiotic Resistance in Gram-Negative Bacteria. Clinical Microbiology Reviews 28: 337–418, 2015.

Lomovskaya O, Bostian KA: Practical applications and feasibility of efflux pump inhibitors in the clinic—A vision for applied use. Biochemical Pharmacology 71: 910–918, 2006.

Lomovskaya O, Warren MS, Lee A, Galazzo J, Fronko R, Lee M, Blais J, Cho D, Chamberlain S, Renau T, Leger R, Hecker S, Watkins W, Hoshino K, Ishida H, Lee VJ: Identification and Characterization of Inhibitors of Multidrug Resistance Efflux Pumps in *Pseudomonas aeruginosa*: Novel Agents for Combination Therapy. Antimicrobial Agents and Chemotherapy 45: 105–116, 2001.

Ma D, Cook DN, Alberti M, Pon NG, Nikaido H, Hearst JE: Genes acrA and arB encode a stress-induced efflux system of Escherichia coli. Molecular Microbiology 16: 45–55, 1995.

Mahmood HY, Jamshidi S, Sutton JM, Rahman KM: Current Advances in Developing Inhibitors of Bacterial Multidrug Efflux Pumps. Current Medicinal Chemistry 23: 1062–1081, 2016.

Mallea M, Mahamoud A, Chevalier J, Alibert-Franco S, Brouant P, Barbe J, Pages JM: Alkylaminoquinolines inhibit the bacterial antibiotic efflux pump in multidrug-resistant clinical isolates. Biochemical Journal 376: 801–805, 2003.

Matsumoto Y, Hayama K, Sakakihara S, Nishino K, Noji H, Iino R, Yamaguchi A: Evaluation of Multidrug Efflux Pump Inhibitors by a New Method Using Microfluidic Channels. Plos one 6: 1–12, 2011.

Merck KGaA. Accessed 24.4.2019a
www.sigmaaldrich.com/catalog/product/sigma/m2319?lang=fi&region=FI

Merck KGaA. Accessed 24.4.2019b
www.sigmaaldrich.com/catalog/substance/epigallocatechingallate4583798951511?lang=fi&region=FI

Merck KGaA. Accessed 24.4.2019c
www.sigmaaldrich.com/catalog/product/sial/04646?lang=fi&region=FI

Merck KGaA. Accessed 24.4.2019d
www.sigmaaldrich.com/catalog/product/mm/816102?lang=fi&region=FI

Miyasaki Y, Rabenstein JD, Rhea J, Crouch ML, Mocek UM, Kittell PE, Morgan MA, Nichols WS, Van Benschoten MM, Hardy WD, Liu GY: Isolation and Characterization of Antimicrobial Compounds in Plant Extracts against Multidrug-Resistant Acinetobacter baumannii. PLOS ONE 8: 1-8, 2013.

Murakami S, Nakashima R, Yamashita E, Matsumoto T, Yamaguchi A: Crystal structures of a multidrug transporter reveal a functionally rotating mechanism. Nature 443: 173–179, 2006.

Murakami S, Nakashima R, Yamashita E, Yamaguchi A: Crystal structure of bacterial multidrug efflux transporter AcrB. Nature 419: 587–593, 2002.

Nakashima R, Sakurai K, Yamasaki S, Hayashi K, Nagata C, Hoshino K, Onodera Y, Nishino K, Yamaguchi A: Structural basis for the inhibition of bacterial multidrug exporters. Nature 500: 102–107, 2013.

Nakashima R, Sakurai K, Yamasaki S, Nishino K, Yamaguchi A: Structures of the multidrug exporter AcrB reveal a proximal multisite drug-binding pocket. Nature 480: 565–569, 2011.

Nakayama K, Ishida Y, Ohtsuka M, Kawato H, Yoshida K, Yokomizo Y, Ohta T, Otani T, Kurosaka Y, Yoshida K, Ishida H, Lee VJ, Renau TE , Watkins WJ: MexAB-OprM Specific Efflux Pump Inhibitors in *Pseudomonas aeruginosa*. Part 2: Achieving Activity *In Vivo* Through the Use of Alternative Scaffolds. Bioorganic & Medicinal Chemistry Letters 13: 4205–4208, 2003b.

Nakayama K, Ishida Y, Ohtsuka M, Kawato H, Yoshida K, Yokomizo Y, Hosono S, Ohta T, Hoshino K, Ishida H, Yoshida K, Renau TE, Leger R, Zhang JZ, Lee VJ, Watkins WJ: MexAB-OprM-Specific Efflux Pump Inhibitors in *Pseudomonas aeruginosa*. Part 1: Discoveryand Early Strategies for Lead Optimization. Bioorganic & Medicinal Chemistry Letters 13: 4201–4204, 2003a.

Nakayama K, Kawato H, Watanabe J, Ohtsuka M, Yoshida K, Yokomizo Y, Sakamoto A, Kuru N, Ohta T, Hoshino K, Yoshida K, Ishida H, Cho A, Palme MH, Zhang JZ, Lee VJ, Watkins WJ: MexAB-OprM specific efflux pump inhibitors in *Pseudomonas aeruginosa*. Part 3: Optimization of potency in the pyridopyrimidine series through the application of a pharmacophore model. Bioorganic & Medicinal Chemistry Letters 14: 475–479, 2004a.

Nakayama K, Kuru N, Ohtsuka M, Yokomizo Y, Sakamoto A, Kawato H, Yoshida K, Ohta T, Hoshino K, Akimoto K, Itoh J, Ishida H, Cho A, Palme MH, Zhang JZ, Lee VJ, Watkins WJ: MexAB-OprM specific efflux pump inhibitors in *Pseudomonas aeruginosa*. Part 4: Addressing the problem of poor stability due to photoisomerization of an acrylic acid moiety. Bioorganic & Medicinal Chemistry Letters 14: 2493–2497, 2004b.

Narwal M, Fallarero A, Vuorela P, Lehtiö L: Homogeneous Screening Assay for Human Tankyrase. Journal of Biomolecular Screening 17: 593–604, 2012.

Neyfakh AA: Mystery of multidrug transporters: the answer can be simple. Molecular Microbiology 44: 1123–1130, 2002.

Nguyen ST, Kwasny SM, Ding X, Cardinale SC, McCarthy CT, Kim HS, Nikaido H, Peet NP, Williams JD, Bowlin TL, Opperman TJ: Structure–activity relationships of a novel pyranopyridine series of Gram-negative bacterial efflux pump inhibitors. Bioorganic & Medicinal Chemistry 23: 2024–2034, 2015.

Nikaido H: Molecular Basis of Bacterial Outer Membrane Permeability Revisited. Microbiology and Molecular Biology Reviews 67: 593–656, 2003.

Nikaido H, Basina M, Nguyen V, Rosenberg EY: Multidrug Efflux Pump AcrAB of Salmonella typhimurium Excretes Only Those b-Lactam Antibiotics Containing Lipophilic Side Chains. Journal of Bacteriology 180: 4686–4692, 1998.

Opperman TJ, Kwasny SM, Kim HS, Nguyen ST, Houseweart C, D'Souza S, Walker GC, Peet NP, Nikaido H, Bowlin TL: Characterization of a Novel Pyranopyridine Inhibitor of the AcrAB Efflux Pump of Escherichia coli. Antimicrobial Agents and Chemotherapy 58: 722–733, 2014.

Opperman TJ, Nguyen ST: Recent advances toward a molecular mechanism of efflux pump inhibition. Frontiers in Microbiology 6: 1–16, 2015.

Pannek S, Higgins PG, Steinke P, Jonas D, Akova M, Bohnert JA, Seifert H, Kern WV: Multidrug efflux inhibition in *Acinetobacter baumannii*: comparison between 1-(1-naphthylmethyl)-piperazine and phenyl-arginine-b-naphthylamide. Journal of Antimicrobial Chemotherapy 57: 970–974, 2006.

Partridge SR: Resistance mechanisms in Enterobacteriaceae. Pathology 47: 276–284, 2015.

Pernodet JL, Fish S, Blondelet-Rouault MH, Cundliffe E: The Macrolide-Lincosamide-Streptogramin B Resistance Phenotypes Characterized by Using a Specifically Deleted, Antibiotic-Sensitive Strain of Streptomyces lividans. Antimicrobial Agents and Chemotherapy 40: 581–585, 1996.

Piddock LJV: Clinically Relevant Chromosomally Encoded Multidrug Resistance Efflux Pumps in Bacteria. Clinical Microbiology Reviews 19: 382–402, 2006.

Piddock LJV: The crisis of no new antibiotics—what is the way forward? Lancet Infect Dis 12: 249–253, 2012.

Price LB, Vogler A, Pearson T, Busch JD, Schupp JM, Keim P: In Vitro Selection and Characterization of Bacillus anthracis Mutants with High-Level Resistance to Ciprofloxacin. Antimicrobial Agents and Chemotherapy 47: 2362–2365, 2003.

Renau TE, Leger R, Flamme EM, Sangalang J, She MW, Yen R, Gannon CL, Griffith D, Chamberland S, Lomovskaya O, Hecker SJ, Lee VJ, Ohta T, Nakayama K: Journal of Medicinal Chemistry 42: 4928–4931, 1999.

Reygaert WC: The antimicrobial possibilities of green tea. Frontiers in Microbiology 5: 1-8 2014.

Roberts MC: Resistance to Macrolide, Lincosamide, Streptogramin, Ketolide, and Oxazolidinone Antibiotics. Molecular Biotechnology 28: 47–62, 2004.

Roberts MC, Sutcliffe J, Courvalin P, Jencen LB, Rood J, Seppala H: Nomenclature for Macrolide and Macrolide-LincosamideStreptogramin B Resistance Determinants. Antimicrobial Agents and Chemotherapy 43: 2823–2830, 1999.

Rodriguez-Martinez JM, Machuca J, Cano ME, Calvo J, Martinez-Martinez L, Pascual A: Plasmid-mediated quinolone resistance: Two decades on. Drug Resistance Updates 29: 13–29, 2016.

Rua J, Fernandez-Alvarez L, de Castro C, del Valle P, de Arriaga D, Garcia-Armesto MR: Antibacterial Activity Against Foodborne Staphylococcus aureus and Antioxidant Capacity of Various Pure Phenolic Compounds. Foodborne Pathogens and Disease 8: 149-157, 2011.

Schuster S, Kohler S, Buck A, Dambacher C, König A, Bohnert JA, Kern WV: Random Mutagenesis of the Multidrug Transporter AcrB from Escherichia coli for Identification of Putative Target Residues of Efflux Pump Inhibitors. Antimicrobial Agents and Chemotherapy 58: 6870–6878, 2014.

Shigemura Ki, Osawa K, Kato A, Tokimatsu I, Arakawa S, Shirakawa T, Fujisawa M: Association of overexpression of efflux pump genes with antibiotic resistance in Pseudomonas aeruginosa strains clinically isolated from urinary tract infection patients. The Journal of Antibiotics 68: 568–572, 2015.

Sjuts H, Vargiu AV, Kwasny SM, Nguyen ST, Kim HS, Ding X, Ornik AR, Ruggerone P, Bowlin TL, Nikaido H, Pos KM, Opperman TJ: Molecular basis for inhibition of AcrB multidrug efflux pump by novel and powerful pyranopyridine derivatives. Proceedings of the National Academy of Sciences of the United States of America 113: 3509–3514, 2016.

Sulavik MC, Houseweart C, Cramer C, Jiwani N, Murgolo N, Greene J, DiDomenico B, Shaw KJ, Miller G, Hare R, Shimer G: Antibiotic Susceptibility Profiles of Escherichia coli Strains Lacking Multidrug Efflux Pump Genes. Antimicrobial Agents and Chemoterapy 45: 1126–1136, 2001.

Theuretzbacher U: Global antimicrobial resistance in Gram-negative pathogens and clinical need. Current Opinion in Microbiology 39: 106–112, 2017.

Tikhonova EB, Yamada Y, Zgurskaya HI: Sequential Mechanism of Assembly of Multidrug Efflux Pump AcrAB-TolC. Chemistry & Biology 18: 454–463, 2011.

Vargiu AV, Nikaido H: Multidrug binding properties of the AcrB efflux pump characterized by molecular dynamics simulations. Proceedings of the National Academy of Sciences of the United States of America 109: 20637–20642, 2012.

Vargiu AV, Ruggerone P, Opperman TJ, Nguyen ST, Nikaido H: Molecular Mechanism of MBX2319 Inhibition of Escherichia coli AcrB Multidrug Efflux Pump

and Comparison with Other Inhibitors. Antimicrobial Agents and Chemotherapy 58: 6224–6234, 2014.

Verma P, Tiwari V: Targeting Outer Membrane Protein Component AdeC for the Discovery of Efflux Pump Inhibitor against AdeABC Efflux Pump of Multidrug Resistant Acinetobacter baumannii. Cell Biochemistry and Biophysics 76: 391–400, 2018.

Vidal-Aroca F, Meng A, Minz T, Page MGP, Dreier J: Use of resazurin to detect mefloquine as an efflux-pump inhibitor in *Pseudomonas aeruginosa* and *Escherichia coli*. Journal of Microbiological Methods 79: 232–237, 2009.

Wachino J, Shibayama K, Kurokawa H, Kimura K, Yamane K, Suzuki S, Shibata N, Ike Y, Arakawa Y: Novel Plasmid-Mediated 16S rRNA m1A1408 Methyltransferase, NpmA, Found in a Clinically Isolated Escherichia coli Strain Resistant to Structurally Diverse Aminoglycosides. Antimicrobial Agents and Chemotherapy 51: 4401–4409, 2007.

Wang Z, Fan G, Hryc CF, Blaza JN, Serysheva II, Schmid MF, Chiu W, Luisi BF, Du D: An allosteric transport mechanism for the AcrAB-TolC multidrug efflux pump. eLife: 1–19, 2017.

Watkins WJ, Landaverry Y, Leger R, Litman R, Renau TE, Williams N, Yen R, Zhang JZ, Chamberland S, Madsen D, Griffith D, Tembe V, Huie K, Dudley MN: The Relationship between Physicochemical Properties, *In Vitro* Activity and Pharmacokinetic Profiles of Analogues of Diamine-Containing Efflux Pump Inhibitors. Bioorganic & Medicinal Chemistry Letters 13: 4241–4244, 2003.

Wolf VG, Bonacorsi C,b Raddi MSG, da Fonseca LM, Ximenes VF: Octyl gallate, a food additive with potential beneficial properties to treat Helicobacter pylori infection. Food & Function 8: 2500–2511, 2017.

World Health Organization: Antimicrobial Resistance Global report on survailance 2014. 2014.

World Health Organization: Antimicrobial Resistance Global report on survailance 2014 Summary. 2014.
Wright GD: Bacterial resistance to antibiotics: Enzymatic degradation and modification. Advanced Drug Delivery Reviews 57: 1451–1470, 2005.

Wright GD: Molecular mechanisms of antibiotic resistance. Chemical Communications 47: 4055–4061, 2011.

Yamaguchi A, Nakashima R, Sakurai K: Structural basis of RND-type multi drug exporters. Frontiers in Microbiology 6: 1–19, 2015.

Yamane K, Wachino J, Suzuki S, Kimura K, Shibata N, Kato H, Shibayama K, Konda T, Arakawa Y: New Plasmid-Mediated Fluoroquinolone Efflux Pump, QepA, Found in

an *Escherichia coli* Clinical Isolate. Antimicrobial Agents And Chemotherapy 51: 3354–3360, 2007.

Yrjänheikki U: Assay Setup for High Throughput Screening to Identify Novel Efflux Pump Inhibitors against Escherichia coli. University of Helsinki, Faculty of Pharmacy, Discipline of Biopharmaceutics, 2018.

Yoshida K, Nakayama K, Kuru N, Kobayashi S, Ohtsuka M, Takemura M, Hoshino K, Kanda H, Zhang JZ, Lee VJ, Watkins WJ: MexAB-OprM specific efflux pump inhibitors in *Pseudomonas aeruginosa*. Part 5: Carbon-substituted analogues at the C-2 position. Bioorganic & Medicinal Chemistry 14: 1993–2004, 2006a.

Yoshida K, Nakayama K, Ohtsuka M, Kuru N, Yokomizo Y, Sakamoto A, Takemura M, Hoshino K, Kanda H, Nitanai H, Namba K, Yoshida K, Imamura Y, Zhang JZ, Lee VJ, Watkins WJ: MexAB-OprM specific efflux pump inhibitors in *Pseudomonas aeruginosa*. Part 7: Highly soluble and *in vivo* active quaternary ammonium analogue D13-9001, a potential preclinical candidate. Bioorganic & Medicinal Chemistry 15: 7087–7097, 2007.

Yoshida K, Nakayama K, Yokomizo Y, Ohtsuka M, Takemura M, Hoshino K, Kanda H, Namba K, Nitanai H, Zhang JZ, Lee VJ, Watkins WJ: MexAB-OprM specific efflux pump inhibitors in *Pseudomonas aeruginosa*. Part 6: Exploration of aromatic substituents. Bioorganic & Medicinal Chemistry 14: 8506–8518, 2006b.

Zechini B, Versace I: Inhibitors of Multidrug Resistant Efflux Systems in Bacteria. Recent Patents on Anti-Infective Drug Discovery 4: 37–50, 2009.

APPENDIX 1: Natural compounds collection used in the test screen.

Table 1. Properties of the natural compounds screened in the efflux pump inhibitor screen at 50 μM concentration in combination with 256 μg/ml of piperacillin against *E. coli* BAA1161.

Number of compound	Name of the compound	Molecular weight of the compound (g/mol)	Supplier of the compound
NC001	Arbutin	272.3	Sigma
NC002	Alpha-naphthoflavone	272.9	Acros
NC003	Apigenin	270.24	Fluka
NC004	Artemisinin	282.35	Extrasynthese
NC005	L-Ascorbic acid	176.1	Sigma
NC006	Baicalein	270.25	Extrasynthese
NC007	Baicalin	446.36	Extrasynthese
NC008	Benzoic acid	122.12	BDH Chemicals Ltd.
NC009	3-Benzoylbenzo(F)coumarin	300.30	Acros
NC010	3-(2-Benzoxazolyl)umbelliferone	279.25	Fluka
NC011	Boldine hydrochloride	363.84	Extrasynthese
NC012	Butylhydroxyanisole	180.2	Sigma
NC013	Butylhydroxytoluene	220.4	Sigma
NC014	Caffeic acid	180.16	Extrasynthese
NC015	(+)-Catechin	290.3	Sigma
NC016	(+/-)-Catechin	290.3	Sigma
NC017	Catechol	110.1	Sigma
NC018	Chrysin	254.25	Extrasynthese
NC019	o-Coumaric acid	164.2	Sigma
NC020	m-Coumaric acid	164.16	Fluka
NC021	4-Coumaric acid	164.16	Extrasynthese
NC022	Coumarin 102	255.32	Acros
NC023	Coumarin 30	347.42	ICN
NC024	Coumarin 7	333.38	Acros
NC025	Coumarin	146.15	Merck
NC026	Daidzein	254.25	Extrasynthese
NC027	Daidzin	416.38	Extrasynthese
NC028	Daphnetin	178.15	Extrasynthese
NC029	7-Diethylamino-3-thenoylcoumarin	327.39	Acros
NC030	2,3-Dihydroxybenzoic acid	154.12	Fluka
NC031	2,4-Dihydroxybenzoic acid	154.12	Fluka
NC032	2,5-Dihydroxybenzoic acid	154.12	Fluka
NC033	2,6-Dihydroxybenzoic acid	154.12	Fluka
NC034	3,4-Dihydroxybenzoic acid	154.12	Fluka
NC035	3,5-Dihydroxybenzoic acid	154.12	Fluka
NC036	2,5-Dimethyl-phenol	122.17	Fluka
NC037	6,2-Dimethoxyflavone	282.3	ICC
NC038	5-Dimethylaminonaphthalene-1-sulfonylchloride	269.75	Fluka
NC039	Ellagic acid	302.2	Sigma
NC040	(-)-Epicatechin	290.3	Sigma
NC041	(-)-Epicatechin gallate	442.37	Extrasynthese
NC042	(-)-Epigallocatechin	306.28	Extrasynthese
NC043	(-)-Epigallocatechin gallate	458.37	Extrasynthese
NC044	Esculetin	178.15	Extrasynthese
NC045	Esculin	340.29	Extrasynthese
NC046	Ethoxyquin	217.3	Sigma

NC047	Ferulic acid	194.19	Extrasynthese
NC048	Flavone	222.25	Carl Roth GmbH
NC049	Fraxetin	208.17	Extrasynthese
NC050	Hesperetin	302.29	Extrasynthese
NC051	Genistein	270.23	Extrasynthese
NC052	Hippuric acid	179.18	APIN Chemicals Ltd.
NC053	Gossypin	480.38	Extrasynthese
NC054	Hamamelitannin	484.37	Extrasynthese
NC055	Hesperidin	610.57	Sigma
NC056	Hydroquinone	110.11	Fluka
NC057	3-Hydroxyacetophenone	136.15	Fluka
NC058	4-Hydroxyacetophenone	136.15	Fluka
NC059	4-Hydroxycoumarin	162.15	Extrasynthese
NC060	2-Hydroxyphenylacetic acid	152.15	Fluka
NC061	3-Hydroxyphenylacetic acid	152.15	Fluka
NC062	4-Hydroxyphenylacetic acid	152.15	Fluka
NC063	Hypericin	504.43	Carl Roth GmbH
NC064	Isopimpinellin	246.22	Carl Roth GmbH
NC065	Bergapten, 5-Methoxypsoralen	216.20	Aldrich
NC066	Isopropyl gallate	212.21	Extrasynthese
NC067	Isorhamnetin	316.28	Extrasynthese
NC068	Kaempferol	286.25	Extrasynthese
NC069	Khellin	260.24	Carl Roth GmbH
NC070	Luteolin	286.25	Extrasynthese
NC071	Luteolin-7-glucoside	448.38	Extrasynthese
NC072	Malvin chloride	691.01	Extrasynthese
NC073	6-Methylcoumarin	160.17	Extrasynthese
NC074	4-Methyldaphnetin	192.17	Extrasynthese
NC075	4-Methyl pyrocatechol	124.14	Merck
NC076	Methyl umbelliferone	176.17	
NC077	Morin dihydrate	338.26	Carl Roth GmbH
NC078	Myricetin	318.25	Extrasynthese
NC079	Myricitrin	464.38	Extrasynthese
NC080	Naringenin	272.27	Extrasynthese
NC081	2'-Methoxy-alpha-naphthoflavone	302.3	ICC
NC082	Naringin	580.53	Carl Roth GmbH
NC083	Nordihydroguaiaretic acid	302.37	Fluka
NC084	Octyl gallate	282.34	Fluka
NC085	Phtalic acid	166.13	Merck
NC086	Protocatechuic acid	154.13	Extrasynthese
NC087	Psoralen	186.17	Extrasynthese
NC088	Pyrogallol	126.11	Riedel-de Haën
NC089	Quercetin krist.	338.27	Merck
NC090	Quercitrin dihydrate	484.43	Carl Roth GmbH
NC091	(-)-Quinic acid	192.2	Sigma
NC092	Resorcin	110.11	Riedel-de Haën
NC093	Resveratrol	228.25	Extrasynthese
NC094	Rhamnetin	316.28	Extrasynthese
NC095	Rosmarinic acid	360.33	Extrasynthese
NC096	Rotenone	394.41	Acros
NC097	Rutin	664.58	Merck
NC098	D(-)-Salicin	286.27	Carl Roth GmbH
NC099	Salicylic acid	138.13	AnalaR
NC100	Scopoletin	192.17	Extrasynthese
NC101	Sennoside B	862.75	Oy Extracta Ltd.
NC102	Silybin	482.43	Carl Roth GmbH
NC103	Sinapic acid	224.22	Fluka

NC104	Sinigrin monohydrate	415.49	Carl Roth GmbH
NC105	Syringic acid	198.2	Sigma
NC106	(+)-Taxifolin	304.27	Extrasynthese
NC107	Tectochrysin	268.28	Extrasynthese
NC108	Thymol	150.22	Riedel-de Haën
NC109	Thymoquinone	164.2	MP Biomedicals, Inc.
NC110	3,4,5-Trimethoxybenzoic acid	212.2	Sigma
NC111	6-Hydroxy-2,5,7,8-tetramethylchroman-2-carboxylic acid (Trolox)	250.29	Aldrich
NC112	Umbelliferone	162.14	Carl Roth GmbH
NC113	Vanillic acid	168.15	Extrasynthese
NC114	Uric cid	168.1	Sigma
NC115	Vanillin	152.15	Merck
NC116	Xanthotoxin	216.19	Extrasynthese
NC117	Gitoxigenin	390.51	Carl Roth GmbH
NC118	Gitoxin	780.96	Merck
NC119	Digoxin	780.96	Fluka AG
NC120	Digitoxigenin	374.5	Sigma
NC121	Lanatosid A	969.15	Carl Roth GmbH
NC122	Lanatosid B	985.1	SERVA
NC123	Lanatosid C	985.14	Carl Roth GmbH
NC124	Chinin	324.43	Fluka AG
NC125	Cinchonidine	294.40	BDH
NC126	Cinchonine	294.40	BDH

APPENDIX 2: Results of the checkerboard assays done in the 96-well plate (96WP) format with two-fold mefloquine and piperacillin concentration ranges.

Mefloquine (µg/ml) \ Piperacillin (µg/ml)	1024	512	256	128	64	32	16	8	4	0
0	99	99	32	8	3	1	2	16	3	0
4	99	99	50	8	6	5	2	3	4	4
8	99	99	99	21	11	9	4	5	9	3
16	99	99	99	99	100	99	99	38	32	32
32	99	99	99	99	99	99	99	99	100	99
64	100	99	100	100	100	100	100	100	100	100

Figure 1. Growth inhibition (%) of the first checkerboard assay done in the 96WP format. In total five checkerboard assays were conducted in 96WP format and in two of those two-fold mefloquine concentration range was used.

Mefloquine (µg/ml) \ Piperacillin (µg/ml)	1024	512	256	128	64	32	16	8	4	0
0	99	99	47	12	7	4	3	3	4	0
4	99	99	57	19	6	4	5	3	6	1
8	99	99	89	32	14	8	14	15	6	4
16	100	99	93	99	99	99	99	51	34	33
32	100	99	99	100	100	100	100	99	99	100
64	100	100	100	100	99	100	100	100	100	100

Figure 2. Growth inhibition (%) of the second checkerboard assay done in the 96WP format. In total five checkerboard assays were conducted in 96WP format and in two of those two-fold mefloquine concentration range was used.

APPENDIX 3: Results of the checkerboard assays done in the 96-well plate (96WP) format with non-geometric mefloquine concentration range.

Mefloquine (µg/ml) \ Piperacillin (µg/ml)	1024	512	256	128	64	32	16	8	4	0
0	99	28	1	2	4	4	1	2	3	0
4	99	31	8	6	2	4	2	3	3	1
6	99	33	28	7	7	4	5	5	4	2
8	99	99	99	13	9	7	11	7	4	3
12	99	99	37	33	39	20	17	24	15	16
16	99	99	99	98	99	99	37	45	39	35

Figure 1. Growth inhibition (%) of the first checkerboard assay done in the 96WP format with non-geometric mefloquine concentration range. In total five checkerboard assays were conducted in 96WP format and in three of those non-geometric mefloquine concentration range was used.

Mefloquine (µg/ml) \ Piperacillin (µg/ml)	1024	512	256	128	64	32	16	8	4	0
0	89	21	5	4	1	2	3	3	2	0
4	100	30	13	6	7	26	5	11	8	7
6	99	37	16	15	7	9	8	10	9	6
8	100	100	18	12	12	7	16	15	16	11
12	99	98	99	100	47	38	30	25	25	25
16	100	100	99	99	99	99	38	43	43	40

Figure 2. Growth inhibition (%) of the second checkerboard assay done in the 96WP format with non-geometric mefloquine concentration range. In total five checkerboard assays were conducted in 96WP format and in three of those non-geometric mefloquine concentration range was used.

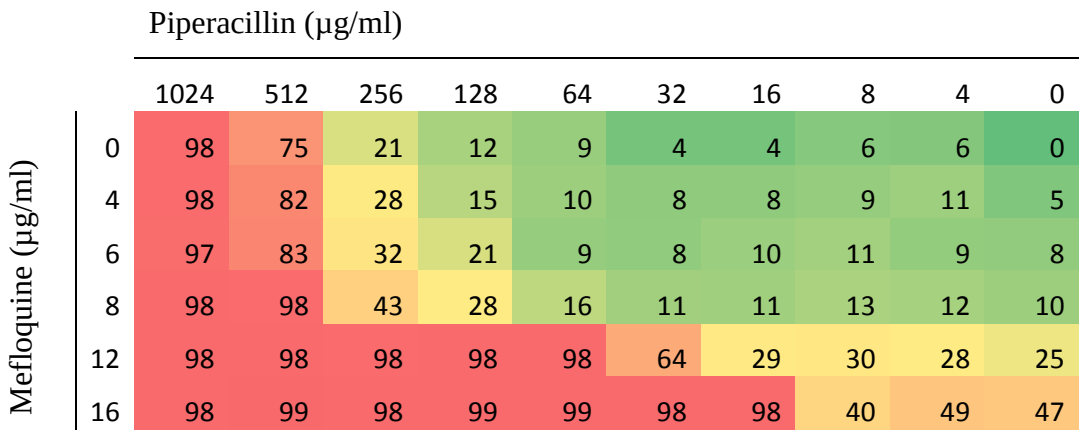

Figure 3. Growth inhibition (%) of the third checkerboard assay done in the 96WP format with non-geometric mefloquine concentration range. In total five checkerboard assays were conducted in 96WP format and in three of those non-geometric mefloquine concentration range was used.

APPENDIX 4: Results of the checkerboard assays done in the 384WP format.

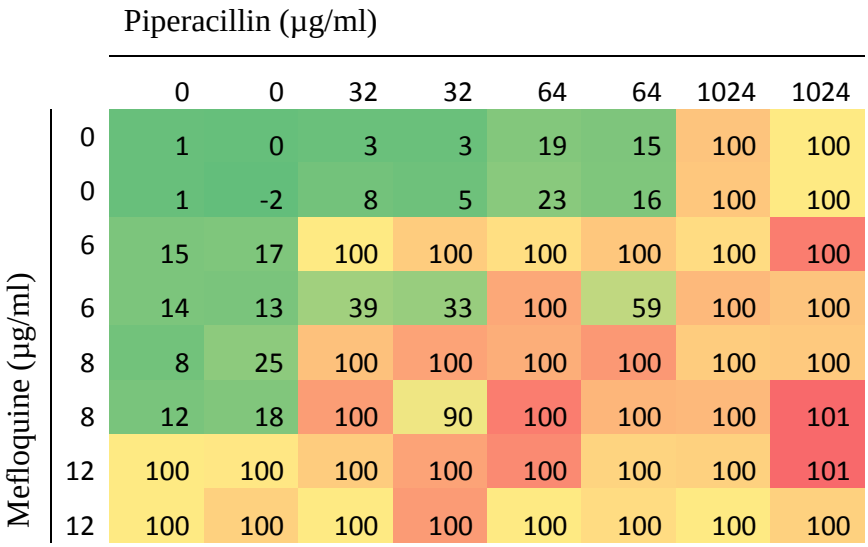

Mefloquine (µg/ml) \ Piperacillin (µg/ml)	0	0	32	32	64	64	1024	1024
0	1	0	3	3	19	15	100	100
0	1	-2	8	5	23	16	100	100
6	15	17	100	100	100	100	100	100
6	14	13	39	33	100	59	100	100
8	8	25	100	100	100	100	100	100
8	12	18	100	90	100	100	100	101
12	100	100	100	100	100	100	100	101
12	100	100	100	100	100	100	100	100

Figure 1. Growth inhibition (%) of the first checkerboard assay done in the 384WP format. In total three checkerboard assays were conducted in 384WP. Results of the third checkerboard assay done in the 384WP format are presented in the results (Figure 20).

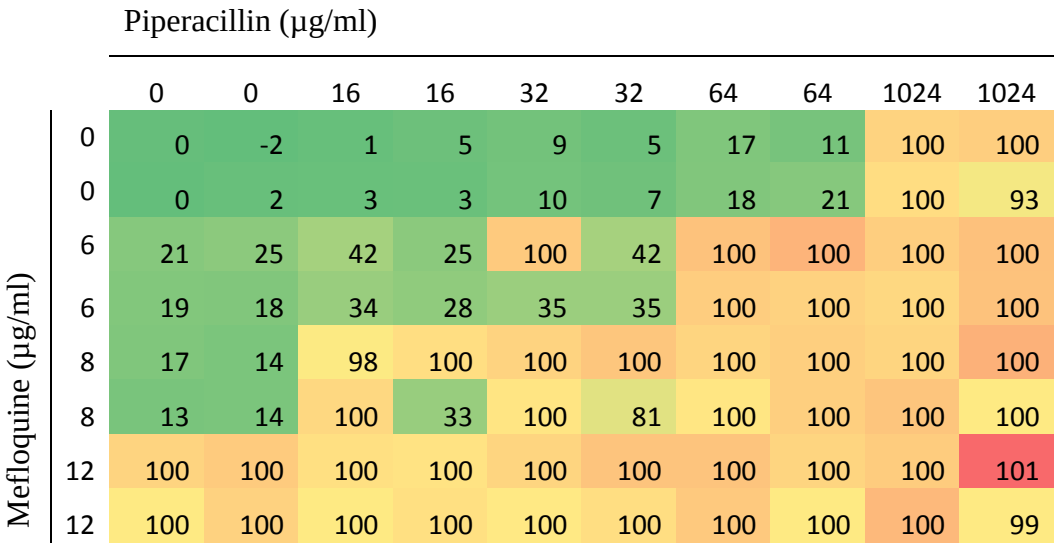

Mefloquine (µg/ml) \ Piperacillin (µg/ml)	0	0	16	16	32	32	64	64	1024	1024
0	0	-2	1	5	9	5	17	11	100	100
0	0	2	3	3	10	7	18	21	100	93
6	21	25	42	25	100	42	100	100	100	100
6	19	18	34	28	35	35	100	100	100	100
8	17	14	98	100	100	100	100	100	100	100
8	13	14	100	33	100	81	100	100	100	100
12	100	100	100	100	100	100	100	100	100	101
12	100	100	100	100	100	100	100	100	100	99

Figure 2. Growth inhibition (%) of the second checkerboard assay done in the 384WP format. In total three checkerboard assays were conducted in 384WP. Results of the third checkerboard assay done in the 384WP format are presented in the results (Figure 20).

APPENDIX 5: Complete results of the plate uniformity assay

Max	Mid	Min	Max	Mid	Min	Max	Mid	Min	Max	Mid	Min	Max	Mid	Min	Max	Mid	Min	Max	Mid	Min	Max	Mid	Min
0.85	0.70	0.00	0.79	0.76	0.00	0.80	0.69	0.00	0.79	0.73	0.00	0.81	0.68	0.00	0.89	0.68	0.00	0.87	0.74	0.00	0.86	0.84	0.00
0.84	0.66	0.00	0.87	0.66	0.00	0.74	0.66	0.00	0.75	0.62	0.00	0.72	0.68	0.00	0.81	0.61	0.00	0.73	0.65	0.00	0.78	0.68	0.00
0.86	0.65	0.00	0.76	0.67	0.00	0.78	0.65	0.00	0.75	0.64	0.00	0.72	0.62	0.00	0.78	0.66	0.00	0.73	0.60	0.00	0.78	0.70	0.00
0.78	0.66	0.00	0.80	0.64	0.00	0.75	0.65	0.00	0.73	0.72	0.00	0.77	0.63	0.00	0.78	0.65	0.00	0.65	0.68	0.00	0.77	0.71	0.00
0.87	0.67	0.00	0.78	0.64	0.00	0.72	0.65	0.00	0.73	0.66	0.00	0.72	0.62	0.00	0.74	0.68	0.00	0.77	0.64	0.00	0.79	0.70	0.00
0.82	0.65	0.00	0.77	0.62	0.00	0.70	0.65	0.00	0.73	0.62	0.00	0.72	0.64	0.00	0.81	0.68	0.00	0.70	0.66	0.00	0.72	0.59	0.00
0.84	0.63	0.00	0.70	0.62	0.00	0.74	0.65	0.00	0.74	0.64	0.00	0.71	0.62	0.00	0.72	0.65	0.01	0.71	0.61	0.00	0.69	0.65	0.00
0.75	0.62	0.00	0.71	0.64	0.01	0.72	0.66	0.01	0.72	0.66	0.01	0.72	0.63	0.01	0.74	0.67	0.00	0.69	0.68	0.00	0.77	0.66	0.00
0.76	0.74	0.00	0.72	0.65	0.00	0.72	0.70	0.01	0.73	0.68	0.00	0.74	0.69	0.00	0.83	0.66	0.00	0.75	0.65	0.00	0.67	0.73	0.00
0.78	0.68	0.02	0.69	0.64	0.01	0.76	0.64	0.00	0.68	0.68	0.00	0.71	0.69	0.00	0.86	0.69	0.00	0.68	0.64	0.00	0.68	0.65	0.00
0.79	0.69	0.00	0.70	0.66	0.00	0.73	0.66	0.00	0.79	0.67	0.00	0.79	0.71	0.00	0.72	0.71	0.00	0.66	0.65	0.00	0.73	0.65	0.00
0.75	0.61	0.00	0.75	0.64	0.00	0.73	0.66	0.00	0.69	0.67	0.00	0.71	0.68	0.00	0.69	0.68	0.01	0.74	0.66	0.03	0.74	0.79	0.00
0.73	0.62	0.00	0.78	0.69	0.00	0.72	0.64	0.00	0.83	0.70	0.00	0.73	0.68	0.00	0.72	0.70	0.01	0.69	0.69	-0.01	0.72	0.72	0.00
0.73	0.66	0.00	0.76	0.64	0.00	0.81	0.69	0.00	0.75	0.67	0.00	0.70	0.70	0.00	0.71	0.71	0.00	0.70	0.64	0.00	0.73	0.69	0.00
0.80	0.68	0.00	0.73	0.74	0.00	0.79	0.75	0.00	0.79	0.68	0.00	0.80	0.67	0.03	0.79	0.69	0.00	0.77	0.68	0.00	0.78	0.68	0.00
0.86	0.71	0.00	0.80	0.68	0.00	0.82	0.76	0.00	0.78	0.73	0.00	0.87	0.69	0.00	0.82	0.75	0.00	0.82	0.68	0.00	0.84	0.81	0.00

Figure 1. Heat map presentation of *E. coli* BAA1161 growth in the first plate uniformity assay plate at 24h. The treatment of column's wells is presented above it in the figure. The treatments were: max: 256 µg/ml piperacillin, mid: 256 µg/ml piperacillin + 6 µg/ml mefloquine, min: 256 µg/ml piperacillin + 16 µg/ml mefloquine. Initial bacterial concentration of all the wells was $5x10^5$ cfu/ml.

Max	Mid	Min	Max	Mid	Min	Max	Mid	Min	Max	Mid	Min	Max	Mid	Min	Max	Mid	Min	Max	Mid	Min	Max	Mid	Min
0.74	-0.01	0.00	0.58	0.42	0.00	0.64	0.38	0.00	0.65	0.42	0.00	0.63	0.39	0.00	0.59	0.00	0.00	0.65	0.41	0.00	0.61	0.42	-0.01
0.60	0.00	0.00	0.55	0.36	0.00	0.55	0.00	0.00	0.54	0.43	0.00	0.54	0.36	0.00	0.54	0.35	0.00	0.54	0.00	0.00	0.52	0.00	0.00
0.59	0.36	0.00	0.52	0.36	0.00	0.48	0.38	0.00	0.54	0.00	0.00	0.56	0.39	0.00	0.51	0.55	0.00	0.60	0.36	0.00	0.56	0.11	0.00
0.59	0.00	0.00	0.53	0.09	0.00	0.54	0.44	0.00	0.53	0.38	0.00	0.50	0.27	0.00	0.52	0.41	0.00	0.51	0.39	0.00	0.46	0.00	0.00
0.58	0.00	0.00	0.52	0.00	0.00	0.53	0.01	0.00	0.56	0.00	0.00	0.51	0.41	0.00	0.53	0.36	0.00	0.49	0.00	0.00	0.53	0.08	0.00
0.56	0.39	0.00	0.51	0.00	0.00	0.51	0.00	0.00	0.48	0.00	0.00	0.53	0.41	0.00	0.46	0.35	0.00	0.48	0.37	0.00	0.51	0.39	0.01
0.63	0.37	0.00	0.52	0.37	0.00	0.56	0.01	0.00	0.54	0.39	0.00	0.54	0.37	0.00	0.54	0.34	0.00	0.51	0.45	0.00	0.52	0.01	0.01
0.61	0.39	0.00	0.56	0.29	0.00	0.51	0.38	0.00	0.53	0.00	0.00	0.52	0.40	0.00	0.50	0.42	0.00	0.53	0.05	0.01	0.49	0.44	0.01
0.63	0.00	0.00	0.49	0.41	0.00	0.61	0.00	0.00	0.50	0.44	0.00	0.51	0.00	0.00	0.54	0.40	0.00	0.53	0.07	0.00	0.46	0.01	0.00
0.58	0.38	0.00	0.53	0.41	0.00	0.53	0.00	0.00	0.51	0.26	0.00	0.50	0.00	0.00	0.49	0.40	0.00	0.50	0.05	0.00	0.52	0.37	0.00
0.61	0.00	0.00	0.50	0.14	0.00	0.50	0.31	0.00	0.52	0.00	0.00	0.53	0.00	0.00	0.52	0.35	0.00	0.52	0.00	0.00	0.52	0.00	0.00
0.63	0.42	0.00	0.52	0.38	0.00	0.52	0.41	0.00	0.59	0.00	0.00	0.52	0.40	0.00	0.54	0.44	0.00	0.52	0.00	0.00	0.56	0.15	0.00
0.67	0.39	0.00	0.52	0.12	0.00	0.52	0.41	0.00	0.55	0.38	0.00	0.53	0.39	0.00	0.52	0.38	0.00	0.55	0.12	0.00	0.58	0.41	0.00
0.60	0.38	0.00	0.60	0.42	0.00	0.50	0.37	0.00	0.56	0.11	0.00	0.57	0.38	0.00	0.56	0.00	0.00	0.57	0.39	0.01	0.52	0.40	0.00
0.56	0.41	0.00	0.58	0.38	0.00	0.58	0.00	0.00	0.67	0.33	0.00	0.57	0.00	0.00	0.59	0.46	0.00	0.56	0.39	0.01	0.73	0.18	0.00
0.72	0.00	0.00	0.68	0.01	0.00	0.62	0.36	0.00	0.65	0.40	0.00	0.63	0.37	0.00	0.59	0.39	-0.01	0.67	0.44	0.00	0.87	0.06	0.00

Figure 2. Heat map presentation of *E. coli* BAA1161 growth in the second plate uniformity assay plate at 24h. The treatment of column's wells is presented above it in the figure. The treatments were: max: 256 µg/ml piperacillin, mid: 256 µg/ml piperacillin + 8 µg/ml mefloquine, min: 256 µg/ml piperacillin + 16 µg/ml mefloquine. Initial bacterial concentration of all the wells was $5x10^5$ cfu/ml.

Min	Max	Mid	Min	Max	Mid	Min	Max	Mid	Min	Max	Mid	Min	Max	Mid	Min	Max	Mid	Min	Max	Mid	Min	Max	Mid
-0.01	0.76	0.78	0.00	0.40	0.67	0.00	0.80	0.83	0.00	0.29	0.75	0.00	0.77	0.77	0.00	0.68	0.80	0.00	0.74	0.80	0.00	0.82	0.80
-0.01	0.74	0.00	0.00	0.36	0.75	0.00	0.00	0.75	0.00	0.78	0.73	0.00	0.49	0.74	0.00	0.86	0.63	0.00	0.83	0.00	0.00	0.65	0.00
-0.01	-0.02	0.47	0.00	0.68	0.65	0.00	0.72	0.00	0.00	0.68	0.00	0.00	0.74	0.46	0.00	0.81	0.00	0.00	0.65	0.73	0.00	0.96	0.09
0.00	0.81	0.58	0.00	0.65	0.69	0.00	0.65	0.00	0.00	0.74	0.81	0.00	0.70	0.00	0.00	0.73	0.62	0.00	0.65	0.72	0.00	0.60	0.77
0.00	0.65	0.00	0.00	0.77	0.47	0.00	0.79	0.69	0.00	0.82	0.00	0.00	0.80	0.00	0.00	0.78	0.73	0.00	0.84	0.73	0.00	0.80	0.73
0.00	0.79	0.70	0.00	0.78	0.67	0.00	0.00	0.71	0.00	0.78	0.00	0.00	0.76	0.77	0.00	0.83	0.66	0.00	0.80	0.72	0.00	0.73	0.76
0.00	0.65	0.83	0.00	0.81	0.69	0.00	0.76	0.66	0.00	0.77	0.00	0.00	0.77	0.69	0.00	0.80	0.79	0.00	0.68	0.67	0.00	0.77	0.69
0.00	0.66	0.66	0.00	0.72	0.00	0.00	0.62	0.69	0.00	0.73	0.00	0.00	0.81	0.52	0.00	0.42	0.77	0.00	0.00	0.71	0.00	0.76	0.77
-0.01	0.66	0.57	0.00	0.81	0.00	0.00	0.74	0.69	0.00	0.79	0.00	0.00	0.53	0.78	0.00	0.83	0.00	0.00	0.76	0.65	0.00	0.80	0.01
0.00	0.70	0.73	0.00	0.78	0.63	0.00	0.80	0.72	0.00	0.80	0.70	0.00	0.73	0.00	0.00	0.70	0.63	0.00	0.81	0.76	0.00	0.74	0.77
0.00	0.42	0.53	0.00	0.84	0.71	0.00	0.77	0.71	0.00	0.76	0.67	0.00	0.60	0.72	0.00	0.78	0.51	0.00	0.74	0.66	0.00	0.79	0.00
0.00	0.81	0.72	0.00	0.80	0.68	0.00	0.75	0.02	0.00	0.71	0.01	0.00	0.62	0.47	0.00	0.75	0.64	0.00	0.76	0.78	0.00	0.71	0.73
0.00	0.78	0.73	0.00	0.77	0.62	0.00	0.76	0.77	0.00	0.86	0.00	0.00	0.78	0.80	0.00	0.70	0.74	0.00	0.83	0.00	0.00	0.00	0.61
0.00	0.82	0.74	0.00	0.70	0.00	0.00	0.74	0.00	0.00	0.59	0.70	0.00	0.79	0.00	0.00	0.93	0.00	0.00	0.73	0.66	0.00	0.81	0.65
0.00	0.92	0.62	0.00	0.76	0.72	0.00	0.78	0.00	0.00	0.81	0.54	0.00	0.82	0.87	0.00	0.81	0.74	0.00	0.85	0.59	0.00	0.77	0.85
0.00	0.88	0.00	0.00	0.80	0.84	0.00	0.81	0.78	0.00	0.80	0.75	0.00	0.86	0.77	0.00	0.80	0.76	0.00	0.80	0.74	0.00	0.84	0.89

Figure 3. Heat map presentation of *E. coli* BAA1161 growth in the Third plate uniformity assay plate at 24h. The treatment of column's wells is presented above it in the figure. The treatments were: max: 256 µg/ml piperacillin, mid: 256 µg/ml piperacillin + 8 µg/ml mefloquine, min: 256 µg/ml piperacillin + 16 µg/ml mefloquine. Initial bacterial concentration of all the wells was $5x10^5$ cfu/ml.

Mid	Min	Max	Mid	Min	Max	Mid	Min	Max	Mid	Min	Max	Mid	Min	Max	Mid	Min	Max	Mid	Min	Max	Mid	Min	Max
0.80	0.00	0.82	0.72	0.00	0.75	0.75	-0.01	0.83	0.71	0.00	0.82	0.68	-0.01	0.83	0.68	0.00	0.99	0.80	-0.01	0.81	0.78	0.00	0.84
0.72	0.00	0.81	0.00	0.00	0.94	0.00	0.00	0.76	0.00	0.00	0.82	0.68	0.00	0.75	0.70	0.00	0.73	0.61	0.00	0.76	0.70	0.00	0.72
-0.01	0.00	0.93	0.69	0.00	0.71	0.52	-0.01	0.75	0.71	0.00	0.71	0.00	0.00	0.66	0.62	0.00	0.83	0.66	-0.01	0.79	0.66	0.00	0.81
0.00	0.00	0.68	0.54	0.00	0.79	0.70	0.00	0.88	0.00	0.00	0.79	0.00	0.00	0.75	0.64	0.00	0.89	0.63	0.00	0.70	0.37	0.00	0.82
0.64	0.00	0.78	0.71	0.00	0.74	0.75	0.00	0.76	0.70	0.00	0.74	0.64	0.00	0.76	0.67	0.00	0.80	0.75	0.00	0.78	0.48	0.01	0.85
0.66	0.00	0.73	0.00	0.00	0.71	0.64	0.00	0.73	0.70	0.00	0.78	0.72	0.00	0.78	0.83	0.03	0.79	0.74	0.00	0.73	0.73	0.00	0.81
0.70	0.00	0.79	0.00	0.00	0.72	0.71	0.00	0.76	0.69	0.00	0.75	0.63	0.00	0.71	0.68	0.01	0.80	0.72	0.01	0.89	0.71	0.00	0.86
0.70	0.00	0.83	0.65	0.00	0.77	0.66	0.00	0.73	0.69	0.00	0.78	0.61	0.00	0.79	0.73	0.01	0.83	0.43	0.00	0.78	0.73	0.00	0.82
0.00	0.00	0.73	0.74	0.00	0.86	0.75	0.00	0.71	0.68	0.00	0.86	0.34	0.00	0.78	0.77	0.01	0.79	0.91	0.00	0.83	0.68	0.00	0.81
0.00	0.00	0.80	0.68	0.00	0.82	0.17	0.00	0.73	0.67	0.00	0.75	0.54	0.04	0.79	0.69	0.00	0.78	0.73	0.00	0.67	0.68	0.00	0.82
0.70	0.00	0.72	0.74	0.00	0.75	0.72	0.02	0.87	0.72	0.00	0.79	0.01	0.01	0.68	0.67	0.00	0.79	0.50	0.01	0.75	0.75	0.00	0.81
0.75	0.00	0.82	0.00	0.00	0.66	0.00	0.00	0.78	0.04	0.00	0.75	0.69	0.00	0.81	0.71	0.00	0.76	0.68	0.00	0.86	0.73	0.00	0.81
0.77	0.00	0.77	0.71	0.00	0.70	0.77	0.00	0.77	0.78	0.00	0.78	0.82	0.02	0.96	0.72	0.00	0.77	0.89	0.00	0.78	0.69	0.00	0.91
0.73	0.00	0.83	0.64	0.01	0.72	0.72	0.00	0.72	0.71	0.00	0.65	0.48	0.00	0.64	0.54	0.01	0.76	0.00	0.00	0.73	0.71	0.00	0.84
0.60	0.00	0.80	0.70	0.00	0.81	0.73	0.00	0.75	0.73	0.00	0.72	0.70	0.00	0.77	0.68	0.00	0.80	0.72	0.00	0.77	0.89	0.00	0.86
0.78	0.00	0.95	0.71	0.00	0.82	0.48	0.00	0.81	0.75	0.00	0.82	0.76	0.00	0.83	0.75	0.00	0.83	0.73	0.00	0.94	0.71	0.00	0.87

Figure 4. Heat map presentation of *E. coli* BAA1161 growth in the fouth plate uniformity assay plate at 24h. The treatment of column's wells is presented above it in the figure. The treatments were: max: 256 µg/ml piperacillin, mid: 256 µg/ml piperacillin + 6 µg/ml mefloquine, min: 256 µg/ml piperacillin + 16 µg/ml mefloquine. Initial bacterial concentration of all the wells was $5x10^5$ cfu/ml.

Min	Max	Mid	Min	Max	Mid	Min	Max	Mid	Min	Max	Mid	Min	Max	Mid	Min	Max	Mid	Min	Max	Mid	Min	Max	Mid
0.00	0.70	0.14	0.01	0.75	0.58	0.02	0.71	0.63	0.01	0.77	0.40	0.02	0.70	0.02	0.01	0.76	0.66	0.01	0.68	0.02	0.02	0.66	0.00
0.00	0.60	0.02	0.02	0.51	0.02	0.02	0.52	0.59	0.02	0.64	0.52	0.02	0.51	0.02	0.02	0.47	0.64	0.02	0.70	0.62	0.02	0.42	0.57
0.01	0.57	0.02	0.02	0.63	0.03	0.02	0.55	0.39	0.02	0.57	0.02	0.02	0.63	0.47	0.03	0.65	0.03	0.02	0.48	0.02	0.02	0.69	0.06
0.01	0.66	0.02	0.02	0.02	0.56	0.02	0.62	0.39	0.02	0.65	0.63	0.02	0.48	0.07	0.02	0.64	0.02	0.02	0.02	0.58	0.02	0.60	0.44
0.01	0.67	0.65	0.02	0.03	0.51	0.02	0.02	0.54	0.02	0.66	0.02	0.02	0.02	0.62	0.02	0.47	0.02	0.02	0.53	0.02	0.03	0.61	0.65
0.01	0.03	0.47	0.02	0.68	0.23	0.02	0.67	0.02	0.02	0.68	0.02	0.02	0.56	0.60	0.02	0.66	0.41	0.02	0.47	0.39	0.02	0.44	0.69
0.01	0.54	0.41	0.01	0.63	0.40	0.02	0.34	0.02	0.02	0.68	0.02	0.02	0.55	0.02	0.02	0.64	0.68	0.03	0.63	0.02	0.02	0.69	0.03
0.01	0.01	0.63	0.02	0.61	0.02	0.02	0.65	0.02	0.02	0.02	0.02	0.02	0.04	0.01	0.02	0.50	0.02	0.02	0.57	0.02	0.03	0.57	0.03
0.01	0.62	0.42	0.02	0.67	0.58	0.02	0.68	0.02	0.02	0.55	0.02	0.03	0.41	0.02	0.02	0.60	0.57	0.02	0.72	0.02	0.02	0.47	0.42
0.01	0.64	0.03	0.02	0.60	0.46	0.03	0.63	0.02	0.02	0.39	0.40	0.02	0.58	0.02	0.02	0.63	0.02	0.02	0.63	0.02	0.02	0.53	0.03
0.02	0.61	0.38	0.02	0.03	0.36	0.02	0.55	0.34	0.02	0.45	0.58	0.02	0.66	0.25	0.02	0.66	0.02	0.02	0.03	0.03	0.03	0.54	0.02
0.01	0.56	0.02	0.02	0.03	0.42	0.02	0.05	0.03	0.02	0.59	0.38	0.02	0.02	0.64	0.02	0.03	0.53	0.02	0.42	0.61	0.02	0.65	0.45
0.02	0.02	0.48	0.02	0.64	0.02	0.02	0.53	0.61	0.02	0.69	0.55	0.03	0.67	0.03	0.02	0.53	0.64	0.03	0.03	0.03	0.03	0.43	0.56
0.01	0.03	0.03	0.02	0.67	0.03	0.02	0.68	0.62	0.03	0.65	0.02	0.02	0.56	0.02	0.02	0.71	0.03	0.03	0.56	0.58	0.02	0.58	0.70
0.01	0.56	0.43	0.02	0.40	0.02	0.02	0.65	0.03	0.02	0.63	0.54	0.02	0.53	0.02	0.02	0.63	0.08	0.03	0.64	0.61	0.02	0.02	0.01
0.00	0.78	0.03	0.01	0.01	0.03	0.02	0.52	0.41	0.02	0.69	0.67	0.02	0.71	0.56	0.01	0.73	0.62	0.01	0.03	0.69	0.01	0.74	0.68

Figure 5. Heat map presentation of *E. coli* BAA1161 growth in the fifth plate uniformity assay plate at 24h. The treatment of column's wells is presented above it in the figure. The treatments were: max: 256 µg/ml piperacillin, mid: 256 µg/ml piperacillin + 6 µg/ml mefloquine, min: 256 µg/ml piperacillin + 16 µg/ml mefloquine. Initial bacterial concentration of all the wells was $5x10^5$ cfu/ml.

Mid	Min	Max	Mid	Min	Max	Mid	Min	Max	Mid	Min	Max	Mid	Min	Max	Mid	Min	Max	Mid	Min	Max	Mid	Min	Max
0.75	0.00	0.73	0.00	0.00	0.68	0.00	0.00	0.71	0.54	0.00	0.73	0.00	0.00	0.78	0.00	0.00	0.75	0.71	0.00	0.46	0.00	0.00	0.62
0.00	0.00	0.59	0.73	0.00	0.65	0.00	0.00	0.64	0.00	0.00	0.00	0.69	0.00	0.53	0.00	0.00	0.77	-0.01	0.00	0.62	0.37	0.00	0.71
0.59	0.00	0.54	0.00	0.00	0.69	0.00	0.00	0.72	0.00	0.00	0.76	0.00	0.00	0.43	0.00	0.00	0.60	0.64	0.00	0.74	0.00	0.00	0.71
0.69	0.00	0.56	0.00	0.00	0.68	0.83	0.00	0.57	0.56	0.00	0.74	0.00	0.00	0.59	0.00	0.00	0.43	0.00	-0.01	0.68	0.69	0.00	0.68
0.00	0.00	0.60	0.62	0.00	0.68	0.70	0.00	0.52	0.64	0.00	0.58	0.00	0.00	0.69	0.00	0.00	0.60	0.71	0.00	0.67	0.00	0.00	0.68
0.00	0.00	0.65	0.00	0.00	0.65	0.00	0.00	0.68	0.70	0.00	0.67	0.00	0.00	0.06	0.65	0.00	0.76	0.59	0.00	0.00	0.00	0.00	0.53
0.00	0.00	0.68	0.71	0.00	0.66	0.00	0.00	0.61	0.00	0.00	0.71	0.40	0.00	0.00	0.57	0.00	0.71	0.00	0.00	0.66	0.45	0.00	0.74
0.00	0.00	0.74	0.00	0.00	0.70	0.62	0.00	0.75	0.00	0.00	0.00	0.00	0.00	0.01	0.67	0.00	0.70	0.00	0.00	0.44	0.39	0.00	0.61
-0.01	0.00	0.41	0.00	0.00	0.66	0.00	0.00	0.54	0.44	0.00	0.86	0.00	0.00	0.71	0.00	0.00	0.73	0.00	0.00	0.85	0.69	0.00	0.53
0.00	0.00	0.73	0.00	0.00	0.65	0.38	0.00	0.15	0.73	0.00	0.69	0.00	0.00	0.59	0.01	0.00	0.78	0.00	0.00	0.49	0.66	0.00	0.75
0.00	0.00	0.70	0.00	0.00	0.63	0.00	0.00	0.61	0.00	0.00	0.60	0.00	0.00	0.41	0.00	0.00	0.75	0.00	0.00	0.01	0.00	0.00	0.76
0.70	-0.01	0.60	0.69	0.00	0.75	0.43	0.00	0.68	0.00	0.00	0.44	0.00	0.00	0.60	0.00	0.00	0.57	0.61	0.00	0.67	0.00	0.00	0.76
-0.03	0.00	0.74	0.26	-0.01	0.21	0.70	0.00	0.66	0.67	0.00	0.72	0.00	0.00	0.61	0.00	0.00	0.72	0.53	0.00	0.74	0.00	0.00	0.70
0.00	0.00	0.70	0.00	0.00	0.69	0.00	0.00	0.00	0.00	0.00	0.57	0.00	0.00	0.66	0.00	0.00	0.73	0.00	0.00	0.67	0.00	0.00	0.61
0.73	-0.02	0.73	0.00	0.00	0.76	0.54	-0.01	0.61	-0.02	0.00	0.80	0.81	0.00	0.58	0.00	0.00	0.55	-0.01	0.00	0.45	0.00	-0.01	0.79
0.49	0.00	0.78	0.00	0.00	0.81	0.66	0.00	0.69	0.00	0.00	0.70	0.67	0.00	0.76	0.00	0.00	0.73	0.75	0.00	0.19	0.00	-0.01	0.93

Figure 6. Heat map presentation of *E. coli* BAA1161 growth in the seventh plate uniformity assay plate at 24h. The treatment of column's wells is presented above it in the figure. The treatments were: max: 256 µg/ml piperacillin, mid: 256 µg/ml piperacillin + 6 µg/ml mefloquine, min: 256 µg/ml piperacillin + 16 µg/ml mefloquine. Initial bacterial concentration of all the wells was $5x10^5$ cfu/ml.

Max	Mid	Min	Max	Mid	Min	Max	Mid	Min	Max	Mid	Min	Max	Mid	Min	Max	Mid	Min	Max	Mid	Min	Max	Mid	Min
0.82	0.46	0.01	0.01	0.01	0.01	0.70	0.01	0.01	0.62	0.04	0.01	0.76	0.01	0.01	0.86	0.01	0.01	0.81	0.01	0.01	0.72	0.56	0.00
0.73	0.01	0.01	0.01	0.01	0.01	0.65	0.01	0.01	0.01	0.00	0.01	0.72	0.00	0.01	0.47	0.01	0.01	0.47	0.01	0.01	0.29	0.01	0.01
0.66	0.37	0.00	0.69	0.37	0.00	0.63	0.01	0.01	0.46	0.01	0.00	0.01	0.01	0.01	0.57	0.52	0.01	0.66	0.01	0.01	0.17	0.00	0.00
0.79	0.38	0.01	0.72	0.01	0.01	0.43	0.01	0.01	0.01	0.01	0.01	0.71	0.01	0.01	0.01	0.01	0.01	0.67	0.76	0.01	0.49	0.00	0.01
0.71	0.00	0.01	0.46	0.01	0.01	0.57	0.01	0.01	0.62	0.01	0.01	0.45	0.46	0.01	0.72	0.58	0.01	0.65	0.01	0.01	0.01	0.70	0.01
0.74	0.01	0.01	0.01	0.01	0.01	0.75	0.47	0.01	0.56	0.02	0.01	0.16	0.01	0.01	0.76	0.68	0.01	0.68	0.01	0.01	0.44	0.00	0.01
0.62	0.00	0.01	0.72	0.61	0.01	0.61	0.58	0.01	0.72	0.17	0.01	0.67	0.01	0.01	0.49	0.42	0.01	0.65	0.01	0.01	0.74	0.01	0.01
0.01	0.01	0.01	0.72	0.01	0.01	0.65	0.64	0.01	0.59	0.01	0.01	0.63	0.01	0.01	0.72	0.01	0.01	0.65	0.01	0.01	0.69	0.59	0.01
0.77	0.00	0.01	0.75	0.01	0.01	0.72	0.01	0.01	0.00	0.43	0.01	0.73	0.01	0.01	0.73	0.01	0.01	0.93	0.01	0.01	0.71	0.00	0.01
0.65	0.00	0.01	0.63	0.01	0.01	0.01	0.62	0.01	0.62	0.01	0.01	0.55	0.62	0.00	0.48	0.03	0.01	0.67	0.01	0.01	0.01	0.61	0.01
0.63	0.00	0.01	0.70	0.51	0.01	0.63	0.01	0.01	0.62	0.64	0.01	0.67	0.62	0.01	0.64	0.69	0.01	0.88	0.21	0.01	0.11	0.01	0.01
0.66	0.65	0.01	0.01	0.06	0.01	0.72	0.01	0.01	0.01	0.01	0.01	0.74	0.01	0.01	0.59	0.01	0.01	0.73	0.61	0.01	0.67	0.65	0.01
0.56	0.00	0.01	0.80	0.01	0.01	0.69	0.01	0.01	0.70	0.01	0.01	0.01	0.01	0.01	0.68	0.01	0.01	0.78	0.01	0.01	0.01	0.01	0.00
0.74	0.01	0.01	0.54	0.01	0.01	0.58	0.00	0.01	0.66	0.01	0.01	0.64	0.01	0.01	0.64	0.63	0.01	0.64	0.63	0.00	0.63	0.71	0.01
0.00	0.01	0.01	0.50	0.01	0.01	0.01	0.01	0.01	0.67	0.62	0.01	0.45	0.01	0.01	0.03	0.01	0.01	0.58	0.01	0.00	0.01	0.01	0.01
0.74	0.63	0.01	0.59	0.00	0.00	0.53	0.01	0.01	0.01	0.01	0.01	0.52	0.59	0.01	0.70	0.70	0.01	0.77	0.02	0.00	0.78	0.63	0.01

Figure 7. Heat map presentation of *E. coli* BAA1161 growth in the eighth plate uniformity assay plate at 24h. The treatment of column's wells is presented above it in the figure. The treatments were: max: 256 µg/ml piperacillin, mid: 256 µg/ml piperacillin + 6 µg/ml mefloquine, min: 256 µg/ml piperacillin + 16 µg/ml mefloquine. Initial bacterial concentration of all the wells was $5x10^5$ cfu/ml.

Max	Mid	Min	Max	Mid	Min	Max	Mid	Min	Max	Mid	Min	Max	Mid	Min	Max	Mid	Min	Max	Mid	Min	Max	Mid	Min
0.88	0.73	0.01	0.61	0.01	0.01	0.78	0.69	0.01	0.63	0.78	0.01	0.88	0.71	0.01	0.81	0.01	0.01	0.76	0.65	0.01	0.83	0.44	0.00
0.76	0.68	0.01	0.58	0.62	0.01	0.72	0.01	0.00	0.80	0.01	0.01	0.77	0.01	0.00	0.75	0.73	0.00	0.48	0.70	0.01	0.01	0.01	0.01
0.59	0.38	0.00	0.74	0.01	0.00	0.57	0.03	0.01	0.69	0.01	0.00	0.73	0.00	0.01	0.77	0.00	0.00	0.79	0.35	0.00	0.01	0.01	0.00
0.59	0.70	0.01	0.67	0.00	0.00	0.76	0.56	0.00	0.78	0.76	0.02	0.69	0.01	0.01	0.70	0.72	0.01	0.82	0.00	0.00	0.75	0.00	0.01
0.73	0.01	0.00	0.00	0.80	0.00	0.83	0.02	0.00	0.83	0.04	0.05	0.65	0.01	0.01	0.73	0.00	0.00	0.90	0.01	0.01	0.66	0.62	0.03
0.75	0.00	0.01	0.74	0.00	0.00	0.67	0.01	0.01	0.71	0.67	0.02	0.56	0.66	0.01	0.02	0.76	0.02	0.44	0.01	0.03	0.09	0.01	0.03
0.66	0.65	0.00	0.81	0.50	0.00	0.64	0.81	0.04	0.82	0.01	0.00	0.78	0.33	0.02	0.67	0.76	0.05	0.65	0.76	0.01	0.79	0.02	0.01
0.74	0.66	0.01	0.37	0.77	0.00	0.78	0.77	0.02	0.64	0.01	0.00	0.56	0.70	0.00	0.83	0.77	0.05	0.03	0.54	0.01	0.70	0.02	0.02
0.77	0.57	0.00	0.61	0.73	0.02	0.70	0.50	0.01	0.05	0.65	0.02	0.83	0.76	0.01	0.70	0.76	0.02	0.81	0.02	0.01	0.81	0.52	0.02
0.73	0.00	0.01	0.50	0.01	0.01	0.76	0.02	0.01	0.77	0.01	0.03	0.86	0.78	0.05	0.90	0.81	0.03	0.75	0.05	0.03	0.52	0.06	0.03
0.77	0.01	0.01	0.76	0.00	0.01	0.79	0.75	0.03	0.83	0.73	0.01	0.66	0.02	0.03	0.57	0.03	0.03	0.71	0.67	0.03	0.76	0.76	0.02
0.70	0.76	0.01	0.50	0.00	0.01	0.43	0.70	0.05	0.86	0.56	0.01	0.84	0.70	0.01	0.82	0.77	0.02	0.64	0.61	0.02	0.47	0.44	0.02
0.93	0.01	0.00	0.76	0.01	0.01	0.76	0.01	0.00	0.78	0.01	0.01	0.76	0.01	0.01	0.75	0.01	0.01	0.65	0.02	0.02	0.83	0.68	0.03
0.80	0.66	0.01	0.73	0.70	0.00	0.61	0.01	0.02	0.68	0.01	0.02	0.75	0.02	0.01	0.79	0.67	0.02	0.75	0.12	0.02	0.77	0.79	0.04
0.72	0.75	0.01	0.30	0.01	0.01	0.75	0.01	0.01	0.60	0.74	0.01	0.53	0.53	0.02	0.01	0.01	0.05	0.74	0.05	0.01	0.39	0.00	0.03
0.84	0.01	0.01	0.52	0.01	0.01	0.79	0.01	0.01	0.81	0.02	0.02	0.75	0.71	0.05	0.80	0.01	0.08	0.81	0.89	0.03	0.64	0.78	0.04

Figure 8a. Heat map presentation of *E. coli* BAA1161 growth in the ninth plate uniformity assay plate at 24h. The treatment of column's wells is presented above it in the figure. The treatments were: max: 256 µg/ml piperacillin, mid: 256 µg/ml piperacillin + 6 µg/ml mefloquine, min: 256 µg/ml piperacillin + 16 µg/ml mefloquine. Initial bacterial concentration of all the wells was $5x10^5$ cfu/ml.

Max	Mid	Min	Max	Mid	Min	Max	Mid	Min	Max	Mid	Min	Max	Mid	Min	Max	Mid	Min	Max	Mid	Min	Max	Mid	Min
0.03	0.02	0.01	0.01	0.01	0.01	0.01	0.01	0.01	0.01	0.12	0.01	0.12	0.01	0.01	0.04	0.01	0.01	0.01	0.01	0.01	0.02	0.01	0.01
0.01	0.01	0.01	0.01	0.01	0.01	0.01	0.01	0.00	0.02	0.01	0.01	0.02	0.01	0.00	0.01	0.02	0.00	0.01	0.01	0.01	0.01	0.01	0.01
0.01	0.01	0.00	0.01	0.01	0.00	0.01	0.00	0.00	0.01	0.00	0.00	0.01	0.00	0.00	0.02	0.00	0.00	0.04	0.00	0.01	0.01	0.01	0.01
0.01	0.02	0.01	0.01	0.00	0.01	0.02	0.00	0.00	0.02	0.12	0.00	0.01	0.00	0.00	0.01	0.03	0.00	0.06	0.00	0.00	0.01	0.00	0.00
0.01	0.01	0.01	0.00	0.09	0.00	0.06	0.01	0.00	0.12	0.00	0.00	0.00	0.00	0.00	0.01	0.00	0.00	0.07	0.00	0.00	0.00	0.00	0.00
0.01	0.00	0.00	0.01	0.01	0.00	0.01	0.00	0.00	0.01	0.02	0.00	0.00	0.01	0.00	0.01	0.10	0.00	0.00	0.01	0.00	0.00	0.00	0.01
0.00	0.01	0.00	0.08	0.00	0.00	0.00	0.20	0.00	0.09	0.00	0.00	0.04	0.00	0.00	0.00	0.07	0.00	0.01	0.08	0.00	0.03	0.00	0.01
0.01	0.01	0.00	0.01	0.14	0.01	0.07	0.13	0.00	0.01	0.00	0.00	0.00	0.02	0.00	0.12	0.04	0.00	0.00	0.00	0.00	0.00	0.00	0.01
0.01	0.01	0.01	0.01	0.03	0.00	0.00	0.00	0.00	0.00	0.01	0.00	0.12	0.13	0.00	0.01	0.13	0.01	0.01	0.00	0.00	0.03	0.00	0.00
0.01	0.00	0.01	0.01	0.01	0.00	0.03	0.00	0.00	0.03	0.01	0.00	0.18	0.03	0.00	0.01	0.09	0.00	0.01	0.00	0.00	0.00	0.00	0.00
0.02	0.01	0.00	0.02	0.00	0.00	0.07	0.19	0.00	0.07	0.00	0.00	0.00	0.00	0.00	0.00	0.00	0.00	0.01	0.01	0.00	0.01	0.02	0.00
0.01	0.05	0.00	0.01	0.00	0.00	0.00	0.01	0.00	0.12	0.01	0.00	0.12	0.01	0.00	0.12	0.09	0.00	0.00	0.01	0.00	0.00	0.00	0.00
0.01	0.01	0.00	0.01	0.01	0.01	0.01	0.00	0.00	0.02	0.01	0.00	0.02	0.00	0.00	0.01	0.00	0.00	0.00	0.00	0.00	0.00	0.00	0.00
0.04	0.01	0.01	0.01	0.01	0.00	0.01	0.00	0.01	0.01	0.01	0.00	0.01	0.00	0.00	0.02	0.01	0.01	0.01	0.01	0.00	0.01	0.02	0.01
0.01	0.02	0.01	0.00	0.01	0.00	0.01	0.00	0.00	0.01	0.01	0.01	0.01	0.01	0.00	0.01	0.01	0.00	0.01	0.00	0.01	0.00	0.00	0.01
0.07	0.01	0.01	0.01	0.01	0.00	0.01	0.01	0.00	0.02	0.01	0.01	0.01	0.01	0.01	0.02	0.01	0.00	0.03	0.03	0.00	0.00	0.03	0.01

Figure 8b. Heat map presentation of *E. coli* BAA1161 growth in the ninth plate uniformity assay plate at 14h. The treatment of column's wells is presented above it in the figure. The treatments were: max: 256 µg/ml piperacillin, mid: 256 µg/ml piperacillin + 6 µg/ml mefloquine, min: 256 µg/ml piperacillin + 16 µg/ml mefloquine. Initial bacterial concentration of all the wells was $5x10^5$ cfu/ml.

Max	Mid	Min	Max	Mid	Min	Max	Mid	Min	Max	Mid	Min	Max	Mid	Min	Max	Mid	Min	Max	Mid	Min	Max	Mid	Min
0.38	0.28	0.01	0.02	0.01	0.01	0.09	0.19	0.01	0.03	0.41	0.01	0.42	0.26	0.01	0.39	0.01	0.01	0.27	0.04	0.01	0.36	0.01	0.01
0.26	0.16	0.01	0.01	0.05	0.01	0.24	0.01	0.00	0.32	0.01	0.01	0.32	0.01	0.00	0.28	0.33	0.01	0.01	0.23	0.01	0.01	0.01	0.01
0.01	0.01	0.00	0.27	0.01	0.00	0.01	0.00	0.00	0.15	0.01	0.00	0.26	0.00	0.01	0.31	0.00	0.00	0.37	0.00	0.00	0.01	0.01	0.01
0.01	0.34	0.01	0.07	0.01	0.01	0.31	0.03	0.00	0.34	0.39	0.00	0.13	0.00	0.00	0.18	0.36	0.00	0.40	0.00	0.00	0.28	0.00	0.00
0.26	0.01	0.01	0.00	0.38	0.00	0.41	0.01	0.00	0.41	0.00	0.00	0.00	0.00	0.00	0.28	0.00	0.00	0.41	0.00	0.00	0.12	0.04	0.00
0.27	0.00	0.00	0.01	0.01	0.00	0.15	0.00	0.00	0.28	0.30	0.00	0.03	0.14	0.01	0.02	0.41	0.02	0.01	0.00	0.00	0.00	0.00	0.01
0.05	0.12	0.00	0.41	0.01	0.00	0.06	0.42	0.00	0.40	0.00	0.00	0.38	0.00	0.00	0.04	0.40	0.02	0.11	0.39	0.00	0.36	0.00	0.01
0.28	0.20	0.00	0.01	0.40	0.00	0.40	0.40	0.00	0.04	0.00	0.00	0.01	0.33	0.00	0.41	0.39	0.01	0.01	0.01	0.00	0.17	0.02	0.01
0.27	0.02	0.00	0.03	0.35	0.00	0.02	0.00	0.00	0.00	0.21	0.02	0.41	0.39	0.00	0.27	0.40	0.00	0.15	0.00	0.00	0.36	0.01	0.01
0.25	0.00	0.01	0.01	0.00	0.00	0.36	0.00	0.00	0.36	0.01	0.01	0.42	0.37	0.02	0.27	0.39	0.00	0.18	0.00	0.01	0.00	0.01	0.00
0.34	0.01	0.00	0.31	0.00	0.01	0.40	0.41	0.00	0.41	0.05	0.01	0.12	0.01	0.01	0.01	0.00	0.00	0.21	0.21	0.00	0.27	0.28	0.00
0.15	0.40	0.00	0.01	0.00	0.00	0.00	0.27	0.00	0.42	0.03	0.01	0.40	0.26	0.02	0.42	0.40	0.00	0.04	0.07	0.00	0.00	0.00	0.00
0.25	0.01	0.00	0.30	0.01	0.01	0.30	0.00	0.00	0.31	0.00	0.00	0.30	0.00	0.00	0.29	0.00	0.00	0.05	0.02	0.00	0.14	0.07	0.00
0.40	0.13	0.01	0.01	0.25	0.00	0.03	0.01	0.01	0.11	0.01	0.02	0.19	0.01	0.00	0.33	0.13	0.01	0.24	0.00	0.00	0.29	0.35	0.01
0.08	0.39	0.01	0.00	0.01	0.01	0.22	0.00	0.00	0.01	0.29	0.01	0.03	0.01	0.00	0.01	0.01	0.00	0.17	0.00	0.00	0.00	0.00	0.01
0.36	0.01	0.01	0.01	0.01	0.00	0.20	0.01	0.00	0.33	0.01	0.02	0.18	0.26	0.01	0.32	0.01	0.00	0.40	0.38	0.00	0.01	0.41	0.01

Figure 8c. Heat map presentation of *E. coli* BAA1161 growth in the ninth plate uniformity assay plate at 17h. The treatment of column's wells is presented above it in the figure. The treatments were: max: 256 µg/ml piperacillin, mid: 256 µg/ml piperacillin + 6 µg/ml mefloquine, min: 256 µg/ml piperacillin + 16 µg/ml mefloquine. Initial bacterial concentration of all the wells was $5x10^5$ cfu/ml.

Max	Mid	Min	Max	Mid	Min	Max	Mid	Min	Max	Mid	Min	Max	Mid	Min	Max	Mid	Min	Max	Mid	Min	Max	Mid	Min
0.54	0.45	0.01	0.40	0.01	0.01	0.42	0.41	0.02	0.41	0.51	0.01	0.56	0.44	0.01	0.50	0.01	0.01	0.47	0.41	0.01	0.50	0.01	0.01
0.44	0.44	0.01	0.36	0.41	0.01	0.46	0.01	0.01	0.50	0.01	0.01	0.49	0.01	0.00	0.47	0.48	0.01	0.08	0.44	0.01	0.01	0.01	0.01
0.39	0.01	0.00	0.47	0.01	0.00	0.37	0.00	0.01	0.44	0.01	0.00	0.47	0.00	0.01	0.50	0.00	0.00	0.52	0.01	0.00	0.01	0.01	0.01
0.38	0.46	0.01	0.43	0.00	0.00	0.50	0.38	0.00	0.51	0.53	0.00	0.45	0.01	0.01	0.46	0.50	0.00	0.55	0.00	0.00	0.48	0.00	0.01
0.44	0.01	0.00	0.00	0.53	0.00	0.55	0.00	0.00	0.53	0.00	0.00	0.17	0.01	0.01	0.47	0.00	0.00	0.58	0.01	0.01	0.42	0.40	0.04
0.46	0.00	0.01	0.33	0.00	0.00	0.44	0.00	0.00	0.47	0.46	0.00	0.33	0.43	0.01	0.02	0.54	0.02	0.06	0.02	0.06	0.09	0.01	0.04
0.40	0.43	0.00	0.54	0.26	0.00	0.42	0.56	0.00	0.54	0.00	0.00	0.51	0.00	0.01	0.41	0.54	0.05	0.44	0.53	0.01	0.52	0.01	0.01
0.46	0.43	0.01	0.01	0.53	0.00	0.52	0.53	0.00	0.42	0.00	0.00	0.36	0.47	0.00	0.55	0.53	0.04	0.04	0.35	0.00	0.45	0.02	0.01
0.45	0.41	0.00	0.42	0.51	0.01	0.39	0.27	0.01	0.05	0.46	0.02	0.56	0.53	0.01	0.47	0.53	0.01	0.48	0.02	0.01	0.52	0.05	0.01
0.45	0.00	0.01	0.17	0.01	0.00	0.51	0.00	0.01	0.51	0.01	0.03	0.59	0.57	0.06	0.59	0.60	0.04	0.54	0.05	0.04	0.15	0.08	0.01
0.47	0.01	0.01	0.50	0.00	0.01	0.52	0.53	0.00	0.53	0.35	0.01	0.43	0.02	0.03	0.34	0.04	0.03	0.46	0.46	0.05	0.48	0.47	0.00
0.42	0.50	0.01	0.16	0.00	0.01	0.02	0.46	0.00	0.56	0.40	0.01	0.55	0.47	0.03	0.55	0.53	0.03	0.42	0.42	0.00	0.03	0.01	0.00
0.59	0.01	0.00	0.49	0.00	0.01	0.50	0.01	0.00	0.50	0.01	0.01	0.49	0.01	0.00	0.48	0.00	0.00	0.43	0.02	0.00	0.44	0.42	0.00
0.50	0.43	0.01	0.26	0.47	0.00	0.41	0.01	0.02	0.44	0.01	0.02	0.49	0.02	0.01	0.49	0.45	0.01	0.47	0.01	0.00	0.47	0.48	0.01
0.42	0.50	0.01	0.01	0.01	0.01	0.47	0.01	0.01	0.40	0.49	0.01	0.22	0.12	0.02	0.01	0.01	0.03	0.46	0.02	0.00	0.01	0.00	0.01
0.58	0.01	0.01	0.17	0.01	0.00	0.46	0.01	0.00	0.49	0.01	0.02	0.45	0.43	0.15	0.48	0.01	0.09	0.49	0.58	0.00	0.42	0.48	0.01

Figure 8d. Heat map presentation of *E. coli* BAA1161 growth in the ninth plate uniformity assay plate at 20h. The treatment of column's wells is presented above it in the figure. The treatments were: max: 256 µg/ml piperacillin, mid: 256 µg/ml piperacillin + 6 µg/ml mefloquine, min: 256 µg/ml piperacillin + 16 µg/ml mefloquine. Initial bacterial concentration of all the wells was $5x10^5$ cfu/ml.

Max	Mid	Min	Max	Mid	Min	Max	Mid	Min	Max	Mid	Min	Max	Mid	Min	Max	Mid	Min	Max	Mid	Min	Max	Mid	Min
0.99	0.89	0.01	0.88	0.01	0.01	1.00	0.88	0.01	0.89	0.94	0.01	1.03	0.89	0.01	1.00	0.01	0.01	0.98	0.87	0.01	1.03	0.67	0.00
0.95	0.87	0.01	0.84	0.83	0.01	0.95	0.01	0.01	0.99	0.01	0.01	0.98	0.41	0.01	0.96	0.91	0.01	0.74	0.90	0.01	0.01	0.01	0.01
0.86	0.62	0.00	0.96	0.01	0.00	0.83	0.44	0.01	0.93	0.01	0.00	0.95	0.00	0.01	0.98	0.00	0.00	1.00	0.54	0.02	0.42	0.01	0.01
0.84	0.88	0.01	0.93	0.01	0.01	0.97	0.78	0.00	0.98	0.93	0.02	0.93	0.01	0.01	0.93	0.91	0.01	1.00	0.00	0.02	0.98	0.01	0.01
0.94	0.01	0.01	0.00	0.95	0.00	1.00	0.02	0.00	0.99	0.04	0.05	0.92	0.29	0.01	0.96	0.00	0.00	1.05	0.42	0.01	0.92	0.85	0.03
0.95	0.01	0.01	0.99	0.01	0.00	0.90	0.01	0.01	0.93	0.86	0.03	0.81	0.87	0.01	0.02	0.93	0.02	0.62	0.02	0.02	0.08	0.01	0.03
0.89	0.83	0.00	0.99	0.72	0.00	0.87	0.95	0.02	0.99	0.00	0.00	0.97	0.52	0.02	0.90	0.94	0.05	0.91	0.94	0.01	1.00	0.02	0.01
0.94	0.83	0.01	0.55	0.93	0.01	0.96	0.93	0.01	0.89	0.01	0.00	0.82	0.89	0.01	1.00	0.93	0.03	0.04	0.77	0.01	0.95	0.03	0.02
0.97	0.78	0.01	0.87	0.92	0.03	0.95	0.71	0.01	0.03	0.85	0.02	1.00	0.92	0.01	0.93	0.93	0.01	1.02	0.02	0.01	1.01	0.91	0.04
0.95	0.01	0.01	0.75	0.01	0.02	0.97	0.42	0.01	0.97	0.01	0.02	1.01	0.95	0.03	1.05	0.97	0.02	0.97	0.03	0.06	0.77	0.05	0.03
0.97	0.01	0.01	0.97	0.00	0.01	0.98	0.92	0.03	1.01	0.95	0.01	0.90	0.01	0.01	0.80	0.02	0.02	0.94	0.90	0.16	1.01	0.98	0.04
0.93	0.92	0.01	0.76	0.00	0.01	0.64	0.91	0.05	1.02	0.78	0.01	1.00	0.91	0.01	1.00	0.95	0.01	0.89	0.83	0.02	0.71	0.62	0.01
1.05	0.01	0.00	0.99	0.07	0.01	0.98	0.01	0.00	1.00	0.01	0.01	0.98	0.01	0.01	0.98	0.15	0.01	0.92	0.02	0.01	0.99	0.89	0.02
0.97	0.85	0.01	1.00	0.91	0.01	0.89	0.01	0.01	0.94	0.01	0.01	0.98	0.02	0.01	1.02	0.88	0.02	0.98	0.48	0.01	1.00	0.98	0.05
0.95	0.92	0.01	0.55	0.01	0.01	0.99	0.01	0.01	0.87	0.93	0.01	0.80	0.82	0.01	0.01	0.01	0.05	1.01	0.05	0.03	0.60	0.03	0.02
0.94	0.01	0.02	0.83	0.01	0.01	1.02	0.02	0.01	1.02	0.02	0.02	0.99	0.91	0.02	1.01	0.01	0.08	1.03	1.02	0.02	0.93	0.93	0.02

Figure 8e. Heat map presentation of *E. coli* BAA1161 growth in the ninth plate uniformity assay plate at 28h. The treatment of column's wells is presented above it in the figure. The treatments were: max: 256 µg/ml piperacillin, mid: 256 µg/ml piperacillin + 6 µg/ml mefloquine, min: 256 µg/ml piperacillin + 16 µg/ml mefloquine. Initial bacterial concentration of all the wells was $5x10^5$ cfu/ml.

APPENDIX 6: Complete results of the DMSO compatibility assays

Piperacillin concentration (µg/ml)	DMSO concentration (%)													
	0	0	0.5	0.5	1	1	2	2	3	3	4	4	5	5
0	8	-3	-11	-8	-12	-12	-10	-5	-8	-4	0	4	19	38
0	3	-9	-15	-16	-13	-14	-10	-10	-5	-9	-1	-2	11	21
256	21	97	22	37	34	90	35	97	46	53	47	56	58	68
256	39	98	98	18	25	47	40	98	46	39	53	49	59	75

Figure 1. Heat map presentation of the *E. coli* BAA1161 growth inhibition in the first DMSO compatibility assay. Bacterial growth inhibition of DMSO was studied with seven DMSO concentrations in presence and in absence of 256 µg/ml PIP. Values presented in the table are growth inhibition percentages measured at 24h time point.

Piperacillin concentration (µg/ml)	DMSO concentration (%)													
	0	0	0.5	0.5	1	1	2	2	3	3	4	4	5	5
0	8	0	-9	-9	-7	-10	-8	-4	-3	-3	6	7	27	39
0	1	-9	-16	-17	-15	-15	-10	-11	-7	-8	2	1	20	30
256	34	19	26	33	94	27	37	34	41	42	50	48	56	63
256	48	26	25	26	30	25	36	37	34	41	47	51	62	69

Figure 2. Heat map presentation of the *E. coli* BAA1161 growth inhibition in the second DMSO compatibility assay. Bacterial growth inhibition of DMSO was studied with seven DMSO concentrations in presence and in absence of 256 µg/ml PIP. Values presented in the table are growth inhibition percentages measured at 24h time point.

APPENDIX 7: Complete results of the test screen

1.1	47.4	49.0	-6.0	9.3	14.4	-2.3	5.5	-4.4	9.5	17.8	18.5	13.2	9.4	9.3	8.9	0.2	-0.4
25.0	1.7	3.9	33.5	-9.1	9.7	6.7	2.2	-1.9	20.9	15.9	15.1	42.0	10.5	-4.7	10.1	92.8	2.4
4.5	13.8	-9.2	5.0	23.0	3.8	-15.5	4.8	5.9	5.3	-1.0	-4.2	-6.5	-6.6	2.0	10.0	39.4	100.1
-5.1	-3.8	0.8	4.2	4.9	-9.6	3.6	-16.4	1.2	-6.0	5.4	10.1	-6.6	-4.6	0.5	-1.6	-1.6	68.3
-5.7	-4.7	-1.7	-6.2	-9.6	22.6	3.2	8.3	0.0	-4.7	35.1	33.3	0.2	-0.9	-1.7	-4.4	14.0	2.5
-3.9	4.0	2.5	18.7	21.8	15.5	10.1	-6.4	11.7	8.5	30.9	32.8	4.0	1.3	-2.5	13.2	-3.7	20.5
4.9	4.4	9.4	-1.0	3.1	26.6	14.3	0.1	-2.3	-2.2	3.3	-4.0	-11.8	0.5	3.8	-13.8	-24.6	-0.8
5.2	10.6	4.4	-5.2	-1.0	10.5	-9.9	-2.6	-2.0	-4.9	-9.2	-5.8	-21.6	8.9	1.0	10.9	-2.2	6.8
7.9	-0.1	10.6	3.2	-6.0	10.1	-7.1	3.1	-3.4	19.2	-2.9	8.3	-1.8	-5.1	-5.3	-1.3	-5.1	-7.1
18.0	-0.2	19.3	1.1	-0.9	1.0	-11.1	-3.8	-0.2	2.0	3.5	5.9	-0.4	-4.5	-2.5	-1.6	-0.5	-5.3
8.2	-9.4	-2.8	36.8	-3.1	-5.6	0.8	-10.3	99.9	6.1	0.9	8.2	28.5	36.6	-10.3	-1.6	0.3	-5.1
99.9	-21.6	-0.2	5.6	7.7	75.7	-3.7	3.1	-3.5	-9.2	1.4	-10.3	32.2	20.9	-4.3	-7.7	2.3	0.5
3.9	23.8	11.6	-0.2	-3.0	9.5	8.6	8.5	3.2	2.7	14.7	12.1	25.6	-4.7	3.7	0.1	-1.1	27.7
-1.8	21.1	-6.3	1.7	-0.3	-0.9	1.8	-3.7	1.5	-1.2	11.6	28.3	17.1	-4.7	-1.1	-1.1	-15.1	3.6

Figure 1. Heat map presentation of the growth inhibition values (%) of the natural compounds in the first plate of the test EPI screen at 24h time point. Growth inhibition effect of 256 µg/ml piperacillin, which in combination with the natural compounds were screened, is subtracted from the presented growth inhibition values. Replicate wells with the same natural compound are separated by the thin lines. In the figure, replicate wells of the compounds which were considered hits and were tested in the follow-up dose-response assays are surrounded by thick lines. From left to right, wells inside the thick lines contained epigallocatechin gallate, hamamelitannin and isopropyl gallate.

7.0	-1.3	2.3	0.5	-1.4	-1.4	-6.8	-0.1	-0.8	4.9	9.8	-0.9	7.2	6.0	10.4	2.4	-2.3	5.5
-1.1	-7.7	12.6	13.9	6.3	-3.6	-0.3	5.5	100.1	5.5	20.9	-2.3	7.8	11.0	4.9	17.4	24.5	20.2
10.4	10.1	-7.8	-16.5	4.3	3.7	-1.7	20.2	7.6	30.0	13.7	3.8	12.3	-18.2	-3.8	37.3	7.7	17.9
7.5	8.2	4.1	2.0	-0.8	-0.6	-5.1	19.0	4.0	-2.9	8.7	-4.7	-0.8	3.7	-20.6	-3.4	-4.0	3.0
4.5	-3.4	11.4	20.3	-15.0	1.0	-0.5	-11.9	2.7	-4.0	-7.9	0.6	1.9	8.0	-5.0	-18.0	-4.4	0.2
-14.7	3.1	14.8	11.4	0.2	-17.8	-15.6	-2.3	-6.5	0.0	3.8	12.2	-2.1	-12.6	5.0	-5.2	-2.4	2.8
2.5	16.2	37.7	48.3	-2.5	3.0	-1.3	-4.4	-5.2	-1.2	2.3	9.7	-9.1	-2.8	-12.9	-1.4	-10.3	1.8
-15.1	37.1	46.3	47.1	1.6	-0.7	-4.7	-7.9	0.7	-7.1	5.7	-1.6	-11.4	2.2	10.0	6.6	-2.6	-0.3
1.8	4.9	-2.7	-16.1	38.2	-7.6	-1.2	-12.4	3.9	11.3	5.6	1.8	-1.6	-4.7	-10.3	30.9	-1.0	-9.8
9.3	-3.7	6.9	-3.1	-3.1	-3.0	3.0	-10.5	-5.7	4.8	-0.1	7.4	-0.5	0.0	1.1	-7.0	1.6	0.9
-4.6	5.5	-4.4	0.4	1.7	0.7	-3.5	-4.7	-5.1	-1.4	11.9	-2.2	7.6	-4.7	-7.0	-3.6	-8.2	-6.9
-9.1	-6.5	7.7	6.6	18.0	-0.4	-0.9	1.4	0.6	10.8	5.9	-4.7	18.3	-4.9	-5.9	3.1	-1.0	-8.5
3.3	16.4	8.1	14.7	6.6	4.9	5.4	10.2	4.1	-1.9	99.9	-1.3	46.8	3.9	1.1	17.8	-1.2	2.0
-2.9	17.6	6.2	-0.1	-5.4	-2.0	7.6	-3.3	-2.9	-7.2	-1.4	3.1	1.9	-1.5	-0.7	8.6	100.1	-8.4

Figure 2. Heat map presentation of the growth inhibition values (%) of the natural compounds in the second plate of the test EPI screen at 24h time point. Growth inhibition effect of 256 µg/ml piperacillin, which in combination with the natural compounds were screened, is subtracted from the presented growth inhibition values. Replicate wells with the same natural compound are separated by the thin lines. In the figure, replicate wells of the octyl gallate, which was considered as a hit and was included in the follow-up dose-response assays, are surrounded by thick lines.

APPENDIX 8: Results of the second dose-response assay

Table 1. Results of the second dose response assay. Growth inhibition effect of the four hit natural compounds (NC) was tested at six concentrations in combination with and without 256 µg/ml piperacillin (PIP). Growth inhibition values (%) of all wells included in the assay are presented in the figure. Inconsistent and random over 97% growth inhibition values were occurring in the wells with 256 µg/ml PIP.

Natural compound*	PIP concentration (µg/ml)	Natural compound concentration (µM)					
		100	75	50	25	12.5	0
EGCG	0	12.3	13.9	10.7	7.5	1.8	-3.9
		15.7	16.4	17.0	12.6	4.1	0.7
		14.6	15.9	12.4	8.3	2.1	-3.4
	256	56.5	52.1	48.4	43.6	42.6	100.2
		53.8	50.4	54.8	61.0	36.2	48.8
		50.4	51.3	55.9	56.7	40.9	46.5
HT	0	5.3	12.8	13.7	4.2	6.0	2.3
		9.9	11.9	11.1	6.5	6.3	2.1
		8.8	12.9	11.7	7.3	5.6	-0.6
	256	53.0	97.4	45.0	40.2	45.7	53.4
		52.0	59.7	48.8	52.3	41.9	25.6
		59.8	61.0	99.1	48.1	42.8	29.6
IG	0	10.1	9.8	12.6	5.9	6.9	2.1
		9.2	9.7	11.1	6.2	5.3	4.3
		10.6	9.8	9.9	7.8	4.9	-0.5
	256	66.9	53.7	63.0	100.0	46.8	100.0
		55.9	54.0	61.7	99.9	53.2	43.9
		68.9	67.5	50.8	99.9	45.1	40.0
OG	0	17.8	17.9	11.7	7.0	2.0	0.1
		12.8	14.0	11.8	1.5	0.1	-1.5
		19.8	14.6	14.8	5.5	3.2	-1.7
	256	99.8	99.9	60.0	49.0	43.2	62.3
		99.8	99.9	55.5	45.0	99.9	33.5
		99.8	99.7	55.3	51.4	44.7	100.0

*EGCG=Epigallocatechin gallate, HT=Hamamelitannin, IG=Isopropyl gallate and OG=Octyl gallate